Pftaire1 (Cyclin Dependent Kinase14): Role and Function in Axonal Outgrowth during the development of the CNS

Fatemeh Kamkar

Thesis Submitted to the

Faculty of Graduate and Postdoctoral Studies

in partial fulfillment of the requirements

for the Doctorate in Philosophy degree

in Cellular and Molecular Medicine

Department of Cellular and Molecular Medicine

Faculty of Medicine

University of Ottawa

ABSTRACT

Cyclin Dependent Kinase (Cdk) family members play a role in CNS development. Cyclin Dependent Kinase 5 (Cdk5) is well known for its fundamental role in neuronal development and axogenesis, as well as, cell death. Other Cdks include Pctaire and Pftaire. Inhibition of Pctaire results in increased axon outgrowth, however, the role and function of Pftaire is unknown. Pftaire1 is a novel member of the Cdk family that was initially detected in a screen for cdc2-like kinases. Unpublished data from our lab reveals that Pftaire1 (Eip63E) deficiency in *Drosophila melanogaster* results in defects in the axon and neuronal structure of the ventral nerve cord (VNC). In mammals, Pftaire1 is highly, expressed in the CNS. Here, we proposed that Pftaire1 might have a role in axon outgrowth. To investigate the role of Pftaire1 in mammals, the first germline Pftaire1 knockout mice were generated. Considering the severe effects of Eip63E deficiency in *Drosophila* and the homology between mammalian and fly Pftaire1, CNS defects in the mouse were anticipated. However, to date, no gross abnormalities have been detected in the overall morphology, fertility, life span, or anatomical brain structures of the Pftaire1 deficient mice. This may be due to the presence of other post-mitotic Cdk proteins that are highly similar to Pftaire1. For instance, mammals possess Pftaire (1, and 2), as well as, Pctaire (1, 2, and 3), while *Drosophila* only possess the Pftaire1 orthologue where the Pftaire2 and Pctaire (1, 2, and 3) are absent. Furthermore, the mice were of mixed background. In spite of this, we demonstrated that Pftaire1 deficient neurons showed increased axon length, in the initial phases of culture. This was confirmed by expression of dominant negative (DN) D228N-Pftaire1 in wild type neurons. Also classification of

axons into different ranges, reveals a higher percentage of hyperextended neurites in D228N and Pftaire1 knockout mice. The mechanism by which Pftaire1 controls axon outgrowth is unknown. In this study we show that, Pftaire1 interacts physically with the small GTPase proteins Rac1, Cdc42, and RhoA. Importantly, we showed that Pftaire1 phosphorylates GDP-RhoA on a serine residue. We propose that this regulates RhoA activity, which in turn controls axon outgrowth.

ACKNOWLEDGEMENTS

The dissertation represented here is the result of contribution, guidance, and efforts of a vast team during my journey as a PhD student at the University of Ottawa. I have been privileged to have their great support and enjoyed working with each and every person.

First, I would like to express my appreciation to my thesis supervisor, Dr. David Park, for giving me the opportunity to discover the wonders of science and providing me with guidance and constructive comments along the way. I have gained invaluable knowledge and expertise from working under your supervision. Thank you for supporting me through this challenging and rewarding experience.

I would like to express my deep appreciation to Dr. Antoine Hakim for his invaluable support through this arduous phase of my life and for giving me hope and courage to continue.

I would like to express my deep and sincere gratitude to Dr. Ruth Slack for her invaluable support in the scientific field as our collaborator, as well as, her caring and moral support. It would have been impossible for me to survive through the difficult moments and be here today without your help.

I would like to express my appreciation to my advisory committee members, Dr. Paul Albert, Dr. Antonio Colavita and Dr. Marc Ekker for their sound advice and insightful comments during the development of my PhD research.

I would like to further extend my thanks to Dr. Paul Albert and Maribeth Lazzaro for providing us with Pftaire1 AV viruses and plasmids. I would like to thank Dr. Gary

Bokoch for providing us with RhoA plasmids and Leticia Sanchez Alvarez for construction of AV viruses.

My warm thanks to the members of the “Park” lab. To those who I am indebted for all the invaluable help during this work, scientific discussions and for the friendly moments at the times of joy and desperation. Thanks to Dr. Yasmilde Rodriguez Gonzalez for her professional and moral support. For her insightful comments and invaluable laboratory assistance. For her critical review of this dissertation. Many thanks to Steve Callaghan and Carmen Estey for their valuable technical and scientific support during all this years. I would like to especially thank Dr. Dianbo Qu, Yi-Hong Zhang, and Dr. Paymaan Jafar-Nejad for their valuable insights and contributions to this work. I would also like to express, my heartfelt thanks to my very good friend, Farzaneh Safarpour, for her great technical, scientific and moral support at all times. My special thanks to Paul Marcogliese and Elizabeth Abdel-Messih for their support and assistance in editing the primary draft of my dissertation and their support at many occasions. I would like to extend my gratitude to all my fellow lab members from the past and the present who made this a memorable experience Dr. Mandana Amini, Dr. Mohammad Parsanejad, Dr. Grace Iyirhiaro, Dr. Zohreh Galehdar, Dr. En Huang, Dr. Emdadul Haque, Wassamon Boonying, Sarah Hewitt, and Katie Don-Carolis.

My special thanks to the Cellular and Molecular Medicine and Neuroscience administrative and technical staff Karen Littlejohn, Bea Robertson, Charlotte McCusker, Sylvie Deblois, Blanche Danielle, Marie La Fontant, Nancy MacDonald, Donna Hooper,

Lynda Jui, Kim Wong, and the rest of my family at the “Neurosciences” and “CMM” for their great assistance and moral support.

Also my special thanks to Devon Svoboda, Dr. Firouz Fallahi and Dr. Golnaz Sedigh, for their expert help

And last but not least, my deep and heartfelt thanks to my family that supported me with love and patience not only during my research life but also through every moment of my life. My dad who was my true inspiration in life with his everlasting passion for learning; my loving mum, my caring sisters Mary and Lily, my brothers Bahram and Moayed for their constant support and encouragement, and my little niece and nephew Parmida and Ryan that helped me survive the frustrations of science with their cheerful spirit.

TABLE OF CONTENTS

LIST OF FIGURES

LIST OF TABLES

LIST OF ABBREVIATIONS

° C	Celsius
14-3-3	14th fraction of bovine brain homogenate, found on positions 3.3
3D	Three dimensional
3'	3rd Carbon in Sugar-Ring of Nucleic Acid, region upstream of gene
5'	5th Carbon in Sugar-Ring of Nucleic Acid, region upstream of gene
A	Alanine
AA	Amino acid
Ab	Antibody
Acetyl-H3	Acetylated histone 3
ALS	Amyotrophic lateral sclerosis
ANOVA	Analysis of variance
APC/C	Anaphase-promoting complex/cyclosome
ApoE	Apolipoprotein E
Arc 2/3	Actin Related Proteins 2 and 3
ATG	Start of protein translation
ATP	Adenosine-5'-triphosphate
AV	Adenovirus
BDNF	Brain-derived neurotrophic factor
β-geo	Fusion of β-galactosidase and the Neomycin-resistance Gene
bHLH	Basic helix-loop-helix

BMP	Bone morphogenic protein
bp	Base pair
BSA	Bovine serum albumin
C	Cysteine
C57Bl/6	C57 black 6
CAM	Cell adhesion molecules
CAK	Cdk activating kinase
CCND3	Cyclin D3
CCNY	Cyclin Y
CCRK	Cell cycle related kinases
Cdc-2	Cell division cycle homolog 2
Cdc25	Cell division cycle 25
Cdc28	Cell division cycle 28
Cdk	Cyclin dependent kinase
CDKI	Cyclin dependant kinase inhibitor
CDKL	Cdk like kinase
cDNA	Complementary DNA
Chk	Checkpoint kinase
Cip/Kip	Cdk interacting protein/ kinase inhibitory protein
CMV	Cytomegalovirus
CNS	Central nervous system
CRD	Cysteine rich domain

CRIB	Cdc42/rac1 interactive binding domain
CRMP2	Collapsin response mediator protein2
C-terminal	Carboxy terminal
CTD	Carboxy terminal domain
Cyc	Cyclin
D	Aspartic acid
D228N	Dominant Negative Pftaire1 (mutation at aa 228 to asparagine)
DA	Dopamine
Da	Dalton
DCC	Deleted in Colorectal Cancer
DIV	Days *in-vitro*
Dlx	Distaless related homologue
D. melanogaster	*Drosophila melanogaster*
DN	Dominant-negative
DNA	Desoxyribonucleic acid
Dock	Dedicator of Cytokinesis
Dreadlocks	Dock/vertebrate nck
DTT	1,4-dithiothreitol
E	Glutamic acid
E	Embryonic day
E2F	E2 promoter binding factor
EDTA	Ethylene diamine tetra-acetic acid

Eip63E	Ecdysone-induced protein
ER	Endoplasmic reticulum
F	Phenyl-alanine
FITC	Fluorescein isothiocyanate
FGF	Fibroblast growth factor
G0	Gap 0 (quiescence)
G1	Gap 1 (interphase)
G2	Gap 2 (interphase)
GABA	Γ-Aminobutyric Acid
GDP	Guanosine diphosphate
GFP	Green fluorescent protein
GnRH	Gonadotropin-releasing hormone
GST	Glutathione S-transferase
GTP	Guanosine triphosphate
GTPyS	Guanosine gamma thiophosphate
h	Hour
HBSS	Hank's balanced salt solution
HCC	Human hepatocellular carcinoma
HDL	High density lipoprotein
HEK	Human embryonic kidney
HEPES	4-(2-hydroxyethyl)-1-piperazineethanesulfonic acid
Hh	Hedgehog

HIF1	Hypoxia-inducible factor 1
HPV	Human papilloma virus
hr	Hour
HRP	Horseradish peroxidase
I	Isoleucine
IgG	Immunoglobulin G
Ink4	Inhibitors of cdk4
IP	Immunoprecipitation
IRES	Internal ribosomal entry site
ISH	In situ hybridization
IZ	Intermediate zone
JNK	C-jun n-terminal kinase
K	Lysine
kb	Kilobase
kDa	Kilodalton
KO	Knockout gene
L	Litre
LDL	Low density lipoprotein
LGE	Lateral ganglionic eminence
LOX	Lipoxygenase
LRP	Low-density lipoprotein receptor related protein
M	Molar

M phase	Mitosis
MAG	Myelin associated glycoprotein
MAO	Monoamine oxidase
MAP	Microtubule associated protein
MAPK	Mitogen-activated protein kinase
MCLK	Myosin light chain kinases
mDia	Diaphanous related formin
MEF	Mouse embryonic fibroblast
MEG	Medial ganglionic eminence
mg	Milligram
min	Minute
MKK	Map Kinase
MLL	Myeloid/lymphoid or mixed lineage leukemia
MOI	Multiplicity of Infection
MPP+	1-methyl-4-phenylpyridinium
MPTP	1-methyl-4-phenyl-1,2,3,6-tetrahydropyridine
mRNA	Messenger RNA
Myc	Myelocytomatosis viral oncogene
mut	Mutant
MZ	Marginal zone
N	Asparagine
n	Nano

n	Number
NeuN	Neuronal nuclei
NF-κB	Nuclear factor kappa beta
NGF	Nerve growth factor
NHBE	Normal human bronchial cells
Nkx2.1	Nk2 homeobox 1
NLS	Nuclear localization sequence
NMDA	*N*-methyl-d-aspartic acid
NO-cGMP	Nitric oxide-cyclic guanosine3',5'-monophosphate signaling pathway
NP-40	Nonidet P-40
NPC	Niemann-Pick type C
N-terminal	Amino-terminal
OB	Olfactory bulb
O.C.T.	Optimal cutting temperature compound
OMgp	Oligodendrocyte myelin glycoprotein
P	Proline
p	Probability value
P19	Pluripotent embryonal carcinoma cell line
PAK	P21-Activating Kinase
PARP	Poly ADP-ribose polymerase
Pax6	Paired box gene 6

PBD	P21 Binding Domain
PBS	Phosphate buffered saline
PC12	Pheochromocytoma cell line
PCR	Polymerase chain reaction
Pctaire	Pctaire kinase
Pctaire (K194R)	Kinase-dead Pctaire
PD	Parkinson's disease
PFA	Paraformaldehyde
Pftaire	Pftaire kinase
Pfu	Plaque-forming unit
PGC1α	Peroxisome proliferator-activated receptor- coactivator
pH	Potential of Hydrogen
PH	Pleckstrin homology
PI3K	Phosphatidylinositol-3-kinase
PID	Pak inhibition domain
PINK1	Pten induced putative kinase 1
PNS	Peripheral nervous system
Poly A	Polyadenylation site
PP1c	Protein Phosphatase 1c
PPAR	Peroxisome proliferator-activated receptor
pRB	Protein retinoblastoma protein
PVDF	Polyvinylidene fluoride

PTEN	Phosphatase and Tensin Homolog
qRT-PCR	Quantitative real-time polymerase chain reaction
R	Arginine
Ras	Rat sarcoma
Rb	Retinoblastoma protein
RB1	Retinoblastoma gene
Rbbp2	Retinoblastoma binding protein 2
RBD	Rho binding domain
RCF	Relative centrifugal force
RNA	Ribonucleic acid
RNAi	Interference RNA
Robo	Roundabout protein
ROCK	Rho-kinase
ROS	Reactive oxygen species
RT	Room temperature
RTK	Receptor tyrosine kinases
S	Serine
S phase	DNA synthesis
SD	Standard deviation
SEM	Standard Error of The Mean
Sema 3	Class 3 semphorin
Sema 4	Class 3 semphorin

SGZ	Subgranular zone
Shh	Sonic hedgehog
shRNA	Short hairpin RNA
siRNA	Small interfering RNA
Stk9	Serine/threonine kinase 9
SV40	Simian virus 40
SVZ	Subventricular zone
SWI/SNF	Switching/sucrose non-fermenting
T	Threonine
TAGLN2	Transgelin2
TIGM	Texas A&M Institute for Genomic Medicine
TNF	Tumor necrosis factor
TRH	Thyrotropin-releasing hormone
Tris	Tris(hydroxymethyl)aminomethane
UAS	Upstream activated sequence
UNC5	Uncoordinated locomotion-5
VASP	Vasodilator stimulated phosphoprotein
VEGF	Vascular endothelial growth factor
VHL	Von hipple lindau
VNC	Ventral nerve cord
VZ	Ventricular zone
WASP	Wiskott -Aldrich -syndrome protein

Wnt	Wingless, integration
Y	Tyrosine
µ	Micro

CHAPTER 1

INTRODUCTION

1. INTRODUCTION

The human brain is an intricate structure containing a complex network of billions of neurons and even more non-neuronal support cells. The development of the brain and the whole nervous system is an intriguing event that relies upon a balance between proliferation and differentiation. The final morphology and function of the nervous system is determined by multiple events including cell division and arrest, differentiation, migration, axonal targeting, synaptogenesis and apoptosis. Tight regulation of these events is important not only in the developing brain but also in the adult brain to maintain plasticity. Dysregulation at any step would result in neurological disorders. Plasticity includes all mechanisms that involve learning, memory and repair so that the proper function of the central nervous system is restored after injury. For instance, after a stroke lesion, profound remodeling processes including neurogenesis, axogenesis, and angiogenesis occur in the penumbra area of an injured adult brain to maintain neuronal plasticity and restore proper function of the nervous system (Dancause 2006, Font, Arboix et al. 2010). Nonetheless, functional recovery after injury is limited in the adult brain. This limited ability may be due to intrinsic factors, loss of the capacity to express growth associated proteins in the neurons to regenerate rapidly, and lack of an environment that is supportive of axon outgrowth (Fawcett 1992, Stuermer, Bastmeyer et al. 1992).

Having an advanced understanding of the processes involved in the development of the nervous system is indispensable for developing new protocols in directing differentiation of stem cells to the neural lineage and other therapeutic protocols. Cyclin Dependent Kinases (Cdks), are a family of kinases with diverse functions in the CNS from

cell cycle regulation to differentiation (Malumbres, Harlow et al. 2009). This chapter will focus on the role of Cdks and their mechanism of action in the central nervous system (CNS).

1.1. Cyclin Dependent Kinases

Cyclin Dependent Kinases, are a family of serine/threonine(S/T) kinases. Currently, twenty-six genes have been distinguished to encode for twenty-one Cdks and five Cdk like (CDKL) kinases (Malumbres, Harlow et al. 2009) that have been associated to cell cycle progress, cell death and differentiation during development of the nervous system, and also in the adult brain (Tsai, Delalle et al. 1994, Park, Levine et al. 1997, Park, Morris et al. 1998, Park, Morris et al. 1998, Giovanni, Wirtz-Brugger et al. 1999, Giovanni, Keramaris et al. 2000, Park, Obeidat et al. 2000, Morris, Keramaris et al. 2001, Wang, Corbett et al. 2002, Rideout, Wang et al. 2003, Smith, Crocker et al. 2003, Weishaupt, Neusch et al. 2003, Rashidian, Iyirhiaro et al. 2005).

1.1.1. Functions of Cdks

Cyclin Dependent Kinases (Cdks) were initially detected in the yeast and include a growing family of cdc-2 related family of Serine/Threonine kinases (Hartwell 1974, Liu and Kipreos 2000). The nomenclature cyclin dependent kinase was adopted since the first identified Cdks, cdc28 and cdc2 (Cdk1), depended on binding to a cyclin regulatory partner to become functional (Kaldis 1999, Liu and Kipreos 2000).

Cdks were initially defined specifically for their role in cell cycle regulation and progression. For instance, Cdk1, Cdk2, Cdk3, Cdk4 and Cdk6 are Cdks with typical roles during the cell cycle (John, Mews et al. 2001). However, later on other Cdks were

identified that had more diverse roles that were independent of their role in cell cycle progress. For instance, Cdk7 (Kaldis 1999) and Cdk5 (Tang, Yeung et al. 1995) were identified for their role in transcription (Kaldis 1999) and differentiation (Tang, Yeung et al. 1995), respectively. Taking this into consideration, the Cdk family can be divided into mitotic and postmitotic Cdks.

1.1.1.1. The Mitotic Cdks

The mitotic Cdks or cell cycle Cdks (Cdk1, 2,3, 4 and 6) have prominent roles in the regulation of the cell cycle (Pines 1993, John, Mews et al. 2001), strictly depend upon a cyclin partner for their regulation, and are responsible for transition between the gap phases (G1 and G2) of cell replication by their kinase activity (John, Mews et al. 2001). Other functions of the mitotic Cdks include, transcription, RNA splicing (Cdk7, 8, 9 and 11) (Loyer, Trembley et al. 2005, Loyer, Trembley et al. 2008), and activation of other Cdks (Cdk7) (Kaldis 1999). In the CNS, mitotic Cdks have an important role in regulating the quantity and time of proliferation of the neural progenitors (Cunningham and Roussel 2001, Li and DiCicco-Bloom 2004, Dehay and Kennedy 2007). For instance, Cdk2-cyclin A2 is suggested to be required for renewal of neural stem cells. Its regulation by p27, an endogenous inhibitor of the Cip/Kid family inhibits neural differentiation and delays migration of the neuronal precursors (Richard-Parpaillon, Cosgrove et al. 2004, Itoh, Masuyama et al. 2007, Jablonska, Aguirre et al. 2007). Cdk4-cyclin D increases the basal progenitor cells and delays neurogenesis (Lange, Huttner et al. 2009).

1.1.1.2. Post-Mitotic Cdks

Post-mitotic Cdks are expressed abundantly in post-mitotic tissue. The role and function of most post-mitotic Cdk family members remains to be fully elucidated. They are distinct from mitotic Cdks since their activation does not specifically depend on binding to a cyclin partner. This group of cdc-2 related kinases include PSSALRE(Cdk5), PFTAIREs (Cdk14/15), PCTAIRE 1-3, KKIALRE, PITALRE, PISSLRE, and PITSLRE which descend from the same evolutionary ancestor (Lazzaro, Albert et al. 1997, Liu and Kipreos 2000). Comparison of the amino acid sequences of Cdk family members reveals high similarity between murine Pftaire-1 with Cdk5 and Pctaire, respectively, at 50-52% and 61% amino acid-identity (Besset, Rhee et al. 1998).

The known functions of Cdks could be summarized as follows, (1) Cdk1-4 and Cdk6, are classified as classical Cdks and regulate cell cycle progression (John, Mews et al. 2001, Malumbres, Harlow et al. 2009); (2) Cdk5, is considered an atypical Cdk and is involved in transcription, differentiation, cell death, migration, and plasticity (Tang, Yeung et al. 1995, Dhavan and Tsai 2001, Malumbres, Harlow et al. 2009, Futatsugi, Utreras et al. 2012) ; (3) Cdk7 is a Cdk activating kinase (CAK) that partners with cyclin H and Mat1 and triggers downstream effectors by phosphorylating Cdks on their T-loop (Kaldis 1999, Malumbres, Harlow et al. 2009); (4) Cdk 8-13 and Cdk 19 (or 11) are transcriptional Cdks that control RNA polymerase II by phosphorylating its carboxy terminal domain (CTD) (Loyer, Trembley et al. 2005, Loyer, Trembley et al. 2008, Malumbres, Harlow et al. 2009) ; (5) Cdk 14-15 (PFTAIRE 1-2) (Lazzaro, Albert et al. 1997, Besset, Rhee et al. 1998, Malumbres, Harlow et al. 2009) and Cdk 16-18 (PCTAIRE1-3) (Okuda, Cleveland et al. 1992, Besset, Rhee et al. 1999, Malumbres, Harlow et al. 2009).

Although, typical Cdks contain a cyclin binding element in their primary structure; some Cdks are activated by binding to non-cyclin partners where association with cyclins is not essentially required for their activity (Meyerson, Enders et al. 1992, Okuda, Cleveland et al. 1992, Brambilla and Draetta 1994, Grana, De Luca et al. 1994, Dhavan and Tsai 2001), (6) Other Cdks have sequences similar to the original Cdks including cyclin activating kinases-CAK (Cdk20-21), as well as, cdc2 like kinases including Cdc2L1 (KKIALRE) (Yen, Kenessey et al. 1995), Cdc2L2 (KKIAMRE) (Sassa, Gomi et al. 2000), and Cdc2L6 and cell cycle related kinases (CCRK)(Malumbres, Harlow et al. 2009, Malumbres 2014). (Table1-1)(Lim and Kaldis 2013)

Table 1-1-Summarized biological properties and functions of Cdks

Cdk	Partner	Type	Function	Reference
Cdk1	Cyc A, Cyc B, Cyc E	Mitotic	Cell Cycle Progression (S, M Phase)	(John, Mews et al. 2001)
Cdk2	Cyc A, Cyc E	Mitotic	Cell Cycle Progression (G1,S,G2 Phase)	(John, Mews et al. 2001)
Cdk3	Cyc C	Mitotic	Cell Cycle Progression (G0,G1 Phase), RNA PII Transcription	(John, Mews et al. 2001)
Cdk4	Cyc D	Mitotic	Cell Cycle Progression (G1 Phase), RB/E2F Transcription	(John, Mews et al. 2001, Lange, Huttner et al. 2009)
Cdk5	Cyc E, p35, p39	Postmitotic	Differentiation, Cell Death, Cell Cycle Regulation (G1 Phase)	(Tang, Yeung et al. 1995, Dhavan and Tsai 2001, Futatsugi, Utreras et al. 2012)
Cdk6	Cyc D	Mitotic	Cell Cycle Progression (G1 Phase), RB/E2F Transcription	(John, Mews et al. 2001)
Cdk7	Cyc H	Mitotic	RNA PII Transcription-CAK	(Kaldis 1999)
Cdk8	Cyc C	Mitotic	Transcription, RNA PII transcription	(Loyer, Trembley et al. 2005, Loyer, Trembley et al. 2008)
Cdk9	Cyc T, Cyc K	Mitotic	Transcription, RB/E2F transcription	(Loyer, Trembley et al. 2005 , Yu, Zhao et al. 2010)

Cdk10	Cyc M	Mitotic	Ets 2 Transcription	(Loyer, Trembley et al. 2005)
Cdk11	Cyc L	Mitotic	Transcription, RNA splicing	(Loyer, Trembley et al. 2005, Loyer, Trembley et al. 2008)
Cdk12	Cyc K,Cyc L	Mitotic	Transcription, RNA PII Transcription	(Loyer, Trembley et al. 2005, Loyer, Trembley et al. 2008)
Cdk13	Cyc K,Cyc L	Mitotic	Transcription, RNA PII Transcription	(Loyer, Trembley et al. 2005, Loyer, Trembley et al. 2008)
Cdk14	Cyc Y, others	Postmitotic	Wnt/β-catenin pathway regulation	(Davidson, Shen et al. 2009, Pollack, Xiao et al. 2015)
Cdk15	unkown	Postmitotic	unknown	
Cdk16	Cyc Y	Postmitotic	spermatogenesis	(Liu, Cheng et al. 2006, Mikolcevic, Sigl et al. 2012)
Cdk17	unknown	Postmitotic	unknown	
Cdk18	unknown	Postmitotic	unknown	
Cdk19	Cyc C	Mitotic	Transcription	(Loyer, Trembley et al. 2005, Galbraith, Donner et al. 2010)
Cdk20	unknown	Mitotic	unknown	
Cdk21	unknown	Mitotic	unknown	

Although differentiation and cell cycle regulation would seem to be completely independent processes there should be a cross-talk between differentiation and cell cycle arrest, as the former normally follows the later (Hindley and Philpott 2012). Previous studies signify the importance of Cdks in the tight regulation of proliferation in the nervous system (Galderisi, Jori et al. 2003, Malumbres 2011). For instance, improper activation of Cdks in a population of neurons that are terminally differentiated results in apoptosis and neuronal death; both, *in vitro* (Freeman, Estus et al. 1994, Park, Farinelli et al. 1996, Park, Levine et al. 1997, Park, Morris et al. 1997, Park, Morris et al. 1998, Park, Morris et al. 1998, Giovanni, Wirtz-Brugger et al. 1999, Padmanabhan, Park et al. 1999, Giovanni, Keramaris et al. 2000, O'Hare, Hou et al. 2000, Park, Obeidat et al. 2000, Morris, Keramaris et al. 2001, Konishi, Lehtinen et al. 2002, Konishi and Bonni 2003, Rideout, Wang et al. 2003, Sumrejkanchanakij, Tamamori-Adachi et al. 2003, Kruman, Wersto et al. 2004, Liu, Biswas et al. 2004, Otsuka, Tanaka et al. 2004), and *in vivo* (Nagy, Esiri et al. 1997, Vincent, Jicha et al. 1997, Coelho and Leevers 2000, Osuga, Osuga et al. 2000, Wang, Corbett et al. 2002, Nguyen, Boudreau et al. 2003, Rashidian, Iyirhiaro et al. 2005).

1.1.2. The Structure of Cdks

Cdks are all relatively small ranging from 34 to 60 kDa and rarely up to 110 kDa on SDS-PAGE gel. Cdk proteins possess a similar structure, in which catalytic domains are conserved. These domains include: (1) “VALK” motif in subdomain II of the kinase domain that facilitates positioning of ATP in the active site, (2) “PCTAIRE/PSTAIRE” motif, a characteristic of Cdk proteins, located in subdomain III of the kinase domain that is mainly responsible for the Cdk/cyclin interaction, (3) ”HRD” motif in subdomain VIb that

catalyzes the transfer of γ-phosphate, (4) ”DFG” motif in subdomain VII that coordinates the position of Mg^{2+} ions and ATP in the ATP-binding domain (Morgan 1995, Morgan 2007). (Figure 1-1)

Cdks have a preference for phosphorylating substrates that possess serine and threonine residues at the consensus sequence of S/TPXK/H/R. (S/T* is the phosphorylated serine or threonine, P is proline in the +1 position, X is any amino acid, K is lysine, and R is arginine). (Dhavan and Tsai 2001, Morgan 2007). In their tertiary structure, Cdks form a bilobal fold that includes a large carboxy-terminal lobe mainly consisting of alpha helices, and a small amino-terminal lobe containing 5 anti-parallel beta sheets, as well as, 1 alpha helix (Pines 1993, Shu, Lv et al. 2007). The carboxy-terminal lobe, includes a flexible threonine-loop (T-loop) that is located adjacent to the active site of Cdks and requires phosphorylation of T161 to acquire maximum activity and bind to substrates (Shu, Lv et al. 2007, Odajima, Wills et al. 2011). Also, adjacent to the T-loop in the carboxy terminal there is a L12 helix located approximately at residues 147-151; which contributes to the structural modification and reorientation of amino acids in the ATP binding site to promote full kinase activity (Pines 1993, Shu, Lv et al. 2007). The conformation of the L12 helix changes from an alpha helix to a beta helix upon binding of cyclin to the Cdk (Pines 1993, Shu, Lv et al. 2007). A conserved glycine-rich loop (G-loop) related to the kinases with the consensus sequence (GxGxxGA) is part of the ATP binding region and facilitates the alignment of ATP’s γ-phosphate (Pines 1993, Shu, Lv et al. 2007). The amino-terminal loop is responsible for the binding of Cdk to a cyclin partner and consists of a glycine rich domain and the highly conserved “PSTAIRE” motif (Pines 1993,

Shu, Lv et al. 2007). The amino-terminal lobe also contains inhibitory threonine (T14) 14 and tyrosine 15 (Y15) phosphorylation sites (Morgan 1995). The amino and carboxy - lobes are connected to each other through a domain that acts like a flexible hinge (Morgan 1995). This region is termed the catalytic cleft or the ATP binding domain. The G-loop forms the peak of the cleft that blocks the catalytic region when the Cdk is inactivated (Morgan 1995). The catalytic domain is composed of aspartate and lysine residues that bind to the substrate and ATP, as well. These residues include aspartate at position (D127), lysine at position (K129) and asparagine at position (N132), as well as lysine (K33) and aspartate (D145) (De Bondt, Rosenblatt et al. 1993, Morgan 1995) (Figure 1-1).

a)

```
CDK2            ----------------------------------MENFQKVEKIGEGTYGV
CDK5            ----------------------------------MQKYEKLEKIGEGTYGT
CDK14           ------TSSTGKESPKVRRHSSPSSPTSPKFGKADSYEKLEKLGEGSYAT
CDK15           ------------EEDLR-QGFQW-RKSLPFGAASSYLNLEKLGEGSYAT
CDK16           YLEKLTLNSPIFDKPLSR-RLRRVSLSEIGFGKLETYIKLDKLGEGTYAT

CDK2            VYKARNKLTGEVVALKKIRXDTETEGVPSTAIREISLLKELNHPNIVKLL
CDK5            VFKAKNRETHEIVALKRVRLDDDDEGVPSSALREICLLKELKHKNIVRLH
CDK14           VYKGKSKVNGKLVALKVIRLQE-EEGTPFTAIREASLLKGLKHANIVLLH
CDK15           VYKGISRINGQLVALKVISMNA-EEGVPFTAIREASLLKGLKHANIVLLH
CDK16           VYKGKSKLTDNLVALKEIRLEH-EEGAPCTAIREVSLLKDLKHANIVTLH

CDK2            DVIHTENKLYLVFEFLHQDLKKFMDASALTGIPLPLIKSYLFQLLQGLAF
CDK5            DVLHSDKKLTLVFEFCDQDLKKYFDSCN-GDLDPEIVKSFLFQLLKGLGF
CDK14           DIIHTKETLTLVFEYVHTDLCQYMDKHP-GGLHPDNVKLFLFQLLRGLSY
CDK15           DIIHTKETLTFVFEYMHTDLAQYMSQHP-GGLHPHNVRLFMFQLLRGLAY
CDK16           DIIHTEKSLTLVFEYLDKDLKQYLDDCG-NIINMHNVKLFLFQLLRGLAY

CDK2            CHSHRVLHRDLKPQNLLINTEGAIKLADFGLARAFGVPVRTYTHEVVTLW
CDK5            CHSRNVLHRDLKPQNPLINRNGELKLADFGLARAFGIPVRCYSAEVVTLW
CDK14           IHQRYILHRDLKPQNLLISDTGELKLADFGLARAKSVPSHTYSNEVVTLW
CDK15           IHHQHVLHRDLKPQNLLISHLGELKLADFGLARAKSIPSQTYSSEVVTLW
CDK16           CHRQKVLHRDLKPQNLLINERGELKLADFGLARAKSIPTKTYSNEVVTLW

CDK2            YRAPEILLGCKYYSTAVDIWSLGCIFAEMVT-RRALFPGD-SEIDQLFRI
CDK5            YRPPDVLFGAKLYSTSIDMWSAGCIFAELANAGRPLFPGN-DVDDQLKRI
CDK14           YRPPDVLLGSTEYSTCLDMWGVGCIFVEMIQ-GVAAFPGMKDIQDQLERI
CDK15           YRPPDALLGATEYSSELDIWGAGCIFIEMFQ-GQPLFPGVSNILEQLEKI
CDK16           YRPPDILLGSTDYSTQIDMWGVGCIFYEMAT-GRPLFPGS-TVEEQLHFI

CDK2            FRTLGTPDEVVWPGVTSMPDYKPS-FPKW-ARQDFSKVVPPLD--EDGRS
CDK5            FRLLGTPTEEQWPSMTKLPDYKPY--PMYPATTSLVNVVPKLN--ATGRD
CDK14           FLVLGTPNEDTWPGVHSLPHFKPERFTLY-SSKNLRQAWNKLSYVNHAED
CDK15           WEVLGVPTEDTWPGVSKLPNYNPEWFPLP-TPRSLHVVWNRLGRVPEAED
CDK16           FRILGTPTEETWPGILSNEEFKTYNYPKY-RAEALLSHAPRLD--SDGAD

CDK2            LLSQMLHYDPNKRISAKAALAHPFFQDVTKPVPH----------------
CDK5            LLQNLLKCNPVQRISAEEALQHPYFSDFCP--------------------
CDK14           LASKLLQCSPKNRLSAQAALSHEYFSDLPPRLWELTDMSSIFTVPNVRLQ
CDK15           LASQMLKGFPRDRVSAQEALVHDYFSALPSQLYQLPDEESLFTVSGVRLK
CDK16           LLTKLLQFEGRNRISAEDAMKHPFFLSLGERIHKLPDTTSIFALKEIQLQ
```

b)

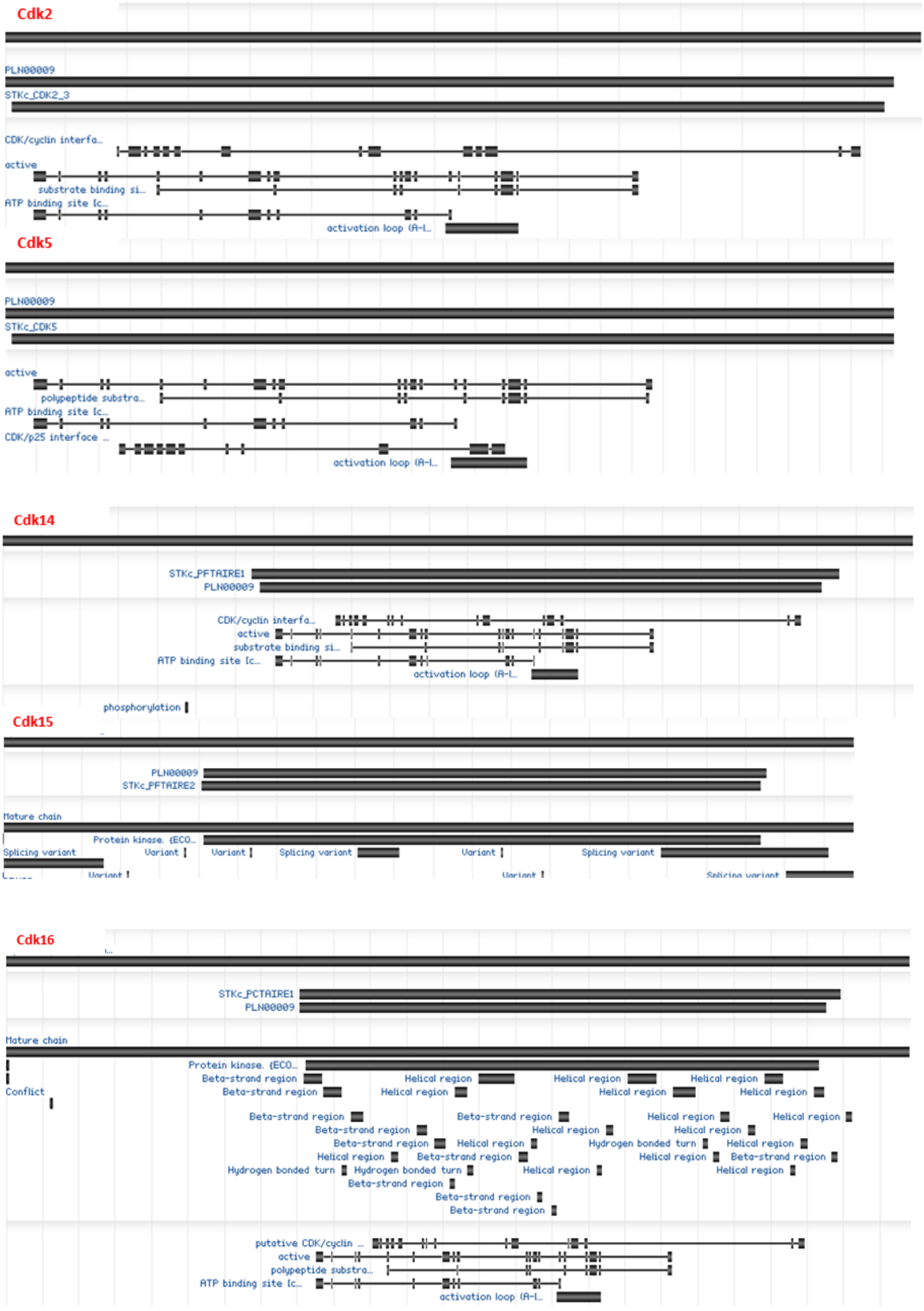
Cdk2
PLN00009
STKc_CDK2_3
CDK/cyclin interfa...
active
substrate binding si...
ATP binding site (c...
activation loop (A-l...
Cdk5
PLN00009
STKc_CDK5
active
polypeptide substra...
ATP binding site (c...
CDK/p25 interface ...
activation loop (A-l...
Cdk14
STKc_PFTAIRE1
PLN00009
CDK/cyclin interfa...
active
substrate binding si...
ATP binding site (c...
activation loop (A-l...
phosphorylation
Cdk15
PLN00009
STKc_PFTAIRE2
Mature chain
Protein kinase. {ECO...
Splicing variant
Variant
Variant
Splicing variant
Variant
Splicing variant
Cdk16
STKc_PCTAIRE1
PLN00009
Mature chain
Protein kinase. {ECO...
Beta-strand region
Helical region
Conflict
Hydrogen bonded turn
putative CDK/cyclin ...
active
polypeptide substra...
ATP binding site (c...
activation loop (A-l...

c)


Cdk2
296 aa
Cdk5
292 aa
Cdk14
451 aa
Cdk15
435 aa
Cdk16
496 aa
S/T kinase
Coiled -coil domain

d)

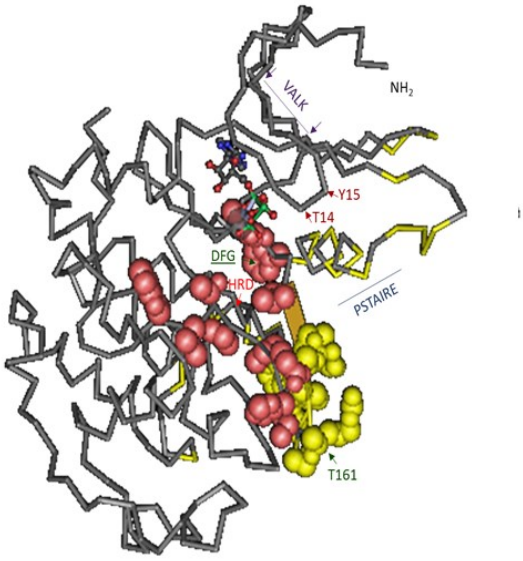
NH2
VALK
Y15
T14
DFG
HRD
PSTAIRE
T161

e)

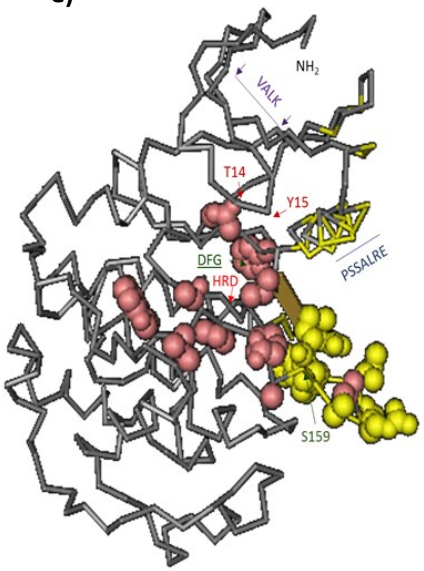
NH2
VALK
T14
Y15
DFG
HRD
PSSALRE
S159

Figure 1-1 Structure of Representative Cdks

a) Alignment of sequences for human CDK2 (Accession: CAA43985.1), CDK5 (Accession: CAG33322.1), CDK14 (Accession: NP001274064.1), CDK15 (Accession: Q96Q40.2), and CDK16 (Accession: Q00536.1). Activation loop (yellow highlight), T14 and Y15 - inhibitory sites (red), S/T- activation site (green), conserved Cdk PSTAIRE motif (blue), VLAK, HRD, DFG domains (respectively purple, red, green) (see text for further description). **b)** Graphical summary of conserved domains of CDK2, CDK5, CDK14, CDK15, and CDK16 respectively with alignment footprint indicating region similarity. **c)** S/T kinases highlighted in red in CDK2, CDK5, CDK14, CDK15, CDK16 (Modified from Table 1 (Malumbres and Barbacid 2005). 3D structure and relative position of conserved domains **d)** CDK2 and **e)** CDK5 using PubMed, Cn3D tool (Wang, Addess et al. 2007, Marchler-Bauer, Zheng et al. 2013).

1.1.3. Modes of Regulation of Cdks

Cdks are commonly regulated through different mechanisms which include: (1) binding to their cyclin partners, (2) phosphorylation of Cdk and/or cylin-Cdk complex at their conserved serine/threonine residue by CAK (Cdk activating kinase), (3) inhibitory phosphorylation of Cdks, (4) CDK inhibitory subunits also known as cyclin-dependent kinase inhibitor protein (CDKIs, CKIs or CDIs) that result in cell cycle arrest during the G_1 phase of cell cycle progression (Morgan 1995, Morgan 2007).

1.1.3.1. Mechanism of Action of Cdks

1.1.3.1.1. Activating Patterns

- **Cyclin Dependent Activation**

Cdks are generally inactive in their monomer form. In their inactive form the T-loop (activation loop) located at the carboxy-terminal blocks the cleft thus the amino acids in the side chain of the Cdk are not accessible for binding of ATP (Morgan 1995, Morgan 2007). Upon binding of cyclin with Cdk at the conserved (PSTAIRE) motif, conformational changes occur in the tertiary structure of the Cdk. The L12 alpha helix at the carboxy-terminal changes to a beta sheet. The T-loop that is adjacent to it has a flexible conformation thus the T-loop rearranges in a manner that it moves outwards from the cleft entrance. Later, the PSTAIRE helix at the amino-terminal moves inwards. This conformational change flattens of the carboxy-terminal lobe; which in turn results in an optimal position for ATP to bind. ATP binds within the cleft in a manner that the phosphates are positioned outwards and accessible for the transfer of phosphate. The

Cdk substrate containing the S/TPXK/H/R sequence binds to the entrance of the cleft and mainly positions towards the carboxy-terminal. (Russo, Jeffrey et al. 1996, Russo, Jeffrey et al. 1996, Kim and Zhao 2005, Morgan 2007). Nevertheless, not all of the classic Cdks become fully active upon binding to their cyclin partner and require binding to other non-cyclin partners. For instance, the Cdk4/cyclin D complex is not fully active and it requires binding to other non-cyclin partners including $p34^{SEI1}$ or Sertad1 for full activity (Sugimoto, Nakamura et al. 1999, Li and DiCicco-Bloom 2004).

Cyclin dependent kinases are regulated by phosphorylation of different residues, at different phases. The phosphorylation of Cdks may occur at residues that enhance the activity of Cdks. For instance, the Cdk-activating kinase (CAK) phosphorylates some Cdks (Morgan 1995) at threonine (T160) and increases the activity of Cdk7/cyclin H complex in combination with MAT1 or Cdk2/cyclin A complex (Gu, Rosenblatt et al. 1992) by stabilizing their binding (Kaldis 1999). Phosphorylation of the conserved tyrosine and threonine residues in the ATP binding region of Cdk results in electrostatic repulsion between the phosphate linked to the kinase and those of ATP (Russo, Jeffrey et al. 1996, Russo, Jeffrey et al. 1996, Kim and Zhao 2005, Morgan 2007).

- **Autophosphorylation**

Despite the similarities in the conformation of the Cdks, Cdk9 has a different phosphorylation pattern in comparison to classical Cdks. The interface area of Cdk9 with its partner cyclin T is 40% less than classical Cdks, such as Cdk2 with its partner cyclin A. Due to this reduced interface area, the threonine (T186) in the T-loop is only able to interact with two arginine residues R148 and R172 on the side chains of Cdk9 and this results in autophosphorylation of Cdk9

(Baumli, Lolli et al. 2008, Echalier, Endicott et al. 2010). Cdk14 has also been reported to have autophosphorylation activity (Lazzaro, Albert et al. 1997) which suggests their independence from Cdk7 kinase activity for becoming activated.

- **Cyclin Independent Phosphorylation**

Some of Cdks classified as atypical Cdks can become activated independent of cyclin. Of pertinence to this matter is Cdk5 that does not bind to a cyclin partner to become activated. Although Cdk5 has the ability to associate with cyclin partners such as cyclin D and E, interaction with a cyclin partner in not essentially required for its activation; (Patrick, Zhou et al. 1998, Dhavan and Tsai 2001, Bartova, Otyepka et al. 2005). Instead, it partners with non-cyclin proteins p35 and p39 which induces transient activation of Cdk5 (Tsai, Delalle et al. 1994, Patrick, Zhou et al. 1998, Dhavan and Tsai 2001, Malumbres 2014). Regulation of Cdk5 will be further discussed in the Cdk5 section.

1.1.3.1.2. Inhibitory Phosphorylation Patterns

- **Glycine-Rich Loop Inhibitory Phosphorylation**

Phosphorylation can also regulate the function of Cdks by inhibiting their kinase activity. This regulatory inhibition is important to control cell arrest or in response to DNA damage. In the classic Cdks, Wee1 and Myt1 kinase inactivate the Cdk, through phosphorylation of the threonine 14 (T14) and tyrosine 15 (Y15) residues that are located on the G-loop. The mechanism of inhibition is different for these two residues. In the case of threonine (T14) residue, an intermediate compound forms with a shift in the position of its Mg^{2+}. This shift causes misalignment of the ATP in the loop. This misalignment in

turn keeps the serine residue of the peptide and ATP apart; thus inhibition occurs. In the case of the tyrosine (Y15) residue, the side chains of ATP will take on a "swing out" position, therefore the binding of substrate is prohibited (Morgan 2007, Zhang, Tan et al. 2007, Echalier, Endicott et al. 2010).

- **Cdk Inhibitory Proteins (CDKIs/CKIs/CDIs)**

CDKIs are responsible for cell cycle arrest at G1. They are mainly classified into two groups based on their structures and their Cdk targets: The INK4 family and the Cip/Kip family (Denicourt and Dowdy 2004).

The INK4 family consists of multiple ankyrin repeats and regulates the activity of Cdk4/Cdk6 by inhibiting the formation of Cdk4 or Cdk6 - cyclin complex. This group includes $p16^{INK4a}$, $p15^{INK4b}$, $p18^{INK4c}$, and $p19^{INK4d}$ (Sherr and Roberts 1999, Denicourt and Dowdy 2004).

The Cip/Kip proteins have a broad spectrum and regulate the activity of most Cdks and cyclins A and E. The Cip/Kip proteins bind to the Cdk and cyclin through the motifs of their amino-terminals. This group includes $p21^{Cip1}$, $p27^{Kip1}$, and $p57^{Kip2}$. They act as inhibitors for cyclins A and E but have an activating effect on cyclin D (Sherr and Roberts 1999, Denicourt and Dowdy 2004).

Cdk4/6 and cyclin D form a complex together and phosphorylate the tumor suppressor protein retinoblastoma protein (pRB) in G1 phase of the cell cycle, as a result the pRb becomes inactivated (Sherr and Roberts 1999, Munger and Howley 2002, Bartkova, Gron et al. 2003, Denicourt and Dowdy 2004, Das, Hashimoto et al. 2005, Korenjak and Brehm 2005). Thus, the inhibition on cell cycle progression is removed and

the cell transits from G1 to S phase. On the other hand, cyclin D sequesters the Cip/Kip proteins. Subsequently, Cdk2 becomes active and forms a complex with cyclin E. Cdk2-cyclin E, then, phosphorylates Rb and p27. Phosphorylation of p27 triggers its degradation through the proteasomal pathway. Phosphorylation of Rb in late G1 disrupts the association of Rb with E2F and disrupts its repression; since the repression is removed the transition throughout S-G2 and M phases is facilitated (Sherr and Roberts 1999, Munger and Howley 2002, Stevaux and Dyson 2002, Denicourt and Dowdy 2004).

1.1.4. Cdk5

Cdk5 has been best characterized among the post-mitotic Cdks. Cdk5 was detected in a screen for cdc2 family members in 1992 (Hellmich, Pant et al. 1992, Lew, Winkfein et al. 1992, Meyerson, Enders et al. 1992). Initially, it was named neuronal-like2 kinase. Cdk5 was classified as a cdc2-like kinase since it was detected in terminally differentiated neurons rather than being active in the cell cycle (Hellmich, Pant et al. 1992).

Cdk5 regulates various functions at the cellular level including morphology, communication, motility (Dhavan and Tsai 2001); with a main role in the development of the CNS, regulating neuronal migration, survival (Ohshima, Ward et al. 1996, Dhavan and Tsai 2001, Ohshima, Hirasawa et al. 2007), dopamine signaling (Bibb, Snyder et al. 1999), axonal transport, and synaptic transmission (Rosales, Nodwell et al. 2000, Dhavan and Tsai 2001, Smith and Tsai 2002, Cheung and Ip 2004, Cheung, Fu et al. 2006, Zhang, Tan et al. 2007), synaptic plasticity, learning and memory (Hawasli and Bibb 2007). Cdk5 dysregulation can trigger neurons to re-enter the cell cycle after arrest and result in

neuronal death (Weishaupt, Neusch et al. 2003, Lopes, Oliveira et al. 2009), both *in vitro* (Patrick, Zukerberg et al. 1999, Coelho and Leevers 2000, Kusakawa, Saito et al. 2000, O'Hare, Kushwaha et al. 2005), and *in vivo.* Thus, Cdk5 dysregulation can be one of the factors resulting in a variety of neurodegenerative diseases, including Alzheimer's disease (Cruz and Tsai 2004), Parkinson's disease (Smith, Crocker et al. 2003), stroke (Wang, Liu et al. 2003, Rashidian, Iyirhiaro et al. 2005), amyotrophic lateral sclerosis (ALS) (Nguyen and Julien 2003), and Niemann-Pick type C (NPC) (Bu, Li et al. 2002).

Expression of the dominant negative form (DN-Cdk5) inhibits axonal outgrowth in cultures of primary cortical neurons (Nikolic, Chou et al. 1998). Deficiency of Cdk5 is lethal in mice and results in embryonic lethality at E18, due, at least, to defective neuronal migration and differentiation of the cortex (Ohshima, Ward et al. 1996, Gilmore, Ohshima et al. 1998). Cell cycle regulation is disrupted in Cdk5 knockout embryos but expression of wild type Cdk5 is able to rescue this deficit (Cicero and Herrup 2005). The migration and lamination of cortical interneurons depends on p35/Cdk5 proper activity. In newborn mice that have p35 deficiency and as a result lack p35/Cdk5 kinase activity, disrupted migration of cortical interneurons results in the formation of new interneurons in the cortex and reverses its typical "inward-outward" lamination (Nikolic, Dudek et al. 1996, Chae, Kwon et al. 1997, Ohshima, Hirasawa et al. 2007, Sonja Rakić 2009). Furthermore, in Cdk5 mutants growth of axons projecting to the thalamus (Gilmore, Ohshima et al. 1998) and development of dendrites (Ohshima, Hirasawa et al. 2007) is disrupted. Also, in Cdk5 deficient mice the morphology of pyramidal neurons is disrupted mainly due to abnormal dendrite structure. Hence, neurons adopt a multipolar morphology rather than

the normal bipolar structure (Ohshima, Hirasawa et al. 2007). Despite the severe effect of Cdk5 deficiency during embryonic development and its lethality, the deficiency of Cdk5 does not completely prevent axons from projecting; (Gilmore, Ohshima et al. 1998, Connell-Crowley, Vo et al. 2007); suggesting that other post-mitotic Cdks may play a role in axogenesis.

1.1.4.1. Regulation of Cdk5 function

Like other Cdks, Cdk5 does not show catalytic activity in its monomeric form and it has been known to bind to non-cyclin partners such as p35 (Tsai, Delalle et al. 1994) or its isoform p39 (Tang, Yeung et al. 1995, Kwon and Tsai 2000, Ko, Humbert et al. 2001) and their cleavage products p25 and p29, respectively (Patrick, Zhou et al. 1998, Dhavan and Tsai 2001). Despite their differences with cyclins in their sequence identity, p35 and p39 resemble cyclins in their ternary structure (Lew, Huang et al. 1994, Tsai, Delalle et al. 1994, Tang, Yeung et al. 1995, Tarricone, Dhavan et al. 2001, Lin, Wang et al. 2008, Jiang, Gao et al. 2009). In spite of the ubiquitous expression of Cdk5, binding to its non-cyclin neural-specific partner, p35 (Tsai, Delalle et al. 1994) or its isoform p39 (Tang, Yeung et al. 1995, Kwon and Tsai 2000, Ko, Humbert et al. 2001) activates Cdk5, predominantly, in the nervous system (Johansson, Lilja et al. 2005, Hawasli and Bibb 2007, Ohshima, Hirasawa et al. 2007).

Cdk5 normally associates with the membrane due to the myristoylation signal on p35 or p39 (Tsai, Delalle et al. 1994, Tang, Yeung et al. 1995, Patrick, Zhou et al. 1998, Tarricone, Dhavan et al. 2001, Asada, Yamamoto et al. 2008, Lin, Wang et al. 2008). p35 directed activation of Cdk5 results in transient activation due to proteasomal

degradation. The deficiency of either Cdk5, or p35 and p39 in mice results in phenotypes that are similar, which confirms the dependence of Cdk5 activity on p35 and p39 (Patrick, Zhou et al. 1998, Patrick, Zukerberg et al. 1999). Furthermore, under pathological conditions, calpain-mediated cleavage of p35 can result in formation and binding of p25 to Cdk5. Since, p25 lacks the myristoylation signal, it results in prolonged activation of Cdk5 in the cytosol (Patrick, Zhou et al. 1998, Dhavan and Tsai 2001) therefore it interacts with a different subset of substrates that induce neuronal death (Dhavan and Tsai 2001) through phosphorylation of MEF2 (Smith, Mount et al. 2006) and Prx2 (Qu, Rashidian et al. 2007) in Parkinson's disease and Stroke (Rashidian, Rousseaux et al. 2009), as well. At early stages of Alzheimer's disease Cdk5 kinase activity is increased. Cdk5/p25 complex hyperphosphorylates Tau and enhances the formation of neurofibrillary tangles (NFTs) which is a hallmark of Alzheimer's and Parkinson's disease (Ishiguro, Takamatsu et al. 1992, Pei, Grundke-Iqbal et al. 1998) . Inhibition of Cdk5 by an inhibitor such as roscovitine inhibits cell cycle progress to death (Lopes, Oliveira et al. 2009). Also, Cdk5 inhibition in models of stroke and MPTP a model of Parkinson's disease, *in-vivo*, results in neuroprotection (Smith, Mount et al. 2006, Qu, Rashidian et al. 2007, Rashidian, Rousseaux et al. 2009).

Despite not always depending on a cyclin partner for activation, association of Cdk5 with cyclins D and cyclin E has been observed (Miyajima, Nornes et al. 1995, Patrick, Zhou et al. 1998, Dhavan and Tsai 2001). Cyclin E has been attributed a role in cell cycle regulation in the CNS and has been detected in conjunction with Cdk5 in adult brains; however, in embryonic brain only Cdk1 and Cdk2 are associated with it (Odajima, Wills et

al. 2011, Lim and Kaldis 2013, Kawauchi 2014). In its inactive state Cdk5 forms a ternary complex with $p27^{kip1}$ in association with cyclin E that is also enriched in adult brain tissue. It is possible that contrary to most cyclins that activate their Cdk partner (John, Mews et al. 2001, Loyer, Trembley et al. 2005, Lange, Huttner et al. 2009), cyclin E inactivates Cdk5 by inhibiting its association with its activating p35/p39 partner (Dhavan and Tsai 2001, John, Mews et al. 2001, Lim and Kaldis 2013, Kawauchi 2014). One possibility is that Cyclin E decreases synapse number and functionality by inactivating Cdk5; thus, contributing to decreased synaptic plasticity in neurological conditions such as Alzheimer's disease (Dhavan and Tsai 2001, Cruz and Tsai 2004). Park2, a Parkinson's disease associated gene with neuroprotective effect exerts its function through targeting cyclin E function and its ubiquitination (Lucking, Durr et al. 2000, Staropoli, McDermott et al. 2003).

1.1.4.2. Cdk5 Structure and Mechanism of Action

Cdk5 contains the conserved PSTAIRE motif of Cdks with alanine (A) and leucine (L) replacing threonine (T) and isoleucine (I); respectively, forming the PSAALRE motif (Zhang, Tan et al. 2007). Similar to other Cdks, Cdk5 has a preference for the consensus sequence (S/T) PX (K/H/R), the proline in +1 position, as well as, basic residues at +3 position (Zhang, Tan et al. 2007). As a result of this change, phosphorylation of the T-loop is not essentially required for Cdk5 activation.

In studies on the mechanism of function of Cdk5, a variety of substrates are involved including cytoskeletal elements (Xie, Samuels et al. 2006), signaling molecules and regulatory proteins. In this section the signaling cues that have a role in Cdk5 regulation will be described briefly. A more detailed explanation will be included later on

in this chapter. Cdk5 has an important role in neurite formation. It inhibits the stimulatory effect of nerve growth factor (NGF) on neurite outgrowth in PC12 cells (Harada, Morooka et al. 2001). Cdk5 regulates both dendrite outgrowth and axonal outgrowth and guidance. In hippocampal neurons, dendrite outgrowth is regulated by phosphorylating Trk B at serine (S478) which in turn activates brain-derived neurotrophic factor (BDNF) (Cheung, Chin et al. 2007). Cdk5 dependent axon outgrowth is regulated via phosphorylation of MAP1b (Del Rio, Gonzalez-Billault et al. 2004) which in turn enhances axon outgrowth and regulates its guidance via netrin1 and ephrinA5, respectively. The kinase activity of Cdk5 is suppressed by s-nitrosylation at cysteine (C83) (Zhang, Yu et al. 2010, Ye, Fu et al. 2012). The loss of kinase activity, inhibits ephrinA5 induced growth cone collapse in retinal ganglion neurons (Cheng, Sasaki et al. 2003). On the other hand, increase in Cdk5 kinase activity through its phosphorylation on tyrosine (Y15) induces epherin4 dendritic spine retraction (Fu, Chen et al. 2007). Contrary to classical cell cycle Cdks, phosphorylation of the tyrosine 15 (Y15) residue in Cdk5 has an activating effect on Cdk5. In classical Cdks, phosphorylation of Tyrosine 15 (Y15) occurs through Wee1 and this causes an inhibitory effect. However, in Cdk5 this phosphorylation occurs through c-abl and Cables (an adaptor protein for Cables), this causes a different conformational rearrangement upon phosphorylation. It is suggested that in this case, the phosphorylated side chains fail to take on a “swing out” position thus binding of the substrate is not inhibited (Zhang, Tan et al. 2007). Rho GTPases are essential factors for the growth cone machinery and are activated as Cdk5 targets. Cdk5 interacts with Rac1 via p35 in a GTP dependent manner (Nikolic, Chou et al. 1998, Rashid, Banerjee et al. 2001). Cdk5/p35, Rac and Pak1 kinase

co-localize in the periphery of the neurites and regulate its outgrowth. Cdk5/p35 kinase complex induces Pak1 hyper-phosphorylation. This downregulates the kinase activity of Pak1, which results in actin re-organization and increases neurite outgrowth (Nikolic, Chou et al. 1998). Cdk5 phosphorylates p27Kip1 in neurons, and this stabilization is critical to keep the proper level of F-actins in the leading processes during migration (Nikolic, Chou et al. 1998, Dhavan and Tsai 2001, Kawauchi, Chihama et al. 2006). Cdk5 increases the activity of Rac and RhoA through phosphorylation of downstream proteins such as kalirin7 (Xin, Wang et al. 2008) and ephexin1 (Fu, Chen et al. 2007?). Cdk5 also activates calpain dependent protein degradation through phosphorylation of RasGRF1 (Kesavapany, Amin et al. 2004, Kesavapany, Pareek et al. 2006).

1.1.5. Other Post-Mitotic Cdks

The amino acid sequence of post-mitotic Cdk's is highly identical. Pftaire-1, Pctaire, show 50-52% and 61% similarity to Cdk5, respectively (Besset, Rhee et al. 1998). Cdk5 has a central role in the in the development of the nervous system and cell death. Similar to Cdk5, Pctaire and Pftaire1 are all highly expressed in the brain (Liu and Kipreos 2000). However, Pctaire1 (Liu, Cheng et al. 2006, Mikolcevic, Sigl et al. 2012) and Pftaire1 (Besset, Rhee et al. 1998), as well as, mitotic Cdk4 has also been detected in non-dividing sertoli cells (Rhee and Wolgemuth 1995). Pctaire is absent in *Drosophila*. Initially, Sauer et al. (Sauer, Weigmann et al. 1996) reported detection of *Drosophila* Pctaire-1 but further investigation by Besset et al. (Besset, Rhee et al. 1998) showed that the detected gene had higher homology with murine Pftaire-1 rather than Pctaire, 75% versus 58%, respectively. Furthermore, comparison of the conserved kinase domain of murine Pftaire-

1 with *Drosophila* reveals higher similarity in their amino acid sequences as compared to other Cdk family members (Besset, Rhee et al. 1998).

1.1.5.1. PCTAIRE

PCTAIRE is another post mitotic Cdk protein, which is highly conserved through evolution (Cole 2009). It is conserved among most of clade holozoa but absent in *Drosophila*. PCTAIRE includes three homologues, Pctaire 1-3 (Cdk 16-18) that are distinct in their c-terminal but more conserved in the N-terminal and central domain (Cole 2009). Pctaire1-3 proteins are expressed at high levels in the testis (Hirose, Kawabuchi et al. 2000, Mikolcevic, Sigl et al. 2012) and the brain (Okuda, Cleveland et al. 1992, Hirose, Kawabuchi et al. 2000, Fu, Cheng et al. 2011, Mikolcevic, Sigl et al. 2012). Pctaire1 has been detected at high levels in growth cones of newly developing neurons and also in dendrites (Fu, Cheng et al. 2011). However, in post-mitotic tissue Pctaire1 is not detected in the axons. It is only present in cell bodies and in the proximal region of neurites which indicate it might not be directly involved in axon outgrowth and only have a role in the transfer of cytoskeletal elements to the neurites (Besset, Rhee et al. 1999). Similarly, Pctaire2 has been detected in neurons and neurites, as well (Hirose, Kawabuchi et al. 2000). The activity of Pctaire1-3 has a negative effect on neurite outgrowth. When the activity of Pctaire 1-3 is abolished, there is an increase in neurite outgrowth; for instance, overexpression of the kinase-dead form of Pctaire (K194R) results in increased neurite outgrowth (Cole 2009). Phosphorylation of Pctaire at serine 153 by PKA decreases the kinase activity of Pctaire1 which increases neurite outgrowth. On the contrary, phosphorylation of Pctaire1 at serine (S95) by Cdk5, in neurons, increases it kinase activity

(Cole 2009). Mutations in the position serine (S95) of Pctaire1 interfere with regular dendrite development (Cole 2009). Cdk5 could be a potential regulator of Pctaire1 activity since the activity of Pctaire1 changes are in line with Cdk5 activity (Fu, Cheng et al. 2011).

1.1.5.2. PFTAIRE: (Pro, Phe, Thr, Ala, Ile, Arg, Glu)

Pftaire1 was, initially, identified in a screen for neuronal cdc2-like kinases by Lazzaro et al in 1997 (Lazzaro, Albert et al. 1997). Later in 1998, Besset et al (Besset, Rhee et al. 1998), reported the detection of the same protein and named it Pftaire1. Nevertheless, the latter group reported a small difference in the cDNA sequence; in which, three single amino acids are varied, as well as, 46 amino acids in the amino-terminal. They reported transcripts that are different from the ones reported by Lazzaro et al (Lazzaro, Albert et al. 1997). The first group had reported one single transcript with the size of 5 kb, expressed almost exclusively in the nervous system; whereas, Besset et al (Besset, Rhee et al. 1998) reported two transcripts at the sizes of 4.9 and 5.5 kb which showed significant expression in the nervous system, testis, and embryo but a ubiquitous and lower expression in the other tissues (Lazzaro, Albert et al. 1997, Besset, Rhee et al. 1998).

At present, the consensus is that PFTAIRE is highly conserved among different species from yeast to mammals (Liu and Kipreos 2000). Nonetheless, the fly and worm genome code for only one complex gene known as Eip63-Ecdysone-induced protein 63E that is 70% identical to the mouse homolog Pftaire1 (Liu and Kipreos 2000, Stowers, Garza et al. 2000) and Pftaire-interacting factor 2-pa (PubMed Gene ID: 9953769). In mammals, PFTAIRE includes 2 separate genes: (1) Pftaire1/ PFTK1/CDK14 (PubMed Gene ID: 5218).

The human PFTAIRE1 and mouse Pftaire1 are located at (7q21-q22) and (5 A1; 2.61 cM) (Lazzaro and Julien 1997), respectively, and show considerably high homology of 95%(Lazzaro, Albert et al. 1997, Yang and Chen 2001). (2) Pftaire2/PFTK2/Als2cr7/CDK15 (PubMed Gene ID: 65061) is recognized in GenBank database; although, to date no research is reported on Pftaire2. The human PFTAIRE2 and mouse Pftaire2 are located at (2q33.2) and (1 C1.3; 1), respectively. There are 14 known transcripts for the mouse Pftaire1 gene (ENSMUSG00000028926). Only six of the isoforms result in a coded protein. Two of the transcripts are putative isoforms and another two are incomplete in the 3' coding region. Thus, only two of the sequences are bona fide (1) Cdk14-002 (ENSMUST00000030763) results in a transcript with a total of 15 exons of which the last exon only contains 3'UTR and no coding sequence. It produces a transcript of 4,851 bps that translates into a protein product with 469 residues; and (2) Cdk14-09 (ENSMUST00000115452) a transcript with a total of 14 exons, of which 13 are coding and results in a 4,866 bps mRNA and a protein product with 451 residues.

Similar to Cdk5, Pftaire1 transcript is concentrated in the brain (Lazzaro, Albert et al. 1997, Besset, Rhee et al. 1998). The localization of Pftaire1 in the brain is exclusive to the marginal layer that consists of differentiated cells. No Pftaire1 was detected in deep layers or layer1, which is mainly composed of axons and dendrites (Lazzaro, Albert et al. 1997, Besset, Rhee et al. 1998). This is different from the expression pattern of cdc2 that is detected in proliferative tissue and only inner layers of the brain (Lazzaro, Albert et al. 1997, Besset, Rhee et al. 1998) and Cdk5 that concentrated in the axons (Tsai, Takahashi et al. 1993). In comparison, Pftaire1 is expressed in neuronal cell bodies and close

proximities (Lazzaro, Albert et al. 1997). The expression of Pftaire1 in comparison to the more ubiquitous expression of cdc-2 (Lazzaro, Albert et al. 1997, Besset, Rhee et al. 1998) suggests a more eminent role for Pftaire1 in the development of the nervous system. Interestingly, Cdk14 is expressed highly in testicular tissue as well (Shu, Lv et al. 2007), (Besset, Rhee et al. 1998). However, there is no evidence with regards to Pftaire1's role in the nervous system.

In the adult mouse, Pftaire1 mRNA is located both in neuroglia and neurons (Lazzaro, Albert et al. 1997, Besset, Rhee et al. 1998) in different regions of the brain such as cortex, hippocampus, thalamus, cerebellum, and also in the spine. Pftaire1 is localized to neuronal cell bodies but not neurite extensions. Pftaire1 mRNA is also strongly expressed in the testis and lung; yet, it does not translate to a protein (Lazzaro, Albert et al. 1997). There is also low expression of Pftaire1 in the heart but no expression is detected in spleen and thymus which supports the notion that Pftaire1 is primarily and mainly expressed in the nervous system in adult mice (Lazzaro, Albert et al. 1997). During mouse development, Pftaire1 mRNA is expressed at very low levels at embryonic days 12.5, 15.5, and even 18.5 but there is a rise right after birth, at P 10.5, it reaches a maximum that is similar to its level in adult mice. This is different from the expression pattern of Cdk5 that has a continuous increase from embryonic day 12, followed by a significant increase at birth (Lazzaro, Albert et al. 1997). The expression pattern of human PFTAIRE1 differs from mouse Pftaire1 to some extent. Similar to mouse Pftaire1, the expression level of human PFTAIRE1 is relatively high in the brain and testis; however, in human it is also highly expressed in the pancreas, kidney, heart and ovary. It is also

detected at lower levels in other tissues such as placenta, lung, liver, skeletal muscle, prostate, small intestine, colon, and peripheral blood leukocyte, but is minimal in spleen and thymus (Yang and Chen 2001, Shu, Lv et al. 2007). The expression pattern of human PFTAIRE2 resembles that of PFTAIRE1 and is expressed highly in the brain and testis and also in prostate, kidney, and skin (Yang and Chen 2001), PubMed Cdk15 Gene ID: 65061).

To determine potential interacting partners of Pftaire1, different methods have been applied. In a 2D-PAGE mass spectrometric analysis ß-actin and Transgelin2 (TAGLN2), a tumor suppressor protein, heat shock protein 70, aldehyde dehydrogenase, and 14-3-3 proteins were identified as Pftaire1 substrates (Leung, Ching et al. 2011). In a yeast two-hybrid screen for proteins interacting with human PFTAIRE1, seven proteins were detected including (1) two non-cyclin proteins such as KIAA0202 (septin8) (Yang, Gao et al. 2002) and 14-3-3 isoforms β,ε,η,τ (Gao, Jiang et al. 2006), (2) cyclin proteins such as cyclin Y (CCNY) (Jiang, Gao et al. 2009) and cyclin D3 (CCND3) (Shu, Lv et al. 2007), (3) p^{21Cip1} (Shu, Lv et al. 2007), (4) PLZF protein (Gao, Jiang et al. 2006).

ß-actin and TAGLN2 (Transgelin2), an actin binding protein, reveal the most intensified signal in a 2D-PAGE mass spectrophotometric analysis. The biological relevance of this interaction was examined *in vitro*. In HEP3B and Human Hepatocellular Carcinoma (HCC) cells upon PFTAIRE1 suppression, the total level of ß-actin remains unchanged; however, the levels of TAGLN2 increases (Leung, Ching et al. 2011). TAGLN2 exhibits actin binding ability in its unphosphorylated state. Increase in PFTAIRE1 levels increases phosphorylation of serine on TAGLN2, upon phosphorylation by PFTAIRE1, at serine 83 and serine 163 residues, the interaction of TAGLN2 and actin is disrupted (Fu,

Subramanian et al. 2000, Leung, Ching et al. 2011) and the inhibitory effect of TAGLN2 on actin dynamics is removed, actin gets depolymerized and HCC become motile (Pang, Bai et al. 2007, Leung, Ching et al. 2011).

Caldesmone, 82 kDa, is another substrate for PFTAIRE1 detected in human hepatocellular carcinoma (HCC) cells. Caldesmone and human PFTAIRE1, physically interact with each other *in vitro,* in Hep3B cells and the level of caldesmone phosphorylation is affected by the kinase activity of hPFTAIRE1. Inhibition of PFTAIRE1 decreases the levels of threonine and tyrosine phosphorylation and disrupts the caldesmone-actin interaction. Phosphorylation of caldesmone enhances the actin binding ability of caldesmone and determines its localization to membrane ruffles and stress fibers (Leung, Ching et al. 2011).

At the subcellular level, ectopically expressed human PFTAIRE1 was localized to the cytosol of Hela cells (Yang and Chen 2001), cytosol and nucleus of immature sertoli cells, primary NHBE (normal human bronchial cells) (Pollack, Xiao et al. 2015), and also in the plasma membrane of HEK293 cells through its interaction with cyclin Y (Jiang, Gao et al. 2009) *in vitro*. Also, in cytosol, nucleus of the cell body of the motor neurons of the spinal cord of adult C3H mice, (Lazzaro, Albert et al. 1997), and mouse testis (Jiang, Gao et al. 2009) *in vivo*. Although, Pftaire1 has two nuclear localization sequences (NLS) at residues 66 to 72 (PEDKKVR) and 113 to 119 (PKVRRHS) (Yang and Chen 2001) it is predominantly localized in the cytosol (Lazzaro, Albert et al. 1997, Yang and Chen 2001) and in the plasma membrane (Jiang, Gao et al. 2009). Generally, proteins that contain a NLS sequence shuttle between the nucleus and the cytoplasm through binding to an

importin α/β complex. It is suggested that KIAA0202 or human septin8 which is a cytosolic protein, interacts with PFTAIRE1 and localizes PFTAIRE1 to the cytoplasm (Yang, Gao et al. 2002). We speculate that the presence of the highly phosphorylated 58-60 kDa protein that was detected among the substrates of Pftaire1 in adult mouse brains lysates (Lazzaro, Albert et al. 1997) and is similar to the size of Septin 8 (Yang, Gao et al. 2002) could be a possible explanation to this. In an assessment for the kinase activity of Pftaire1 in a mouse brain lysate sample, a subset of three endogenous phosphoproteins were suggested to interact with Pftaire1. Of the three substrates, the 58-60 kDa protein was highly phosphorylated and considered specific to Pftaire1; whereas, the phosphoproteins in 200-205 kDa range are believed to be unspecific and detected in association with Cdk5 (Lazzaro, Albert et al. 1997). Similar to all Cdk proteins, Pftaire1 contains three conserved regulatory phosphorylation residues that include serine (S99), tyrosine (Y100), and serine (S243). The equivalent of these residues in other Cdk family members are threonine (T14), tyrosine (Y15), and threonine (T161) (Lazzaro, Albert et al. 1997).

As mentioned above, the 14-3-3 proteins also interact with PFTAIRE1. Four of the 14-3-3 (β, ε,, η,, τ) isoforms are detected in association with PFTAIRE1 (Gao, Jiang et al. 2006). These isoforms are mainly cytoplasmic and abundant in the CNS. It is suggested that similar to KIAA0202, 14-3-3 proteins have the ability to localize PFTAIRE1 to the cytoplasm (Muslin and Xing 2000, Voigt, Liebich et al. 2000, Gao, Jiang et al. 2006). Two consensus binding motifs (1) RSxpSxP, and (2) $Rx_{1-2}Sx_{2-3}S$ (Fu, Subramanian et al. 2000) are detected in 14-3-3 proteins. It is suggested that the consensus motif RHSSPSS (117 to 120) of 14-3-3 overlaps with the second NLS of the PFTAIRE1 protein and interacts with it

through phosphorylation of 14-3-3 on the serine (S199) residue (Muslin and Xing 2000, Voigt, Liebich et al. 2000).

Retinoblastoma protein (Rb) is a substrate for hPFTAIRE1 *in vitro* in many different cell lines including human embryonic kidney cells (HEK-293) (Shu, Lv et al. 2007, Jiang, Gao et al. 2009), SH-SY5Y, and SK-N-SH human neuroblastoma cells (Shu, Lv et al. 2007). The phosphorylation of retinoblastoma protein (Rb) is activated by the association of human PFTAIRE1 with CCND3 (cyclin D3) and inhibited by interaction with p^{21Cip1} (Shu, Lv et al. 2007). This might suggest that the activity of PFTAIRE1 is regulated by (CCND3) cyclin D3 (Shu, Lv et al. 2007) and CCNY (cyclin Y) (Jiang, Gao et al. 2009) and inhibited by the p21 (Shu, Lv et al. 2007). Since, phosphorylation of Rb results in inhibition of its activity (Shu, Lv et al. 2007); this indicates a role in cell cycle regulation for Pftaire1. Furthermore, overexpression of human PFTAIRE enhanced cell cycle progression in human osteosarcoma U2OS cell line through transition from G1 to S (Shu, Lv et al. 2007). Although phosphorylation of Rb occurs only in the cytoplasm, interaction of PFTAIRE1 with the membrane-associated cyclin Y *in vitro,* in HEK cells, recruits PFTAIRE1 to the plasma membrane through its N-terminal myristoylation (Jiang, Gao et al. 2009). This interaction is facilitated through phosphorylation of CCNY on the serine residues by PFTAIRE1 kinase activity (Jiang, Gao et al. 2009). The interaction of PFTAIRE1 with Cyclin Y phosphorylates low density lipoprotein receptor related protein 6 (LRP6) in *vivo*, which also requires Cdc25 activity (Davidson, Shen et al. 2009). LRP6, on the other hand, modulates the Wnt signaling pathway that is involved in neurogenesis (Ille, Atanasoski et al. 2007, Davidson, Shen et al. 2009). Wnt signaling in combination with CCND regulate

spermatogenesis during mouse development (Golestaneh, Beauchamp et al. 2009, Kerr, Young et al. 2014) and in postmitotic cells, as well (Pollack, Xiao et al. 2015). Downregulation of Pftaire1 disturbs Wnt signaling and β-catenin levels (Pollack, Xiao et al. 2015) and result in cell-cycle arrest (Shu, Lv et al. 2007).

PLZF protein interacts with other proteins including hPFTAIRE1 and PCTAIRE1, through (1) a proline-rich domain (Pro domain) in the linker region, (2) the 9 Krüppel zinc finger domains in its carboxy terminal, and (3) the conserved POZ/BTB domain at its amino terminal (Li, English et al. 1997). PLZF proteins are highly conserved (Cook, Gould et al. 1995) and contain a consensus sequence for cdc2 phosphorylation (Cook, Gould et al. 1995) that contains serine and threonine residues (Ball, Melnick et al. 1999). PLZF negatively regulates cell cycle progress by inhibiting cyclin A (Yeyati, Shaknovich et al. 1999). Ectopic expression of PLZF inhibits growth and results in apoptosis by arrest of cell cycle progression at G1 (Shaknovich, Yeyati et al. 1998). Taking this into consideration, we hypothesize that Pftaire1 might also regulate cell cycle through PLZF and cyclin A. Nevertheless, no biological function for this interaction has been examined yet.

Thyrotropin-Releasing Hormone (TRH) is a neuropeptide expressed in hypothalamus and other regions of the brain. TRH regulates the expression of Pftaire1 in mice cerebellum through NO-cGMP pathway. TRH acts on anterior pituitary cells that secrete thyroid stimulating Hormone (TSH). This suggests an active role for Pftaire1 in postnatal tissue, as a downstream target of TRH, perhaps playing a role in differentiation rather than cell proliferation (Hashida, Yamada et al. 2002).

In *Drosophila,* the Pftaire homologue Eip63E is crucial for development and its absence is embryonically lethal (Stowers, Garza et al. 2000). Expression of its conserved kinase domain can reverse this lethality (Stowers, Garza et al. 2000). Also, data from our lab described later in this chapter, suggests the importance of Eip63E in axogenesis in *Drosophila* (Rodríguez González and S. 2011). Our study on Pftaire1 is novel, as it focuses on the neuronal function and targets of Pftaire1. To date, no reports exist on the role and mechanism of action of Pftaire1 in the nervous system.

1.2. Neuronal Development and Migration

Cdks regulate different aspects of neurogenesis from proliferation and differentiation to apoptosis and cell death. One of the pathways that are renown for regulating progenitors and cell lineage fate is Wnt signaling which is important in insects and vertebrates , (Zechner, Fujita et al. 2003, Ille, Atanasoski et al. 2007, Grigoryan, Wend et al. 2008). As mentioned earlier Pftaire1 mediates Wnt signaling (Davidson, Shen et al. 2009). Neurogenesis is defined as the process by which neurons are developed from neural stem cells and progenitor cells. In addition to neurons, glial cells originate from the stem cells. Neurogenesis is highly active both perinatally and later during adulthood. During development, initially proliferative divisions occur in stem cells, they increase in number and produce progenitor cells. Upon neurogenesis, the progenitor cells undergo an asymmetrical division and different types of progenitor cells are produced (Kawauchi, Shikanai et al. 2013). This division is followed by symmetric, differentiating divisions of progenitor cells that produce immature neurons (neuroblasts), which still do not possess processes. Commonly, the new neurons are formed in locations, different

from the position that they finally acquire. These immature neurons have the ability to migrate to new positions and reside at their final destination in the mature brain (Rakic 1990). The migration of these neuroblasts is controlled by “leading processes” that are structures at the tip of the migrating neurons. The leading processes sense the environmental cues and direct the neuroblasts to their new locations (Tabata and Nakajima 2003). Migration occurs in two stages, locomotion and somal translocation (Nadarajah, Brunstrom et al. 2001). During locomotion (1) neuroblasts extend a leading process, (2) nucleokinesis occurs and the prenucleous compartment (centrosome and Golgi apparatus) moves into the leading process along with the nucleus. Remodeling of the leading process facilitates its movement. Once the migrating neuron reaches its destination, it undergoes somal translocation and once again remodeling and nucleokinesis occur in the leading process of the neuroblast, then the extended leading tip shrinks (Rakic 1990, Miyata, Kawaguchi et al. 2001, Nadarajah and Parnavelas 2002, Tabata and Nakajima 2003, Miyata and Ogawa 2007, Marin, Valiente et al. 2010).

Migration mainly occurs through two main modes: radial migration and tangential migration (Umeshima and Kengaku 2013). Radial migration occurs mainly during early development of the brain, as opposed to tangential migration that occurs during final stages of development. The ventricular zone contains the soma of radial glial cells and gives rise to the neurons that form the cortical plate. The neuroblasts migrate perpendicular to the ventricular zone and all the way through the developing cortex to reach their final destination. A single extended process named the leading process aids the neuroblasts in locating their path during migration as they follow the long processes

of the radial glial cells (Rakic 1990, Campbell and Gotz 2002, Marin, Valiente et al. 2010). Membrane bound cell adhesion molecules such as astrotactin, neuregulin, and integrins aid the interaction of the neurons with the radial glial cells during migration (Anton, Marchionni et al. 1997, Anton, Kreidberg et al. 1999, Adams, Tomoda et al. 2002, Marin, Valiente et al. 2010). Other regulators of the migration process include environmental cues such as slits, netrins, semaphorins, and reelin (Marin, Valiente et al. 2010). Inhibition of Cdk5 activity results in lengthening of radial fibers into the white matter of cerebellum and disrupted radial migration of neurons (Umeshima and Kengaku 2013).

In tangential migration of neuroblasts, the leading process forms two branches with a steady angle. They possess a dynamic structure and depending on the direction of migration, only one branch remains active at each migratory cycle and the other branch retracts (Ward, Jiang et al. 2005, Martini, Valiente et al. 2009). The migration path of tangential cells is parallel to the ventricular surface and orthogonal to the radial glia palisade (Polleux, Whitford et al. 2002, Yokota, Gashghaei et al. 2007, Martini, Valiente et al. 2009). Rather than interacting with radial glial cells (Corbin, Nery et al. 2001, Marin and Rubenstein 2001) , the tangentially migrating neurons interact with a variety of cells either homotypic or heterotypic in nature as they pass through different environments (Marin, Valiente et al. 2010). Homotypic interactions usually occur when neurons migrate through unpermissive environments. In this case, a cluster of neuroblasts migrate together and utilize neighbouring cells as their substrate (Marin, Valiente et al. 2010). An example of homotypic interaction is the formation of the interneurons of the olfactory bulb which migrate through the lateral ventricles of the telencephalon (Wichterle, Garcia-

Verdugo et al. 1997, Marin, Valiente et al. 2010). Contrary to the movement of neuroblasts in clusters, inhibitory homotypic interactions may occur. This assists the neuroblasts to move to low density areas. An example of this movement is the dispersion of Cajal-Retzius cells (which originate from the cortical hem) over the surface of the cerebral cortex, during early corticogenesis (Borrell and Marin 2006). Tangential migration may also be heterotypic in which case the direction of migration is determined by the environmental cues that are present in the surface of other cells including axons. For instance, the neurons that produce Gonadotropin-releasing hormone (GnRH) pass through the forebrain following vomeronasal axons (Wray 2002, Marin, Valiente et al. 2010). The guidance cues that regulate tangential migration of neuroblasts are mainly the same cues that regulate axon guidance, which include slits, netrins, semaphorins, as well as, growth factors including BDNF, NT4, and HGF or morphogenetic proteins (Polleux, Whitford et al. 2002, Pozas and Ibanez 2005, Marin, Valiente et al. 2010). Once the neuroblasts reach their final destination, the new neurons become polarized and take up various morphological changes dendrites and axons form and extend toward long-distance targets (Kawauchi and Hoshino 2008).

1.3. Axon Outgrowth and Cellular Signaling

In addition to the aforementioned functions the timing of Pftaire1 expression could be an important factor in regulating axon outgrowth and fasciculation (Sanchez-Soriano and Prokop 2005). Precise connectivity within the nervous system is important for proper development and plasticity in the adult nervous system. Our knowledge about the patterns of axogenesis in the nervous system began over a century ago, when Golgi

and Cajal stained brain sections using the Golgi method (Cajal 1906, Mazzarello 1999). This resulted in Cajal's remarkable discovery of the axonal structure and the growth cone and our cellular and molecular understanding of the biology of neurons and their outgrowth has continued to develop especially during the recent decades. The polarized structure of neurons plays an important role in relaying information in the nervous system. The growth cone is the motile terminal of the neurite that leads the axon through the complex environment of the tissues. The structure of a growth cone includes actin microfilaments and cytoskeletal microtubules in the peripheral and central region, respectively (Nikolic 2002, Huber, Kolodkin et al. 2003). The peripheral actin microfilaments are connected to the central microtubular region by the actin arc. Upon axonal outgrowth cohered rearrangements occur in the actin superstructure of a growth cone (Condeelis 1993, Rodriguez, Schaefer et al. 2003).

This guidance of an axon is modulated through multiple events at the growth cone and axogenesis occurs in a few stages, as defined in neuronal cultures *in vitro*. At the time of plating, unpolarized sphere-shaped neurons are cultured. The neuron then becomes polarized and axogenesis initiates: (1) During initiation, the actin structure of the immature postmitotic neurons goes through rearrangement and cellular protrusions appear in the form of sheet like structures and lamellipodia and filopodia microspikes; respectively (Nikolic 2002); (2) Lamellipodia and filopodia give rise to immature neurites; (3) In the next step elongation occurs, the neuron becomes asymmetrical, one particular neurite grows rapidly and forms the axon while the remaining become retracted and form dendrites. The attribute to become an axon or dendrite is inherited from the progenitor

cells that give rise to these neurites *in vivo* (Polleux and Snider 2010). One possible mechanism in determining the fate of an axon is that the axon sends out inhibitory signals to dendrites and excitatory signals to itself; (4) While the axon continues to grow rapidly, arborization of the dendrites occurs; (5) Neurons become differentiated, axons and dendrites become specialized, the dendritic spines and synapses form (Dotti, Sullivan et al. 1988, da Silva and Dotti 2002).

Polarity in the neuron and axon outgrowth is modulated by signaling cues. During axon outgrowth, extracellular guidance cues bind to the receptors at the periphery of the growth cone and link to downstream signaling cascades (Nikolic 2002, Jaffe and Hall 2005). The signaling pathways may become activated or deactivated (Huber, Kolodkin et al. 2003) depending upon repulsive and attractive cues. While excitatory cues enhance axon outgrowth, the Inhibitory cues result in growth cone collapse and arrest of axon growth (Nikolic 2002, Lowery and Van Vactor 2009). The direction and rate of axon growth also depends upon these signaling cues (Dickson 2002, Huber, Kolodkin et al. 2003) which are present in a gradient. The growth cone integrates different guidance cues, modifies the actin superstructure and alters the morphology of the growth cone. Thus, axons are either directed to their targets or retracted from them (Nikolic 2002).

Signaling cues including intrinsic factors, Rho GTPase regulatory molecules, developmental morphogens, mature neurotrophins, receptors, neurotransmitters, extracellular matrix and adhesion molecules and cell adhesion molecules (CAMs), regulate the formation of neurites (Nikolic 2002, Jaffe and Hall 2005).

Intrinsic factors that appear to be important and regulate cytoskeletal dynamics and axon growth include proteins such as transcription factors, GAP-43, cell adhesion molecules, cytoskeletal proteins, the Rho-family of GTPases (Hall and Lalli 2010), and Cdk5 (Ye, Fu et al. 2012). We hypothesize that Pftaire1 plays a role in the growth cone machinery, as well.

Developmental morphogenes are signaling cues that are present in a gradient and exert different responses with regards to axon outgrowth depending on their absolute concentration. They alter the transcription of their target cells. (Gurdon and Bourillot 2001, Schnorrer and Dickson 2004). Among the morphogenes are sonic hedgehog (Shh) (Charron, Stein et al. 2003), Wnt (Yoshikawa, McKinnon et al. 2003) and bone morphogenic protein (BMP)s (Butler and Dodd 2003).

Neurotrophins play an important role in neurite outgrowth and differentiation. Neurotrophin precursors split and form mature neurotrophins (Sun, Lim et al. 2012) and usually enhance axon outgrowth through Trk receptors. The Ras linked tyrosine kinase receptor Trk is a regulator for the Rho family of GTPases (Nusser, Gosmanova et al. 2002, Huang and Reichardt 2003). Nerve Growth Factor NGF regulates neurite formation by activating Rac1 and Cdc42 (Aoki, Nakamura et al. 2004) and deactivating RhoA (Nusser, Gosmanova et al. 2002, Huang and Reichardt 2003). The Brain derived neurotrophic factor (BDNF) enhances neurite outgrowth in an inhibitory environment (Huang and Reichardt 2003, Williams, Williams et al. 2005). There are also various downstream molecules that trigger intercellular signaling. For instance, Pak interacts with LIM kinases that are serine/threonine kinases that phosphorylate and deactivate the destabilizing

protein cofilin (Maekawa, Ishizaki et al. 1999). This induces the formation of stress fibers and enhances the outgrowth of axon (Yang, Higuchi et al. 1998, Amano, Tanabe et al. 2001, Bernard 2007). Pak can inactivate myosin light chain kinases (MCLK) and as a result control retrograde formation of F-actin (Arber, Barbayannis et al. 1998, Yang, Higuchi et al. 1998). Also, the Src-family of tyrosine kinases including Src, Fyn, Lck regulate axon and dendrite outgrowth through their effector the small GTPase TC10, a Cdc42-GAP, and the CAP-associated complex (Liu, Nakazawa et al. 2006). A number of actin-binding proteins like cofilin and profilin inhibit neurite formation. Profilin II is mainly expressed in the brain (Witke, Podtelejnikov et al. 1998, Da Silva, Medina et al. 2003). In addition, profilin-binding proteins of the vasodilator stimulated phosphoprotein (Ena/VASP) or EVH family regulate actin polymerization (Bear, Svitkina et al. 2002, Huber, Kolodkin et al. 2003). Other effector proteins include Wiskott -Aldrich -syndrome protein (WASP) and neuronal N-WASP that are scaffolding proteins that are regulated by Cdc42 and regulate branching (Rohatgi, Ma et al. 1999). SCAR/WAVE proteins that are regulated by Rac and subsequently regulate the actin related proteins 2 and 3 (Arp2/3 complex) which increase actin nucleation (Machesky, Mullins et al. 1999, Rohatgi, Ma et al. 1999, Higgs and Pollard 2001). Filamin (Revenu, Athman et al. 2004) is another effector that regulates cytoskeleton remodeling and neurite outgrowth (Stuermer, Bastmeyer et al. 1992, Hall 1998, Burridge and Wennerberg 2004, Langhorst, Jaeger et al. 2008, Hall and Lalli 2010, Stuermer 2010). Inhibitory molecules such as those with the inhibitory effect of glia (Schwab and Thoenen 1985, Carbonetto, Evans et al. 1987, Savio and Schwab 1989), oligodendrocyte myelin glycoprotein (OMgp) (Wang, Corbett et al. 2002), myelin

associated glycoprotein (MAG) (McKerracher, David et al. 1994, Mukhopadhyay, Doherty et al. 1994), Nogo (Caroni and Schwab 1988) are responsible for the collapse of the growth cone and retraction of the axon (Negishi and Katoh 2002, Fujita Y 2014). cAMP mediated inhibition of NogoA through the proteosomal pathway induces axon outgrowth (Sepe, Lignitto et al. 2014). *In vivo* studies show that in NogoA mutant mice axon outgrowth is enhanced. However, deficiency of MAG and OMgp does not affect neuron outgrowth *in vivo* (Filbin 2003, Cafferty, Duffy et al. 2010).

There are four key families of proteins that act as signaling molecules in axonal guidance and include semaphorins, ephrins, slits and netrins (Huber, Kolodkin et al. 2003). The receptors are usually located at the extracellular side of the growth cone membrane (Stuermer 2010) and detect these molecules. Semaphorins or collapsins, are membrane associated proteins that are detected by plexin proteins and interact directly with Rac or indirectly with RhoA (Huber, Kolodkin et al. 2003, Govek, Newey et al. 2005). Semaphorins include 3A (Sema3A), semaphorin 3D (Sema3D)(Vastrik, Eickholt et al. 1999) , semaphorin 4D (Sema 4D) and collapsin response mediator protein2 (CRMP2) that is a substrate of Rho kinase proteins and modulates the actin cytoskeleton to induce growth cone collapse and prevent outgrowth of the axon (Arimura, Inagaki et al. 2000, Hall, Brown et al. 2001). Ephrins, act as ligands for the receptor tyrosine kinases (RTK) and are classified as ephrin A and ephrin B which are involved in growth cone collapse and axon retraction (Wilkinson 2001, Cutforth and Harrison 2002, Huber, Kolodkin et al. 2003). Slit proteins, modulate axon guidance/repulsion at the midline by recruiting dedicator of cytokinesis (Dock) and p21-activating kinase (Pak) to the roundabout (Robo) receptor (Fan, Labrador et al. 2003).

Netrins, are a family of proteins that modulate the guidance of commissural and peripheral axons by acting as chemoattractants (Sun KLW 2011). Their function is controversial. Different netrin receptors include uncoordinated locomotion-5 (UNC5) and is absent in colorectal cancer (DCC) family members. If netrin binds to DCC homodimers it acts as a chemoattractant but if it binds to UNC5/DCC heterodimer it acts as a chemorepellent (Huber, Kolodkin et al. 2003).

NMDA and GABA neurotransmitters regulate axon outgrowth and fasciculation. They exert their action on axonal guidance through glutamate and Ca^{2+} influx (Georgiev, Taniura et al. 2008, Sernagor, Chabrol et al. 2010). Ca^{2+} has an important role in regulating neuronal development. Changes in the frequency of Ca^{2+} release regulate neurotransmitter expression and neurite outgrowth. This regulation is achieved through fast Ca^{2+} spikes and slow Ca^{2+} waves, respectively (Gu, Olson et al. 1994, Gu and Spitzer 1995, Gomez and Spitzer 1999, Ciccolini, Collins et al. 2003).

CAMs include cadherins and integrins, which are important regulators of plasticity in the nervous system, as mentioned earlier in this chapter. They modulate a variety of processes from migration to differentiation, axon outgrowth, synapse (Walsh, Meiri et al. 1997, Hansen, Berezin et al. 2008) formation by regulating intracellular Ca^{2+} levels and are usually located at the extracellular side of the membrane (Stuermer 2010, Sheng, Leshchyns'ka et al. 2013).

1.4. Rho Family of GTPases

Cell signaling at the growth cone is essential for proper axonal outgrowth and guidance. Rho GTPase family members are critical regulators in the process of axon

specification and elongation. Rho GTPases were initially identified about 30 years ago (Madaule and Axel 1985) but their Rho GTPase activity was not discovered until 1992 (Ridley and Hall 1992). The Rho family of small GTPases is a subfamily of the Ras superfamily of GTPases (Negishi and Katoh 2002). The Rho family includes 7 subgroups of small monomeric GTPases with 23 representatives in mammals (Wherlock and Mellor 2002); including Rac (1,2,3), Cdc42, Rho(A,B,C,D), and Rho(G and H) (Negishi and Katoh 2002, Burridge and Wennerberg 2004). Rac1, Cdc42, and RhoA, respectively, stimulate formation of veil-shaped lamellipodia, mirospiked filopodia, stress fibers, and focal adhesions (Nobes and Hall 1995, Hall and Lalli 2010). They have an essential role in neurite outgrowth and guidance by regulating the dynamics of the actin and microtubule cytoskeleton via their associated kinases and these roles may overlap at times (Jalink, van Corven et al. 1994, Luo, Hensch et al. 1996, Zhao and Manser 2005).

1.4.1. Structure of Rho GTPases

The structure of Rho GTPases governs its spatiotemporal regulation. They contain: (1) a conserved G domain that includes 5 motifs (G1-G5) involved in the positioning of Mg^{2+} and nucleotide binding for the base guanine (Vetter and Wittinghofer 2001, Wennerberg, Rossman et al. 2005, Wittinghofer and Vetter 2011); (2) 2 homologous switch domains which are responsible for GEF binding (V43 in RhoA) and GTP hydrolysis (Z63). Formation of hydrogen bonds between the ϒ-phosphate of GTP and T37 and G62 residues in Rho-GTPases results in conformational changes that regulate the interaction of effector proteins (Vetter and Wittinghofer 2001, Wennerberg, Rossman et al. 2005, Wittinghofer and Vetter 2011); (3) an insert region, involved in the binding of

GEF and effector proteins which in RhoA includes residues 123-137; (4) a hypervariable C-terminal and a CAAX motif that mediate association with the membrane (Wennerberg, Rossman et al. 2005, ten Klooster and Hordijk 2007) and binding of effector proteins (Schaefer, Reinhard et al. 2014). (Figure 1-2)

a)

```
CDC42          MQTI--KCVVVGDGAVGKTCLLISYTTNKFPSEYVPTVFDNYAVTVMIGG
RAC1           MQAI--KCVVVGDGAVGKTCLLISYTTNAFPGEYIPTVFDNYSANVMVDG
RHOA           MAAIRKKLVIVGDGACGKTCLLIVFSKDQFPEVYVPTVFENYVADIEVDG
                             G1                  G2

CDC42          EPYTLGLFDTAGQEDYDRLRPLSYPQTDVFLVCFSVVSPSSFENVKEKWV
RAC1           KPVNLGLWDTAGQEDYDRLRPLSYPQTDVFLICFSLVSPASFENVRAKWY
RHOA           KQVELALWDTAGQEDYDRLRPLSYPDTDVILMCFSIDSPDSLENIPEKWT
                        G3

CDC42          PEITHHCPKTPFLLVGTQIDLRDDPSTIEKLAKNKQKPITPETAEKLARD
RAC1           PEVRHHCPNTPIILVGTKLDLRDDKDTIEKLKEKKLTPITYPQGLAMAKE
RHOA           PEVKHFCPNVPIILVGNKKDLRNDEHTRRELAKMKQEPVKPEEGRDMANR
                                  G4

CDC42          LKAVKYVECSALTQRGLKNVFDEAILAALEPPETQP-KRKCCIF
RAC1           IGAVKYLECSALTQRGLKTVFDEAIRAVLCPPPVKKRKRKCLLL      RHOA
RHOA           IGAFGYMECSAKTKDGVREVFEMATRAALQARR-GKKKSGCLVL
                        G5
```

b)

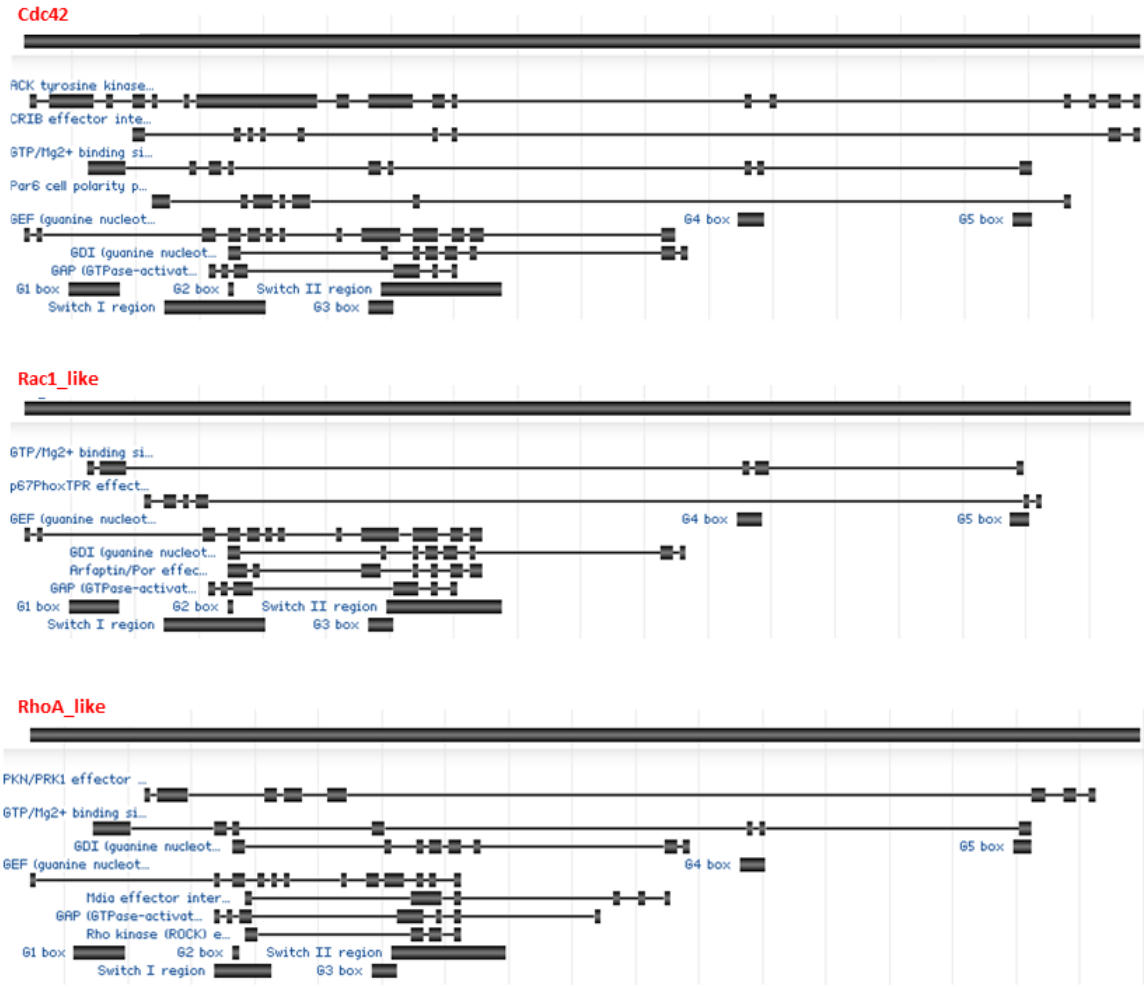
Cdc42
ACK tyrosine kinase...
CRIB effector inte...
GTP/Mg2+ binding si...
Par6 cell polarity p...
GEF (guanine nucleot...
G4 box
G5 box
GDI (guanine nucleot...
GAP (GTPase-activat...
G1 box
G2 box
Switch II region
Switch I region
G3 box
Rac1_like
GTP/Mg2+ binding si...
p67PhoxTPR effect...
GEF (guanine nucleot...
G4 box
G5 box
GDI (guanine nucleot...
Arfaptin/Por effec...
GAP (GTPase-activat...
G1 box
G2 box
Switch II region
Switch I region
G3 box
RhoA_like
PKN/PRK1 effector ...
GTP/Mg2+ binding si...
GDI (guanine nucleot...
G5 box
GEF (guanine nucleot...
G4 box
Mdia effector inter...
GAP (GTPase-activat...
Rho kinase (ROCK) e...
G1 box
G2 box
Switch II region
Switch I region
G3 box

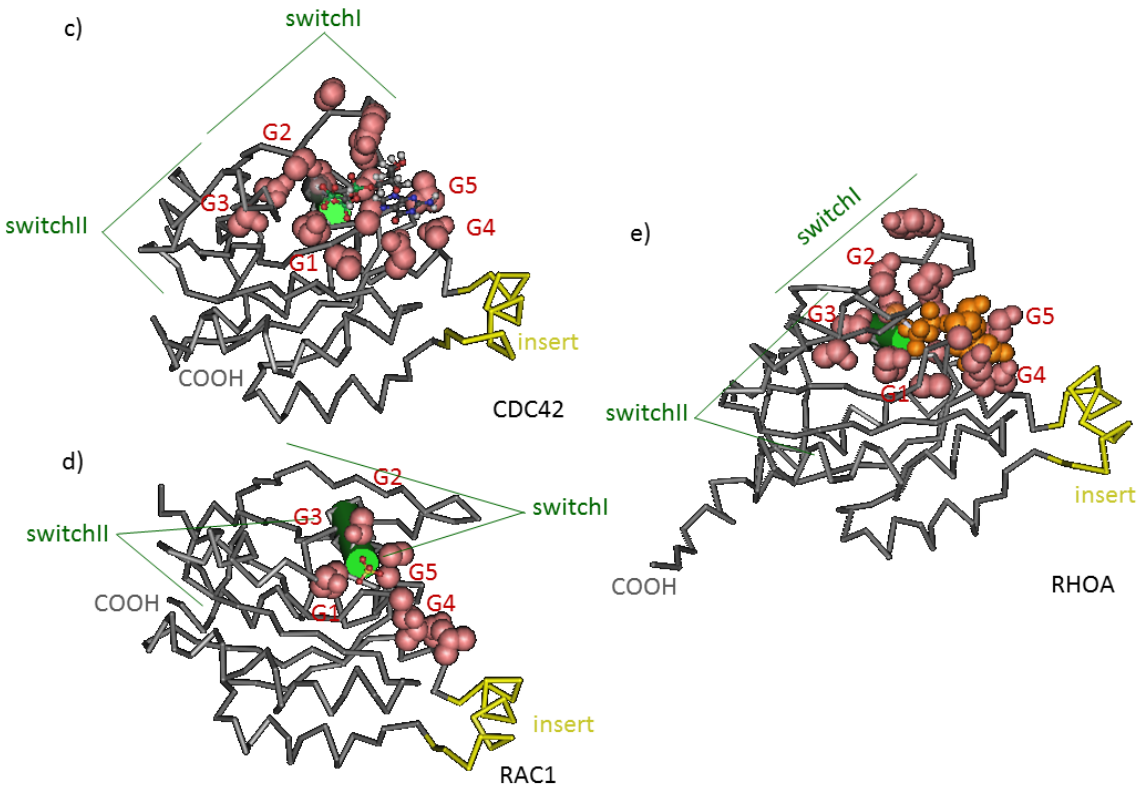
c)
switchI
switchII
G2
G3
G5
G4
G1
insert
COOH
CDC42
d)
G2
switchI
switchII
G3
G5
COOH
G1
G4
insert
RAC1
e)
switchI
G2
G3
G5
G4
G1
switchII
insert
COOH
RHOA

Figure 1-2 Structure of CDC42, RAC 1, RHO A

a) Alignment of the CDC42 (AAM21109.1), RAC1 (AAM21111.1) and RHOA (AAM21117.1) amino acid sequences. G domain sequences (red), Switch I, switch II, respectively (green highlight), the insert region (yellow highlight) and the hypervariable C-terminus (grey highlight). **b)** Graphical summary of conserved domains of GTPase proteins, CDC42, RAC1 and RHOA, respectively with alignment footprint indicating region similarity. 3D structure of and relative position of conserved domains **c)** CDC42, **d)** RAC1 and **e)** RHOA using PubMed, Cn3D tool (Wang, Addess et al. 2007, Marchler-Bauer, Zheng et al. 2013).

Cdc42/Rac1 and RhoA bind to downstream effectors such as Pak (p21-activated kinase) and ROCK (Rho-kinase) (Manser, Leung et al. 1994, Totsukawa, Yamakita et al. 2000). They contain (1) a kinase domain (Amano, Chihara et al. 1999), (2) a Rho Binding Domain (RBD) which is located within a putative α-helix coiled coil (Dvorsky, Blumenstein et al. 2004, Tu, Li et al. 2011) or a p21 Binding domain (PBD) (Manser, Leung et al. 1994, Daniels and Bokoch 1999) also known as Cdc42/Rac1 Interactive Binding domain (CRIB) (Burbelo, Drechsel et al. 1995, Daniels and Bokoch 1999, Stepanova and Chernoff 2008), (3) a pleckstrin domain (PH), and a Cysteine Rich Domain (CRD) in RhoA (Dvorsky, Blumenstein et al. 2004, Zhao and Manser 2005) or 5 proline rich domains in Pak (Daniels and Bokoch 1999, Stepanova and Chernoff 2008). GTP-Rho or activated Rho binds to the RBD and releases it from the kinase domain; thus, the inhibition on ROCK is disturbed and the Rho GTPase becomes activated and recruits effector proteins to the membrane (Ishizaki, Maekawa et al. 1996, Riento, Guasch et al. , Riento and Ridley 2003, Kubo, Yamaguchi et al. 2008, Fujita Y 2014) (Figure1-3) (Daniels and Bokoch 1999, Dvorsky, Blumenstein et al. 2004, Zhao and Manser 2005, Stepanova and Chernoff 2008, Tu, Li et al. 2011).

Typically, Rac and Cdc42 induce neurite formation through phosphorylation of Pak (Manser, Leung et al. 1994, Daub, Gevaert et al. 2001). On the contrary, Rho usually inhibits neurite formation through ROCK (Luo, Hensch et al. 1996, Totsukawa, Yamakita et al. 2000, Etienne-Manneville and Hall , Da Silva, Medina et al. 2003).

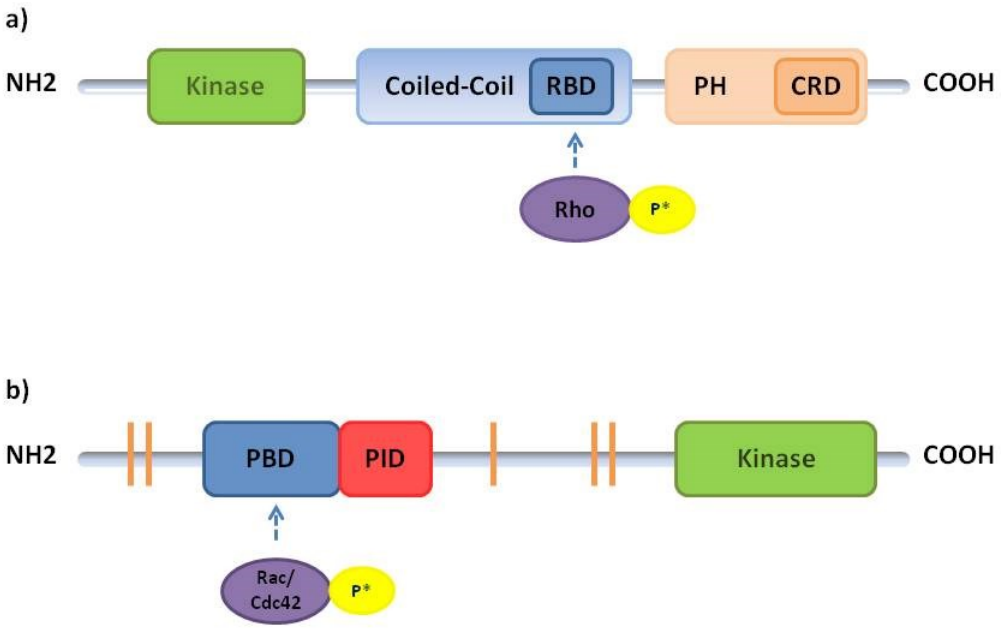
a)
NH2
Kinase
Coiled-Coil
RBD
PH
CRD
COOH
Rho
P*
b)
NH2
PBD
PID
Kinase
COOH
Rac/
Cdc42
P*

Figure 1-3 Schematic view of ROCK1 and Pac1 domains

a) ROCK I consists of an N-terminal serine/threonine kinase domain (green), a Rho binding domain (RBD) located within the central putative coiled-coil domain (blue), and a C-terminal cysteine-rich domain (CRD) that is located within a pleckstrin homology (PH) domain (orange). Upon activation of Rho, GTP-Rho it binds to the RBD and disturbs the inhibition on ROCK (modified from Figure1A (Dvorsky, Blumenstein et al. 2004)). **b)** p21-activated kinase (Pak) consists of an N-terminal p21-binding domain (PBD) (blue) followed by a Pak inhibition domain (PID) (red), 5 proline rich domains that are the binding site for -SH3 units (orange), and a C-terminal kinase domain (green). Upon activation of (Rac/Cdc42) GTP-Rac/Cdc42 binds to the PBD, unfolds the molecule and activates Pak (Modified from Figure (Stepanova and Chernoff 2008)).

1.4.2. Regulators of Rho GTPases

Rho GTPase molecules transit between a GTP-bound and a GDP-bound state in the cell. Generally, the GTP-bound state of the GTPase is deemed active; however, occasionally the GDP state acts as regulatory; for instance, GDP-Cdc42 regulates MAPK (Arozarena, Matallanas et al. 2001). The higher concentration of GTP in the cell acts in favor of GTP-bound state (Schaefer, Reinhard et al. 2014). Guanine nucleotide Exchange Factors (GEFs), GTPase activating proteins (GAPs), and guanine nucleotide dissociation Inhibitors (GDIs) regulate this transition and Rho GTPase signaling (Jaffe and Hall 2005, Hall and Lalli 2010).

GEFs are multidomain proteins, most of them consisting a Dbl homology (DH) domain and a Pleckstrin homology (PH) domain.GEFs enhance the GTP bound state by catalyzing GTP (Schmidt and Hall 2002). The invasion inducing-lymphoma and metastasis1 protein (Tiam1) is a Rac-GEF that is expressed in the developing nervous system (Ehler, van Leeuwen et al. 1997) and is enriched in the neurite that is destined to become an axon and also in the growth cone of the developing axon (Kunda, Paglini et al. 2001). Other GEFs include Kalirin that contains GEF domains for both Rac1 and RhoG and modulates axon protrusion (Ma, Johnson et al. 2001, Penzes, Johnson et al. , May, Schiller et al. 2002) . The Rac-GEF, SIF and Tiam like exchange factor (STEF) that is involved in neurite formation (Hoshino, Sone et al. 1999), Ost (Horii, Beeler et al. 1994), Dock 180, Sos (Ng and Luo 2004), and Rho-GEF KIAA0380 that is usually present in the tip of neurites (Togashi, Nagata et al. 2000).

On the contrary are GAPs that enhance the hydrolytic activity of GTPase and act in favor of the GDP bound state by dissociating GTP. GAP proteins include CrGAP/Vilse, p190RhoGAP (Brouns, Matheson et al. 2001), α-chimaerin (Hall, Michael et al. 2001),and oligophrenin-1 (Billuart, Bienvenu et al. 1998, Bernards and Settleman). GAPs usually interact with the P-loop and switch I and II regions of GTPases and their activity normally results in neurite retraction (Dvorsky and Ahmadian 2004, Cherfils and Zeghouf 2013, Schaefer, Reinhard et al. 2014).

GDIs are Chaperon proteins, which lack enzymatic activity and consist of an N-terminal domain that interacts with switch domains I and II within the GTPase and a C-terminal that binds to the switch II region and acts as an membrane anchor (Longenecker, Read et al. 1999, Hoffman, Nassar et al. 2000, Scheffzek, Stephan et al. 2000, Schaefer, Reinhard et al. 2014). GDIs inhibit dissociation of GDP and transfer of phosphate. RhoGDIγ is an example of a GDI that is mainly located in the nervous system (Adra, Manor et al. 1997).

Nonetheless, the regulation of axon outgrowth is not always a straightforward process and depending on the receptors different results could be observed. This variation depends on the developmental stage and type of neuron and also the subcellular localization of the GTPases, as well as, the upstream and/or downstream signaling that becomes activated. In their active state, Rho GTPases recruit effector proteins to the membrane. Rac, as well as Rho, have dual functions. For instance, if Rac is modulated through Rac GEFs (such as Tiam, STEF and Dock 180) and then activates IQGAP3 as its downstream target, axon outgrowth is stimulated (Aoki, Nakamura et al.

2004). On the contrary, Rac suppress axon outgrowth if it is activated by Trio to phosphorylate cofilin through Pak and LIMK (Aoki, Nakamura et al. 2004). Also, Slit dependent activation of Rac which is regulated by GEF Sos and GAP CrGAP/Vilse via Drosophila Dock/vertebrate Nck (Dreadlocks), Pak and Robo complex results in axon retraction (Hall and Lalli 2010). Interaction of Rac with plexinA1 causes a change in the cytoplasmic tail of plexin and results in receptor endocytosis (Hall and Lalli 2010). This enhances the activity of Rho/Rock signaling cascade and the inhibition of axonal outgrowth. Furthermore, Rac inhibits axon outgrowth when it is activated as a downstream target of plexinB1 (Hall and Lalli 2010). p190RhoGAP which is a RhoA-specific GAP transiently downregulates the activity of Rho but activates Rho activity through Rho GEFs (PDZ-RhoGEF and LARG) in a Sema dependent manner (Hall and Lalli 2010). In contrast, if Rho is activated through a GEF such as Kailirin9 or if it functions through Diaphanous related formin (mDia), axon outgrowth is stimulated (Hall and Lalli 2010). Inactivation of Rho through Rap/RA-Rho GAP or p190RhoGAP stimulates axon growth, as well; whereas, phosphorylation of cofilin through ROCK and Pak activated LIMK inhibits axon outgrowth (Govek, Newey et al. 2005). IRSp53 modulates neurite outgrowth by recruiting actin cytoskeleton effectors (Kast, Yang et al. 2014). Cdk5/p35 complex hyperphosphorylates Pak and disrupts its kinase activity (Govek, Newey et al. 2005). (Figure1-4) (Modified from (Govek, Newey et al. 2005, Hall and Lalli 2010)).

The activation and inactivation of the Rho GTPases controls downstream signaling cascades; which regulate actin disassembly and growth cone regulation including outgrowth and axonal guidance (Nikolic 2002, Jaffe and Hall 2005). Cdc42 may play an

important role in polarity of neuron as it is a downstream effector of small GTPase (Ras proximate1). Accumulation of active Rap1 and the selective degradation of its inactive form is one possible mechanism of regulation while the neuron acquires polarity (Schwamborn and Puschel 2004, Schwamborn, Muller et al. 2007). Cdc42 may also interact with atypical protein kinase C (aPKC) through mPar6 and modulate apical/basal polarity of *Drosophila* neuroblasts and rat astrocytes (Kemphues 2000, Ohno 2001, Etienne-Manneville and Hall 2002). In *Drosophila*, mutant forms of Rac1 inhibit axon outgrowth whereas dendrites are not affected (Hakeda-Suzuki, Ng et al. 2002, Ng, Nardine et al. 2002). In comparison, Cdc42 mutants affect both axon and dendrite outgrowth and migration and RhoA mutants have no effect on axon outgrowth but extend the dendrite and reduce its branching (Lee, Winter et al. 2000, Aoki, Nakamura et al. 2004). Loss- of- function mutations in the Rac genes of *Drosophila* result in defects in axonal outgrowth and guidance (Hakeda-Suzuki, Ng et al. 2002). Deficiency of Ena/Vasp family members in flies, worms, and mice causes defects in axonal outgrowth and guidance (Lanier, Gates et al. 1999, Wills, Bateman et al. 1999, Yu, Hao et al. 2002).

The Rac signaling pathway is modulated by Cdk5. In *Xenopus,* neuronal morphology of retinal ganglion cells (RGCs) is regulated by Rac via Cdk 5/p35 (Ruchhoeft, Ohnuma et al. 1999). Cdk5 interacts with Rac1 via p35 in a GTP dependent manner (Nikolic, Chou et al. 1998, Rashid, Banerjee et al. 2001). P35/Cdk5, Rac and Pak1 kinase co-localize in the periphery of the neurites and regulate its outgrowth. P35/Cdk5 kinase complex induces Pak1 hyper-phosphorylation. This downregulates the kinase activity of

Pak1 and actin re-organization which results in increased neurite outgrowth (Nikolic, Chou et al. 1998).

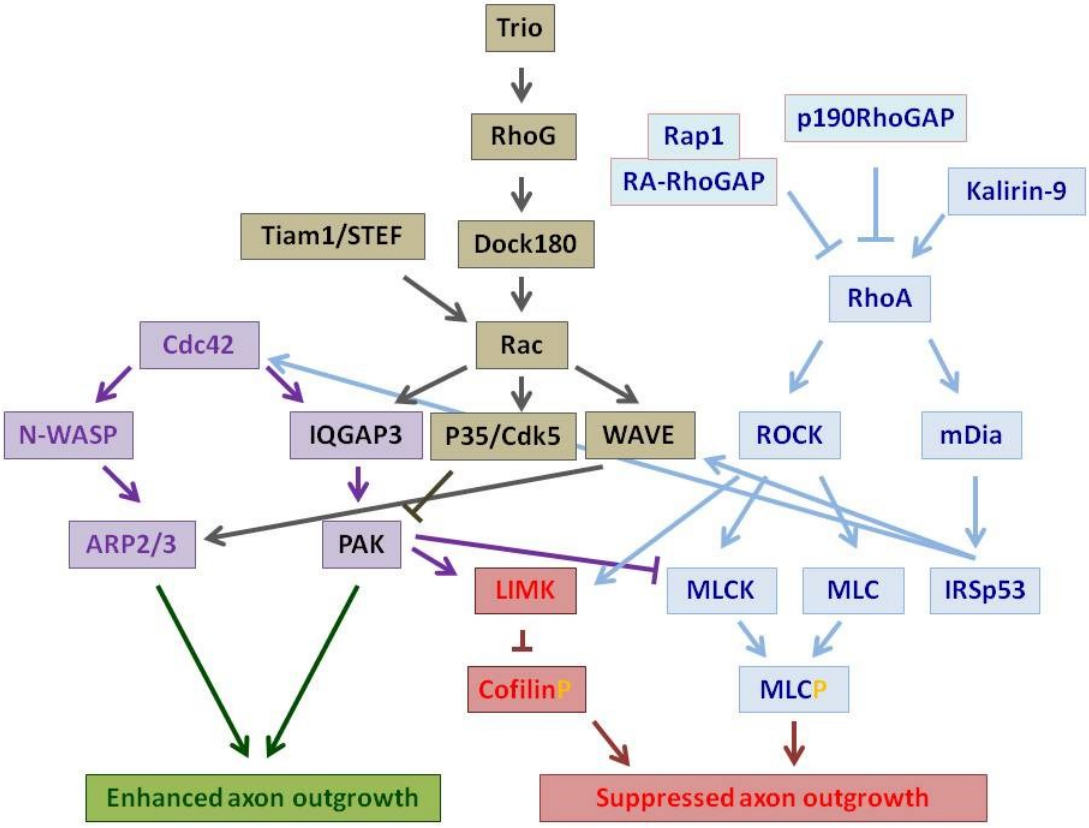
Trio
RhoG
Rap1
RA-RhoGAP
p190RhoGAP
Kalirin-9
Tiam1/STEF
Dock180
RhoA
Cdc42
Rac
N-WASP
IQGAP3
P35/Cdk5
WAVE
ROCK
mDia
ARP2/3
PAK
LIMK
MLCK
MLC
IRSp53
CofilinP
MLCP
Enhanced axon outgrowth
Suppressed axon outgrowth

Figure 1-4 Schematic illustration of main Rho GTPase effectors involved in axon outgrowth

Rho and Rac can inhibit or activate axon outgrowth depending on their upstream and/or downstream effectors. To simplify the pathway, different colors are utilized for illustrating each GTPase protein and its upstream and downstream effectors, i.e. Rac, Cdc42, RhoA and their effectors are illustrated in black, purple and blue, respectively. Also, the final enhancement (green) and suppression (red) of axon outgrowth is illustrated (See text for further description- Modified from Figure1 (Govek, Newey et al. 2005) and Figure3 (Hall and Lalli 2010))

1.5. Statement of Study

1.5.1. Rationale

Pctaire, Pftaire and Cdk5 are post-mitotic Cdk proteins that share the same most recent common ancestor. Previous research indicates that Cdk5 and Pctaire have important roles in the nervous system. For instance, Cdk5 inactivation leads to inhibition of axonal growth (Nikolic, Dudek et al. 1996, Nikolic, Chou et al. 1998). Furthermore, deletion of Cdk5 results in abnormal brain structure and embryonic lethality at embryonic day 18 (Ohshima, Ward et al. 1996). Pctaire has been detected at high levels, in growth cones of newly developing neurons and also in dendrites (Hirose, Kawabuchi et al. 2000, Fu, Cheng et al. 2011). The activity of Pctaire1-3 negatively regulates neurite outgrowth (Cole 2009). In addition, Pctaire seems to be a target of Cdk5 since the activity of Pctaire1 changes is in line with Cdk5 activity (Fu, Cheng et al. 2011).

Pftaire1 is highly expressed in the nervous system (Lazzaro, Albert et al. 1997, Yang and Chen 2001). Our lab has previously, examined the role of Pftaire (Eip63E, ecdysone-induced protein) in *Drosophila*. Initially, Jafar-nejad P (unpublished data), showed that commissural and longitudinal axons of the VNC were defasciculated and disrupted in two Eip63E mutant *Drosophila* lines (1) Df (L63) E1 and (2) $L63^{81}$. Homozygosity for both of these mutant alleles are embryonic lethal. Df(L63)E1 consists of a large deletion including the transcription initiation point and almost the entire conserved kinase domain resulting in no L63 (fly PFTAIRE) expression; whereas $L63^{81}$ represents a smaller 48bp (226-241) in-frame deletion within the conserved kinase domain resulting in a allele that is possibly null (Stowers, Garza et al. 2000) due to the loss of a highly conserved lysine residue K234

that is a part of the ATP binding domain in the Cdk2 protein (Jeffrey, Russo et al. 1995). Deficiency of the Pftaire1 homologue in *Drosophila* results in severe defects in axon patterning. This includes axon misguidance and defasciculation accompanied by disorganization of neuronal and cell bodies, as well as, abnormal arrangements of both commissural and longitudinal axons of the Ventral Nerve Cord (VNC) (Rodríguez González and S. 2011). Furthermore, our lab showed disorganization of cell bodies and diffused expression of elav, (neuronal marker for soma), in Eip63E mutants. Additionally, staining with HRP (sensitive axonal marker), reveals premature axonal growth along with defasciculation and misguidance. Eip63E deficiency results in concerted defects in axons and neurons of the *Drosophila* VNC. The defects emerge at stage 11 of embryonic development. The penetrance of the defects increases during development (Rodríguez González and S. 2011) and the flies dye at early larval stages (Stowers, Garza et al. 2000). The majority of the flies die during larval development; a few of them survive to form pupae that are smaller in size and rarely a fly survives to adult life. Taking into consideration the smaller size of the fly, one could infer that Eip63E may play a direct or indirect role in the size of the organism. For instance Eip63E may indirectly affect the size of the flies through disrupting the proper development of the nervous system (Stowers, Garza et al. 2000).

By analogy to Cdk5 and Pctaire, we speculated that Pftaire1 may play a role in neuronal development that could be more significant than that of Pctaire, as Pctaire is absent in *Drosophila* whereas Pftaire1 is highly conserved through evolution (Liu and

Kipreos 2000). This hypothesis is further supported through the study our lab is conducting on flies in parallel as mentioned above (Rodríguez González and S. 2011).

We also speculate that Pftaire1 may interact with Rho GTPases since they are involved in the regulation of neurite outgrowth. Nikolic et al. had shown that Cdk5 kinase interacts with Rac and regulates the activity of Pak1 (Nikolic, Chou et al. 1998). Since, Cdk5 interacts with the Rac family members, we propose that Pftaire1 may interact with Rho GTPases, as well. Our lab's study on flies supports this notion as functional interaction of Eip63E and RhoA is observed and the co-expression of Eip63E and RhoA modifies the axonal defects.

1.5.2. Hypothesis

We hypothesized that Pftaire1 is critical for neuronal development and differentiation, particularly in axon outgrowth and guidance, during the CNS development. However, we did not expect the lack of Pftaire1 to be lethal in mice due to the presence of the other homologues including Pftaire2 and Pctaire 1, 2, and 3; thus, only some degree of CNS abnormalities was anticipated.

We next proposed that Pftaire1 may functionally interact with known pathways relevant to axon guidance / outgrowth. Rho family GTPases (Rac1/RhoA/cdc42) may interact with Pftaire1 and modulate Pftaire1's function in the neurons. Based on previous reports by Nikolic et al. on Cdk5 (Nikolic, Dudek et al. 1996, Nikolic, Chou et al. 1998), we wonder if Pftaire1 negatively regulates axogenesis, similar to the function of Pctaire and opposite to Cdk5 (Nikolic, Dudek et al. 1996).

1.5.3. Objective

The purpose of this study was to examine the effect of Pftaire1 on axonal features. To execute this goal, the length of axons of Pftaire1 mutants in primary cortical cultures was compared with wild type controls. We also examined the interaction between Pftaire1 and the well-known Rho GTPases, which are confirmed to regulate neurite outgrowth.

To have a better understanding of the function of Pftaire1 *in vivo,* TIGM (Texas A&M Institute for Genomic Medicine) commercially designed Pftaire1 standard knockout mice specifically for our use[1]. Morphological, functional, and anatomical factors were examined in this transgenic mouse model, which lacked the Pftaire1 allele. To this end, we compared the differences between this group and their wild type littermates to pinpoint possible abnormalities that were caused by the absence of the gene and which would aid in determining the cellular role of Pftaire1.

We are cognizant that due to the presence of two highly similar Pftaire genes in the mammalian system, Pftaire2 could compensate for any defects related to the disruption of Pftaire1. To have a clearer understanding, this study needs to be continued with analyses of the Pftaire2 gene individually and in conjunction with Pftaire1.

[1] Pftaire1 was commercially obtained from TIGM (Texas A&M Institute for Genomic Medicine)

CHAPTER 2

METHODOLOGY

2. METHODOLOGY

2.1. Transgenic Mice Systems

All experimental animal studies were conducted in accordance with the guidelines of the University of Ottawa Animal Care Committee and conformed to the guidelines set forth by the Canadian Council on Animal Care and Canadian Institutes of Health Research.

2.1.1. Generation of Pftaire 1 deficient Mice

Pftaire1 heterozygote mice were generated for the first time, specifically for our use, by the Gene Targeting and Transgenic Facility of Texas A&M Institute for Genomic Medicine (TIGM), on mixed (129/ SvEvBrd x C57BL/6) background. To generate the mutant allele, Pftaire1 Gene (MGI: 894318) and the transcript sequence of Pftaire1 or (Cdk14-002 ENSMUST00000030763) located on chromosome 5 (4,803,391-5,380,197) (reverse strand) was targeted. Exon 6 of Pftaire1 was partially deleted, starting from nucleotide 18 of exon 6, extending up to nucleotide 1 of exon 7. The targeted genomic sequence is highlighted below:

(GCTTCCCTGTTGAAAGG“**ACTAAAGCACGCCAACATCGTGTTGCTTCACGACATCATCCACACTAAGGAAACCCTGACCCTTGTCTTTGAATACGTG”gtaagcgagataagaaggggtctagactgcatgtgtcacgtttgaataaaactctcagtgttagtgagttggtttttaagttgctctatgaaatgaatgtttttttctgagtacatgtgacatacatttgcataaaatcatggccatgtgacaggcttttgagtatgcatttcgttagacatgtggtttatttatagcct”**).

A b-geo (IRES/ bGeo/ PolyA) cassette was introduced in place of the deleted sequence via homologous recombination.

The mutant allele was transformed into 129/SvEvBrd embryonic stem cells via homologous recombination. Positive ES clones were isolated and screened. Their

sequences were confirmed by Polymerase Chain Reaction (PCR) and Southern blot hybridization analysis. Positive clones were delivered into C57BL/6 blastocysts by microinjection and implanted into pseudo-pregnant foster mothers to produce chimeras. Chimeric mice were bred with wild type mice to produce the Pftaire1 heterozygote deficient mice. PFTAIRE F1 generation homozygote/null mice were obtained by breeding heterozygous parents and their genotypes were confirmed by Polymerase Chain Reaction (PCR). To establish Pftaire1 knockout line on a pure C57BL6 background we backcrossed mixed (129/SvEvBrd x C57BL/6) heterozygote mice from the Pftaire1 deficient line with C57BL6 for 10 generations (Figure 3-2 b)

Germ line chimera was confirmed by Southern blot followed by PCR analysis using primers recommended by the Jackson Laboratory as described in their protocol. To confirm genotypes, primers for Southern blot screening were designed as follows: 5'probes, A: (5'–CATACATCAGGCATCCAGGGTA) and B: (5'– GGCTGGACTCCTGACTTCACCA); to generate a 644 bp product. 3'probes, C: (5'– CTTAGGAGAATTTGACATCCTCA) and D: (5' – CAGTGAGTTCCGGAGCTAGTCT); to generate a 684 bp product. Furthermore, to confirm successful disruption of Pftaire1 gene in Pftaire1 final mouse strain, PCR primers were designed as follows: (fwd. 5'-TGACCCTTGTCTTTGAATACGTG-3' and 5'-GGAAGCCTAAATTGTAAGGATCAGG-3') and (fwd. 5'–GCAGCGCATCGCCTTCTATC-3' and 5'-GGAAGCCTAAATTGTAAGGATCAGG-3'); to generate a 418 bp product and reverse to generate a 341 bp product for wild type and knockout, respectively.

PCR mix was run with GoTaq Green Master Mix 2x (Promega, M712B). The PCR amplification process was as follows: initial amplification designed as touchdown PCR

including: 6 cycles of denaturation 98 °C for 17 sec, annealing 69 °C (touchdown, -1°C per cycle) for 15 sec, amplification 72°C for 15 sec, and further amplification of the target genes was as follows: 35 cycles of 98 °C for 17 sec, 60 °C for 15 sec, and 72 °C for 15 sec. PCR products were resolved on a 1.5 % agarose gel- Ultra Pure Agarose (Invitrogen, 15510-027) and visualized by ethidium bromide (Ethyl hexadecyl dimethyl bromide $C_{20}H_{44}BrN$) (Sigma Ultra, C5335-1000).

2.2. Real Time PCR (Quantitative RT- PCR)

All steps were performed in RNAase-free environment. To ensure RNA-free surface, RNase away (MBP Molecular Bioproducts, 7003) was applied. Total RNA was extracted from mouse embryo whole brains/cortices at embryonic day E 13.5-14.5 using Trizol Reagent (Ambion, 15596026) based on Invitrogen protocols. 25 ng of extracted RNA was used per reaction. To determine disruption of Pftaire1 transcription the SuperScript III Platinum SYBR Green One-Step RT-PCR kit (Invitrogen, 204174) was used. Negative controls, no RNA and no RT were run in parallel with both the GAPDH housekeeping gene and Pftaire1. Each sample was run in quadruplets and n=3. Results were normalized against GAPDH. Primers used for amplification of the target genes were as follows: (GAPDH-Fwd.: 5'-GGTGAAGGTCGGTGTGAACG-3', GAPDH-Rev: 5'-CTCGCTCCTGGAAGATGGTG-3') to generate a 233 bp product and (Pftaire1-Fwd: 5'-CAGCGATCTGCCTCCACGGC-3') designed within exon13. (Pftaire1-Rev: 5'-GGCCCTCATGCTCTCTCCAGC-3') designed within exon 14, to generate a 341 bp product. The primers would also be able to produce a short heptamer within mutated region (exon 8); thus, it could not interfere with mRNA levels for Pftaire1-KO. The program for RT-PCR

amplification was as follows: 48 °C for 30 min, 95 °C for 10 min, and 40 cycles of 95 °C for 15 sec, 60 °C for 30 sec and 72°C for 30 sec. The RT-PCR products were resolved on a 1.5 % agarose-ethidium bromide gel as well.

2.3. Semi-Quantitative Reverse Transcriptase RT-PCR

All steps were performed in RNAase-free environment. To ensure RNA-free surface, RNase away (MBP Molecular Bioproducts, 7003) was applied. Total RNA was extracted from whole brains/cortices of WT-Pftaire1 and KO-Pftaire1 mouse embryo at embryonic day E 13.5-14.5 using Trizol Reagent (Ambion, 15596026) based on Invitrogen protocols. 50 ng of extracted total RNA was used per reaction for cDNA synthesis and gene amplification using SuperScript III Platinum SYBR Green One-Step RT-PCR kit (Invitrogen, 204174). Targeting primers designed for RhoA were as follows: (RhoA-fwd: 5'-GACCTTCGGAATGACGAGCA-3' and RhoA-Rev: 5'-TTCCCACGTCTAGCTTGCAG-3'). Results were normalized against S12 and primers were as follows (5'-GGAAGGCATAGCTGCTGG-3' and 5'-CCTCGATGACATCCTTGG-3') (Gonzalez, Zhang et al. 2008, Biswas, Zhang et al. 2010). cDNA synthesis was performed at 45°C for 45 min. Then, amplification was performed by a 2 min initial denaturation step at 94°C, followed by 24 cycles of 94°C for 30 sec, 60°C melting temperature (Tm) for 30 sec, and 72°C for 1 min, and 72°C for 10 min . RT-PCR products were resolved on a 2% agarose (Invitrogen)–ethidium bromide gel, and correct band for RhoA, 197 bp was processed by densitometry using Image J. Transcript levels were normalized against S12 signals and results were reported as relative mRNA level (normalized value). Data is represented as (Mean ±SEM) of at least three independent experiments.

2.4. Cell Culture

2.4.1. Immortalized Cell Line

Human Embryonic Kidney cells (HEK-293T) were cultured in Dulbecco's Modified Eagle Medium (DMEM) (High Glucose 4500 mg/L with 4 mM L-Glutamine without Sodium Pyruvate 0.1 µm sterile filtered) (ThermoScientific, SH30022-01) supplemented with 10 % Fetal Bovine Serum (FBS) (Hyclone, SH30397.03) and 1 % Antibiotic/ Antimicotic Solution100x (10,000 units/ml of penicillin, 10,000 µg/ml of streptomycin, and 25 µg/ml of Amphotericin B , 0.2 µm filtered) (ThermoScientific, SV30079.01) at 37°C in a 5% CO_2 atmosphere.

2.4.2. Primary Cortical Neuron Cultures

Cortical neuron cultures were prepared either from wild-type CD1 mouse embryos purchased from Charles River or from heterozygous crosses between Pftaire1 mice, at gestational day /embryonic day E 13.5-14.5. Embryos were considered E 0.5 d, at the time vaginal plug was detected. Embryos were removed from the uterine horns and transferred to Hanks' Balanced Salt Solution (HBSS) (modified without Calcium and Magnesium) (Hyclone Gibco, SH3003102). Brains were excised by cutting the skull open at the midline, from base of the head towards the front. Two lateral incisions were made under the cerebral cortices and skull was peeled off, meninges were removed and individual cortices were transferred to HBSS containing 8 µl Trypsin (25g/L in 0.9 % NaCl) (Sigma, T4549), incubated for 20 min at 37 ^{o}C with agitation. 10.7 µl of Trypsin inhibitor in neurobasal medium was added to stop trypsinization, and 13.34 µl DNase1 (10 mg / ml) (Boehringer Mannheim Roche Diagnostics, 10137100) to degrade extracellular DNA

medium were added to the solution. Cells were pelleted at 1000 x, for 5 min at 4 °C and 10.7 µl of trypsin inhibitor and 13.34 µl of DNase were added. Cells were triturated; viable cells were counted using sterile filtered trypan blue solution (0.4 %) (Sigma, T8154). (Number of cells per ml was calculated by: cell count in the central square x dilution factor x 10^4). Cells were diluted to desired concentration for culture, in Complete Neurobasal Medium containing: Neurobasal medium (Gibco LifeTechnologies, 21103-049), B27 supplement (Invitrogen, 17504-044), N2 supplement (Invitrogen, 17502-048), L-Glutamine 200 mM (Gibco, 25030-081) and Penicillin-Streptomycin. Primary cortical neuron cells were plated into 24 or 6 well plates. Plates were coated with Poly-D-Lysine-Hydrobromide (1 mg/ml, sterile) (Sigma, P0899) prior to use. Poly-D-Lysine incubation was performed for at least 30 min and then plates were washed. For immunostaining, sterilized coverslips were placed into 24 well culture dishes and then coated with poly-D-lysine. Cultures were incubated at 37 °C in a 5% CO_2 atmosphere and fixed or lysed at varied times.

2.5. Exogenous Gene Expression

2.5.1. Expression Vectors

Plasmids for transfection: GFP subcloned into pCig2 vector (generously gifted by Carola Sherman), FLAG-Tagged: WT-Pftaire1 and D228N-Pftaire1 cDNA (mutation of conserved aspartic acid residue to asparagine, by a point mutation) (1284 kb) subcloned into pCMV vector (generously gifted by Dr. Paul Albert and Maribeth Lazzaro) (Lazzaro, Albert et al. 1997); GST-Tagged: WT-Rac1, G12V-Rac1, S17N-Rac1 subcloned in pEBG vector; GST-tagged: WT-Cdc42, G12V-Cdc42, S17N-Cdc42 subcloned in pEBG vector and

MYC-tagged: WT-RhoA, CA-RhoA Q63L, DN-RhoA L19N in pRK5 vector. Rho GTPases (generously gifted by Dr. Gary Bokoch and Dr. Margaret Chou, University of Pennsylvania). Constructs were sequenced at Ottawa Genomic Center, using following primers: (1) For Rac1 and Cdc42 constructs in the pEBG backbone: (pGEX 5' Sequencing Primer: 5'-[GGGCTGGCAAGCCACGTTTGGTG]-3' and pGEX 3' Sequencing Primer 5'-[CCGGGAGCTGCATGTGTCAGAGG]-3') (2) To sequence Pftaire1, CMV virus backbone: (pCMV 5' Sequencing Primer: 5'-CGCAAATGGGCGGTAGGCGTG-3' Pftaire1 GC rich region at 3' end: 5'-GGGGGAGTTGAAGCTGGCAG-3'). Sequencing was performed 100 bp upstream of start codon and 100 bp downstream of stop codon. Plasmids were transformed with Top10 competent cells. Transformed cells were cultured on Ampicillin resistant agar plates (LB Agar Granulated, Molecular Genetics BP-1423-500). A single colony was picked and grown in Luria-Bertani (LB) Broth (Miller Amresco, J-106-500G). DNA was purified using the Pure Yield Plasmid Midi Prep System (Promega, A2495).

2.5.2. Transient Transfection with Lipofectamine

HEK 293T Cells were cultured to 70% confluency, then co-transfected with Flag tagged (WT-Pftaire1 or D228N-Pftaire1) and GST tagged [WT-Rac1, G12V-Rac1 (constitutively active), S17N-Rac1 (dominant negative inactive)] or GST tagged [WT-Cdc42, G12V-Cdc42 (constitutively active), S17N-Cdc-42 (dominant negative inactive)] or GST tagged [WT-RhoA, Q63L- RhoA (constitutively active), L19N-RhoA (dominant negative inactive)], as well as, the reporter vector (GST::PEGB, MYC::PRK5, Flag::CMV using lipofectamine 2000 reagent (1mg/ml) (Invitrogen, 11668-019). Opti-MEM (Minimal Essential Medium), 1x Reduced Serum (Gibco, 31985-070) was used to dilute the plasmid

and lipofectamine according to the manufacturer's instructions. Diluted plasmid and lipofectamine were mixed and incubated for 20 minutes at room temperature. Cell culture medium was changed to media without FBS at the time of transfection. The plasmid-lipofectamine complex was added to culture media in droplets. 24 hours post transfection, cells were triturated off culture plates by scraping, cells were collected into ice cold PBS and spun down at 1.4 x g for 1 min for pull down assay.

2.5.3. Viral Infection

Gene delivery via Adenoviral (AV) infection was performed at the time of plating. Adenovirus expressing WT-Pftaire1 (Ad ET-CMV-3x Flag-WT-Pftaire1, Pfu: 1.00 x 10^{12} CsCl Pure, Plaque pure), D228-Pftaire1 (Ad ET-CMV-3x Flag-D228N-Pftaire1, Pfu: 9.20 x 10^{11} CsCl Pure, Plaque pure), and GFP (Ad ET-CMV-EGFP, Pfu: 4.89 x 10^{11} CsCl Pure, 3x Plaque pure), was mixed with neuronal cortical culture cells at 50 -100 MOI (multiplicity of infection). Cells were fixed or lysed, at different time points, post-culture, for further analysis, depending on the nature of the experiment.

2.6. Neuronal Death Assay

Cortical culture cells from mouse embryos at E13.5-14.5 were seeded at (1 x 10^5) in 96 well plates and infected/co-infected with AV viruses (GFP alone or GFP + WT-Pftaire1, D228N-Pftaire1) at MOI=100 at the time of plating, for survival assay. Cells were washed with 1X PBS and then fixed with 4% PFA 12, 16 and 24 hours post-infection and then stained with Hoechst 33258 (1:10000) (Sigma-Aldrich B2883) in 1x PBS and incubated for the minimum of 30 min for nuclei staining. Intact nuclei were counted against condensed and fragmented nuclei to determine live neurons versus dead ones.

To determine survival the number of live GFP positive neurons were assessed in each well, each treatment was performed in triplets, and the average for each treatment was calculated. Survival was assessed for WT-Pftaire1 or D228N-Pftaire1 as the percent of live GFP positive neurons in comparison to GFP. Survival percentage represents the ratio of GFP expressing neurons with morphologically intact nuclei at (12, 16, and 24 h) in WT-Pftaire1 or KO-Pftaire1 to the total number of GFP expressing neurons. The values were normalized to GFP alone as control. Data are presented as (Mean± SEM) of at least three independent experiments.

2.7. Total Protein Extraction

To compare protein expression levels, whole brain lysates were prepared from mouse brains at E13.5-14-5 or from mouse pups at P21. Basically, mouse brains were dissected and washed with ice-cold PBS. Brains were homogenized in lysis buffer: [50mM Tris-HCl (pH=7.5), 150mM NaCl,1 mM $MgCl_2$, 1mM EDTA, 1% triton X-100 (Boehringer Mannheim, 789704), 1mM L-Dithiothreitol (DTT , $C_4H_{10}O_2S_2$) (Sigma Aldrich, D0632-5G), protease inhibitor (Halt Protease inhibitor Cocktail EDTA-free 100x (Roche, 87785)] for 20 min, at 4 °C, with agitation. Lysates were clarified by centrifugation at 19500 x g, 4 °C, for 20 min. Supernatant was collected (approximately 2mg of protein was collected per brain), mixed with 0.1% w/v bromophenol blue/ DTT sample buffer and heated at 100°C, for 10 min.

2.8. Immunoprecepitation (IP)

All steps were performed on ice. Cell lysate was prepared as described, previously. Lysate was prepared using lysis buffer 50 mM Tris-HCl (pH=7.5), 150 mM NaCl, 1 mM

$MgCl_2$, 1mM EDTA, 1% Triton X-100 (Boehringer Mannheim, 789704), 1mM DTT (L-Dithiothreitol, $C_4H_{10}O_2S_2$) (Sigma Aldrich, D0632-5G), protease inhibitor, for 20 min, at 4°C with agitation. Lysates were clarified by centrifugation at 19500 x g, 4°C, for 20 min. Supernatant was collected and incubated with 20 µl of washed bead per reaction. After immunoprecipitation, beads were pelleted at 1000 x g , washed five times with wash buffer (Tris-HCl (pH≈7.3-7.5), NaCl, EDTA, Triton 10 % , DTT), then mixed with 0.1 % w/v bromophenol blue / DTT sample buffer, and heated at 100°C, for 10 min to release the protein complex. Proteins were resolved on 12 % SDS-polyacrylamide gels.

For immunoprecipitation of ectopically expressed GST tagged proteins, GST beads - (Glutathione Sepharose 4b beads, particle size 45 µm - 165 µm, GE Healthcare 17-0756-05) were incubated with the lysate overnight, at 4 °C, on a rotor. For immunoprecipitation of endogenous protein, Trueblot Anti Rabbit IgIP beads - (eBioScience, 00-8800-25) or Anti mouse IgIP beads - (eBioScience, 00-8811-25) were used, depending on the origin of the bait antibody. Lysate was collected and precleared by incubating 20 µl of the washed bead that was to be used for IP, for 30 min, at 4 °C, on a rotor. Supernatant was cleared by centrifugation at 1000 x g, 1 min, at 4°C. 4 - 8 µg of antibody per reaction, normal mouse IgG (SantaCruz, sc-2025) or normal rabbit IgG (SantaCruz, sc-2027) and Pftaire-1 (H-140) (1:500) rabbit polyclonal IgG (SantaCruz, sc-50475), RhoA (1:500) mouse monoclonal IgG (SantaCruz, sc-418), Rac1 (C-11) (1:500) rabbit polyclonal IgG (SantaCruz, sc-95), Cdc42 (1:500) rabbit polyclonal IgG (SantaCruz, sc-87) was incubated with the cleared supernatant, overnight, at 4°C, on a rotor. Pftaire1 was used to IP GTPase and vice

versa. 20 µl of the washed beads were incubated with the antibody-lysate mix for 3 hours, at 4 °C, on a rotor to precipitate the antibody.

2.9. SDS-PAGE and Western Blot

Protein extracts were resolved on a 10 or 12 % SDS - polyacrylamide gel, along with Molecular Marker, Blueye Prestained Protein Ladder (GeneDirex, P14007-0500). Transfers were done on 0.45 µm PolyVinylidene DiFluoride (PVDF) Transfer membrane (Immobilon-P, IPVH00010). Membrane was blocked in 10 % non-fat dry milk in 1 x PBST [Phosphate Buffered Saline (pH=8.0) and 0.1 % Tween] at room temperature, for 1 hour. Proteins were detected using antibodies. Primary antibodies were diluted in [3 % Bovine Serum Albumin (BSA) fraction V (Fisher, BP1600-100) in PBST and 0.1 % Sodium Azide NaN_3 (Sigma Ultra, s-8032)] as follows: Pftaire1 (H-140) (1:500) rabbit polyclonal IgG, (SantaCruz, sc-50475), Pftaire2 (CDK15) (1:500) rabbit polyclonal (Life Span Biosciences, LS-C119219/34326), RhoA (1:500) mouse monoclonal IgG (SantaCruz, sc-418), Rac1 (C-11) (1:500) rabbit polyclonal IgG (SantaCruz, sc-95), Cdc42 (1:500) rabbit polyclonal IgG (SantaCruz, sc-87), Cdk5 (C-8) (1:500) rabbit polyclonal IgG (SantaCruz, sc-173), Pctaire1 (CDK16) (1:500) rabbit polyclonal, (Life Span Biosciences, LS-C112292/34325), Anti-Flag (1:500) rabbit monoclonal IgG (Sigma, F7425), Anti-GST (1:500) mouse monoclonal IgG (SantaCruz, sc-138) and incubated with the membranes overnight, at 4 °C, with agitation. Membranes were washed and then incubated with secondary antibodies diluted in 5 % non-fat milk, for 1 hour, at room temperature [goat anti-mouse 170-6516 or goat anti-rabbit 170-6515 IgG (H+L) HRP conjugate (Bio-Rad)] were all used at 1:2000 in 3 % BSA in 0.1 % Tween 20 (PBS/T). Immunoreactivity was detected using Immobilin Western

Chemiluminescence HRP substrate (Millipore, WBKLS0500) or Pierce ECL Western Blotting Substrate (Thermo Scientific, 32106) and visualization HyBlot CL Autoradiography film, Denville Scientific. Protein levels were normalized against β-actin signals, and results were reported in reference to control values (untreated control for each individual experiment).

2.10. Pftaire1 Kinase Assay

Kinase assay was performed using immunoprecipitated WT-Pftaire1 protein or IgG as a control. Briefly, Neuronal cortical cells prepared from WT-Pftaire1 mouse embryos E13.5-14.5 were cultured in Neurobasal media (Gibco, 21103-049) containing B27 (Invitrogen, 17504-044) and N2 (Invitrogen, 17502-048), in 12 well plates, at the ratio of 1 embryo per well, for 18-20 hour, at 37°C, 5 % CO_2. After washing with ice-cold 1x PBS, lysates were collected directly from plates by scraping into ice-cold immunoprecipitation (IP) buffer (Tris-HCL 25mM (pH 7.4) , $Na_4P_2O_7$ 10 mM, Na_3VO_4 25 mM, NaF 50 mM, EDTA 1 mM , Digitonin 2 mg/ml) and sonicated twice, for 3 cycles, with a 20 minute incubation in between the 2 set of cycles, and then supernatant was cleared by centrifugation at 14000x g, 4°C, for 10 min. 1 mg of protein(adjusted to the volume of 300 µl was incubated with 4 µg antibody either normal rabbit IgG (200 µg/0.5 ml) or Pftaire1 (200 µg/ml) antibodies, overnight, at 4°C, on the shaker. IP-ed, WT-Pftaire1 and IgG were mixed with 40 µl of pre-equilibrated (performed washes with IP wash buffer) Trueblot anti-rabbit IgIP beads per reaction and incubated for 2 hours, at 4°C, on the shaker. Beads were then washed and pelleted at 2000rpm, for 1 min, at 4°C, with IP wash buffer and kinase assay buffer [HEPES 50 mM (pH 7.5) and 1mM DTT], respectively. Next, kinase reaction buffer

(HEPES 50 mM (pH 7.5), 1 mM DTT, 10 mM MgCl, and 20 µM ATP)) was added to a final volume of 25 µl. 10 µg of RhoA substrate His-Recombinant human RhoA (Prospec, pro-057), was added to reactions with or without (5 µl, 100 x) GDP. Reactions were incubated overnight, at 30°C. Samples were then centrifuged at 2000 rpm, for 1 min, at 4°C, then supernatant was collected and subjected to either western blot for rabbit polyclonal IgG phosphoserine (Invitrogen, 61-8100) signal; or G-LISA assay to assess RhoA activity as described below.

2.11. Assessment of Rho GTPase Activity

Activation of RhoA, as a function of Pftaire1 kinase activity was determined using commercially available "RhoA Activation Assay Kit (CellBioLabs, STA-403-A)" according to the manufacturer's instructions. Primary Cortical Culture Cells were prepared from Het x Het crosses at embryonic day 13.5-14.5, at the density of 1 embryo per well, in 1.5 ml, cultured in complete Neurobasal media supplemented with B27 and N2 , in 12 well plates, and incubated at 37 °C and 5 % CO_2. 18-20 hours post-plating cells were washed with ice-cold PBS and GTPase assay was performed according to the manufacturer's kit. To decrease rapid hydrolysis of active GTP bound to inactive GDP bound protein all following procedures were performed on ice. Briefly, cells were incubated on ice, for 20 minutes, with 1x Assay / lysis buffer provided with the kit (Part No. 240102) (containing 125 mM HEPES, pH 7.5, 750 mM NaCl, 5% NP-40, 50 mM MgCl2, 5 mM EDTA, 10% Glycerol) and then collected by scraping. Due to very low expression of RhoA same-genotype extracts were pooled to achieve large amounts of Protein. Total protein was quantified by Bradford protein assay to achieve at least 800ug of protein for each sample/assay. Cell

lysates were clarified by centrifugation at 14,000 g x, at 4 °C, for 10 min. (at least 800 µg protein per reaction). 100x GTPγS (Part No. 240103) and GDP (Part No. 240104) were added to the cells for positive and negative control, respectively. Control samples were incubated for 30 minutes, at 30 ^{o}C, with agitation, and the reaction was terminated by adding 1M $MgCl_2$ to the samples. Volume of sample per reaction was adjusted to be identical in all reactions and 40 µl of bead added per reaction. Active-proteins were immunopercipitated with respective rhotekin RBD agarose beads for RhoA. Beads were pelleted by centrifugation at 14000 x g, for 10 seconds, and washed three times with 1x Assay buffer supplied in the kit. Afterwards, beads were resuspended in SDS-PAGE sample buffer and boiled for 5 minutes for detection by western blotting. Separated proteins were visualized using RhoA, Mouse Monoclonal antibody (Part No. 240302) provided with the kit.

To quantify Rho GTPase activity after the pftaire1 Kinase assay, in a more accurate/sensitive manner, G-LISA RhoA activation assay biochem kit (Absorbance based) (Cytoskeleton, BK124) was used according to the manufacturer's protocol. Samples from the kinase reactions, (IgG-IP: RhoA, IgG-IP: RhoA+GDP, Pftaire1-IP: RhoA and Pftaire1-IP: RhoA+GDP) were diluted and pre-equalized with ice cold lysis buffer /binding buffer (Part # GL37). To pre-equalize samples, protein concentration was determined at 600nm, using Precision Red^{TM} Advanced Protein Assay Reagent (Part # GL50) as suggested by the manufacturer. Same buffer mix (no protein) and RhoA (provided by manufacturer), were respectively, used as blank and positive control for the assay. Next, samples were transferred to 96 well Rho-GTP binding plates (Part # GL25), equipped with pre-washed

GLISA assay strips, incubated at 4°C, on an orbital microplate shaker at 400 rpm, for 30min. Samples were then washed with wash buffer (Part # GL38) and incubated with Antigen Presenting Buffer (Part # GL45) for 2 min, washed again with wash buffer, then incubated at room temperature for 45 min, on orbital microplate shaker at 400rpm, with anti-RhoA primary antibody (Part # GL01) (1:250) in Antigen dilution buffer (Part # GL40) and washed subsequently. Samples were next incubated with (1:62.5) secondary horseradish peroxidase (HRP) conjugate antibody (Part # GL02) at room temperature, for 45 min, on an orbital microplate shaker at 400 rpm and washed afterwards. Then samples were incubated with HRP detection reagents A (Part # GL43) and B (Part # GL44) (1:1 ratio) for 15 min, at 37 °C, and reaction was stopped by adding HRP Stop Buffer (Part # GL80), and absorbance measured at 490 nm using a microplate spectrophotometer. To measure RhoA activity, values were determined as follows, $(\frac{\text{GLISA value(ng)}}{\text{ELISA value(ng)}} \times 100 = \text{normalized \% of active RhoA})$. The detected signal was normalized against total RhoA using G-LISA and E-LISA (BK # 150) kits side by side. To determine if any significant difference existed in the activity of RhoA among samples, two way ANOVA was performed in the grouped data followed by Bonferroni's post-hoc test. Results were presented as average of at least three independent experiments.

2.12. Histology and Staining

2.12.1. Brain Sectioning

Brains were collected from the Wt-Pftaire1 and KO-Pftaire1 mice at 8 weeks of age. Animals were humanely anesthetized with euthasol and transcardially perfused with 0.9 % saline, followed by fixative solution 4 % Paraformaldehyde (PFA) (EMD, PX0055-3)

in 1x PBS at pH=7.4. Brains were then removed from the skull and fixed further with 4 % PFA, at 4 °C, for 24 hrs. Fixed brain tissue was cryopreserved in 20 % sucrose in 0.1 M phosphate buffer and stored at 4°C, over a 3 day course, and the solution was changed 3 times per day. Brains were then snap-frozen with Nitrogen balanced with CO_2 and then embedded with O.C.T. (Tissue - Tek /O.C.T compound, 4583) for sectioning. 14 µm coronal sections were collected from the brains; starting at the frontal cortex at Bregma: ~ 2.710 mm up to the 4th ventricle at Bregma: ~ - 4.20 mm. For collecting, 3 sections were skipped in between each selection. Sections were directly mounted onto SuperFrost Plus microscopic slides 25 x 75 x 1.0 mm (Fisher brand, 12-550-15) and subjected to2 % cresyl violet staining as described below.

2.12.2. Cresyl Violet Staining

Sections were thawed on slide warmer for 15-20 min, at 35 °C, and then placed in distilled water for 5 min. Sections were then stained with 2 % filtered cresyl violet (pH=3.5) cresyl violet acetate ($C_{18}H_{15}N_3O_3$, Sigma C5042-10G), for 10-30 minutes depending on the stain concentration. Sections were then dehydrated in graded ethanol solutions from 50 % to 100 %, followed by defatting with xylene. Sections were mounted with coverslips using toluene.

2.12.3. Immunostaining

Cells plated on glass coverslips were fixed in 4 % PFA in 1 x PBS, for 15 min. Fixed cells were permeabilized and blocked simultaneously in 0.1 % Triton X-100, and 5 % BSA in 1x PBS, respectively, for 20 min, at room temperature. Coverslips were incubated with primary antibodies diluted in 5 % BSA in 1x PBS: Tau1 clone 46 (1:500) mouse monoclonal

IgG (Sigma-Aldrich, T-9450), GFP (H-140) (1:500) mouse monoclonal IgG (Abcam, ab1218), Pftaire1 (H-140) (1:500) rabbit polyclonal IgG (SantaCruz, sc-50475), MAP2 (H-300) (1:500) rabbit polyclonal IgG (SantaCruz, sc-20172) for 1hr, at room temperature. Coverslips were washed; incubated with FITC-secondary antibodies: Alexafluor 488 (1:1000) Goat-Anti-mouse (Molecular Probes, A11001), Streptavidin Alexafluor 488 (1:1000) Goat-Anti-mouse (Molecular Probes, S11223), Streptavidin Alexafluor 546 (1:1000) Goat-Anti-mouse (Molecular Probes, S11225), Alexafluor 594 (1:1000) Goat-Anti-mouse (Molecular Probes, A11005), Alexafluor 594 (1:1000) Goat-Anti-rabbit (Molecular Probes, A11037), Alexafluor 594 (1:1000) Donkey-Anti-Goat (Molecular Probes, A11058) were diluted in 5% BSA in 1x PBS, and then incubated with coverslips for 30 min, at room temperature. To detect intact nuclei, cells were stained with Hoechst 33258 (1:10000) (Sigma-Aldrich B2883) in 1x PBS, incubated for the minimum of 30 min, at room temperature. Slides were immersed in distilled water to remove excess salt and then mounted on slides applying approximately 25 µl of Vectashield Mounting Medium (Vector laboratories, H-1200).

2.13. Microscopy and Imaging

Images were taken using upright Zeiss Axioskop 2 Mot or inverted Zeiss AxioObserver-Z1 fluorescent microscope with Northern Eclipse Software or Zeiss and Axiovision Rel. 4.8 software, captured in XY mosaic format, in rectangle mode. Images were taken at 20x, 32x, and 40 x magnification lenses. To determine the total diameter of the field of view for each objective, Ocular Field of View (F.O.V.) number (32) was divided by objective magnification and following measurements were obtained: for 20x (1500

μm), for 32x (719 μm), and for 40x (575 μm). Images were processed for length measurements using Axiovision software Rel. 4.8, spline mode to trace axon length or Stereo Investigator microscopy imaging system (version 6; MicroBrightField, Williston, VT) software using contour mapping mode and tracing the length of axons. The distance from the cell body of the GFP expressing neuron or Tau1 to the distal region of the longest neurite was measured as axon/lengthiest neurite.

2.14. Quantification of Signal Density on Images

Immunoblots were further analyzed by Image J software to compare the density/intensity of the bands of an agar gel or a western blot membrane. Following imaging of the blots, representative bands were selected and their intensity was quantified. Then quantified measurements were transferred to excel and results were normalized against relative controls (β-actin for western blot and S12 for RT-PCR).

2.15. Statistical Analysis

Experiments were performed for a minimum of 3 times and each treatment was done in replicates of 3. Data and graphs were represented in the format of (Mean ± SEM) or percentage. Graphs were plotted as column charts for probability of getting a specific range of values, to compare the mean of the experimental groups. To compare axon lengths among different litters and to avoid divergence and variability between different litters, data was either transformed to log10 format or classified into length intervals and then data was plotted onto a linear or bar graph, respectively. To classify measurements, the average and median axon lengths were calculated for each time-point. The maximum and minimum numbers related to average and median were considered as average range

for that time-point and neurites diverting from this range were considered as either short or long, relatively. Comparison against different litters was performed, as well. Statistical analysis was performed using excel, Eviews 6 and SPSS software and processed using chi square, Levene's Test for Equality of Variances, student's two tailed t-Test considering the variance between the two experimental groups equal, or one way and two way ANOVAs followed by Student-Newman-Keuls post-hoc test or Bonferroni's test.

CHAPTER 3

RESULTS

3. RESULTS

3.1. Pftaire1 Transgenic Mice

3.1.1. Generation of Pftaire1 Transgenic Mice

To examine the role of PFTAIRE1 in the CNS, Pftaire1 deficient mice were generated*[2]. These mice are the first of their type since no other Pftaire1 deficient mice exist, to date. To generate the Pftaire1 deficient mouse, Pftaire1 heterozygotes were designed by replacing the majority of exon 6, starting from nucleotide 18, of the *Mus Musculus* Pftaire1 transcript (ENSMUST00000030763) (Figure 3-1, 3-2 a) with the neomycin (Neo) resistance cassette via homologous recombination (Figure3-2 b). The transgenic mutation produced in the Pftaire1 gene causes a frame shift which alters the open reading frame and leads to a premature stop codon and produces a truncated protein that does not have the full kinase domain (Figure3-3); thus, is expected to degrade or lack kinase activity. The DNA sequence of the 129/SvEvBrd embryonic cells that were transformed with Pftaire1 mutant allele was confirmed by Polymerase Chain Reaction (PCR) and Southern blot hybridization analysis. The transformed Pftaire1 allele was easily detectable in the transformed mice through the agouti coat color of the chimeras. The produced chimeric mice were viable and fertile; after being crossed with wild type mice they also produce the Pftaire1 heterozygote deficient mice that were viable and fertile. Pftaire1 F1 generation, homozygote (null) mice, which were obtained by breeding

[2] Pftaire1 deficient mouse was designed and developed for our use by the TIGM (Texas A&M Institute for Genomic Medicine) company.

heterozygous parents were also viable and fertile. To establish Pftaire1 knockout line on a pure C57BL6 background we backcrossed mixed (129/SvEvBrd x C57BL/6) heterozygote mice from the Pftaire1 deficient line with C57BL6 for 10 generations, which continue to be viable (Figure 3-2 b). Nevertheless, due to the length of time the complete cleaning of the genomic background entitles; in most cases the results included in this thesis were obtained using mice of 6^{th} backcross generation or lower.

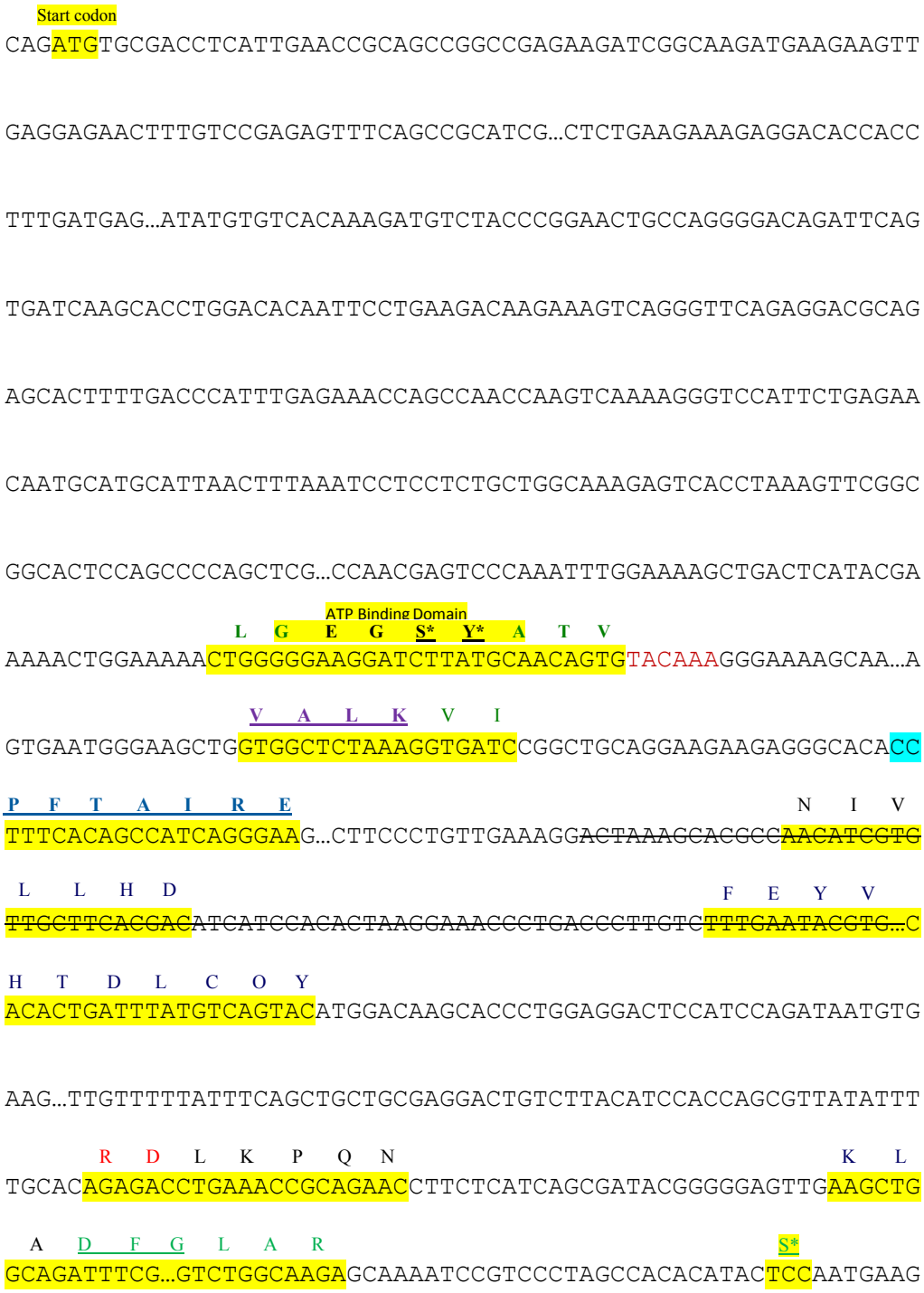
Start codon
CAGATGTGCGACCTCATTGAACCGCAGCCGGCCGAGAAGATCGGCAAGATGAAGAAGTT
GAGGAGAACTTTGTCCGAGAGTTTCAGCCGCATCG…CTCTGAAGAAAGAGGACACCACC
TTTGATGAG…ATATGTGTCACAAAGATGTCTACCCGGAACTGCCAGGGGACAGATTCAG
TGATCAAGCACCTGGACACAATTCCTGAAGACAAGAAAGTCAGGGTTCAGAGGACGCAG
AGCACTTTTGACCCATTTGAGAAACCAGCCAACCAAGTCAAAAGGGTCCATTCTGAGAA
CAATGCATGCATTAACTTTAAATCCTCCTCTGCTGGCAAAGAGTCACCTAAAGTTCGGC
GGCACTCCAGCCCCAGCTCG…CCAACGAGTCCCAAATTTGGAAAAGCTGACTCATACGA
ATP Binding Domain
L G E G S* Y* A T V
AAAACTGGAAAAACTGGGGGAAGGATCTTATGCAACAGTGTACAAAGGGAAAAGCAA…A
V A L K V I
GTGAATGGGAAGCTGGTGGCTCTAAAGGTGATCCGGCTGCAGGAAGAAGAGGGCACACC
P F T A I R E
N I V
TTTCACAGCCATCAGGGAAG…CTTCCCTGTTGAAAGGACTAAAGCACGCCAACATCGTG
L L H D
F E Y V
TTGCTTCACGACATCATCCACACTAAGGAAACCCTGACCCTTGTCTTTGAATACGTG…C
H T D L C O Y
ACACTGATTTATGTCAGTACATGGACAAGCACCCTGGAGGACTCCATCCAGATAATGTG
AAG…TTGTTTTTATTTCAGCTGCTGCGAGGACTGTCTTACATCCACCAGCGTTATATTT
R D L K P Q N
K L
TGCACAGAGACCTGAAACCGCAGAACCTTCTCATCAGCGATACGGGGGAGTTGAAGCTG
A D F G L A R
S*
GCAGATTTCG…GTCTGGCAAGAGCAAAATCCGTCCCTAGCCACACATACTCCAATGAAG

T L W Y R P P D V L

TGGTTACCTTGTGGTACAGACCTCCAGATGTTCTTCTGGGCTCTACAGAATATTCCACC

D M W G V G C I

TGCCTTGACATGTG…GGGAGTTGGCTGTATCTTCGTTGAGATGATCCAAGGAGTTGCTG

D O L E R I F L V L G

CGTTTCCAGGAATGAAAGACATTCAGGATCAACTTGAACGGATATTTCTG…GTTCTTGG

T P N E D T W P

AACACCGAATGAGGACACGTGGCCTGGAGTTCATTCTTTACCACATTTTAAGCCAG…AA

CGCTTTACCGTGTACAGCTCTAAAAGCCTTAGACAAGCATGGAATAA…GCTCAGCTATG

L O C S P K N

TAAATCATGCTGAAGACTTGGCCTCCAAGCTTCTCCAGTGTTCCCCAAAGAACAGGCTA

TCAGCACAGGCCGCCTTGAGCCATGAGTATTTCAGCGATCTGCCTCCACGGCTATGGGA

GCTGACTGATA…TGTCTTCTATTTTTACCGTCCCAAATTGAGATTGCAACCAGAAGCTG

GAGAGAGCATGAGGGCCTTTGGAAAAAACAATAGTTATGGGAAAAGCCTATCGAACAGC

AAACACTGA

Stop codon

Figure 3-1 The 14 coding exons of Pftaire1 in *Mus Musculus*

Coding sequence for Pftaire1-(ENSMUST00000030763), ~~Strikethrough~~ font illustrates the deleted nucleotides in the pftaire1 knockout allele. The deletion results in a frame-shift. For the wild type allele, exons 4-13 translate into kinase domains, ATP binding site (yellow highlight), inhibitory sites (red), and S/T activation site (green). Conserved PFTAIRE motif highlighted (blue); VLAK, HRD and DFG domains, respectively, (purple), (red), (green). Potential phosphorylation sites presented by (*). Start and stop codon (grey highlight). Dotted regions illustrate introns.

a) Deleted Sequence

GCTTCCCTGTTGAAAGGACT
AAAGCACGCCAACATCGTG
TTGCTTCACGACATCATCCA
CACTAAGGAAACCCTGACC
CTTGTCTTTGAATACGTGgta
agcgagataagaaggggtctagact
gcatgtgtcacgtttgaataaaactc
tcagtgttagtgagttggtttttaagtt
gctctatgaaatgaatgtttttttctga
gtacatgtgacatacatttgcataaa
atcatggccatgtgacaggcttttga
gtatgcatttcgttagacatgtggttt
atttatagcct

b) Mutant Allele

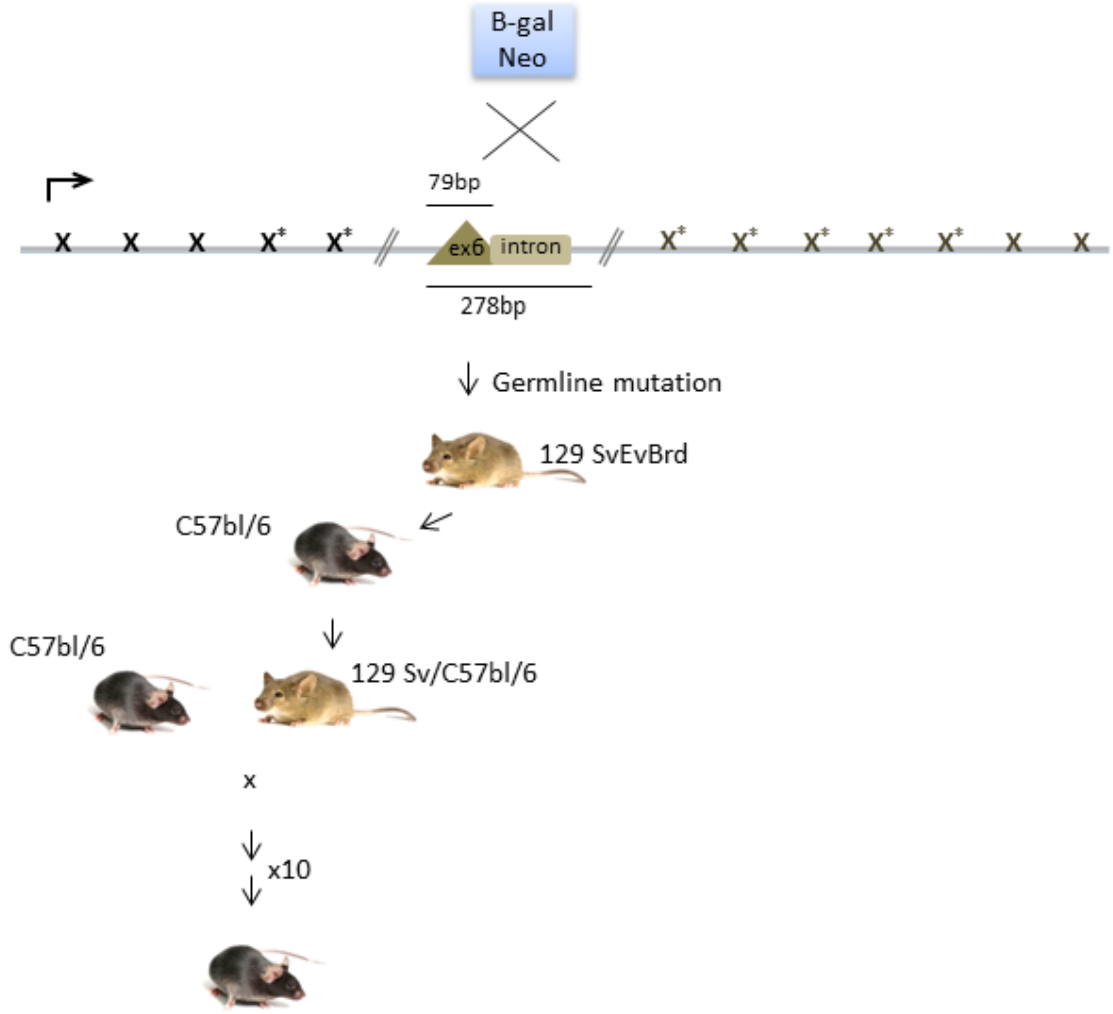

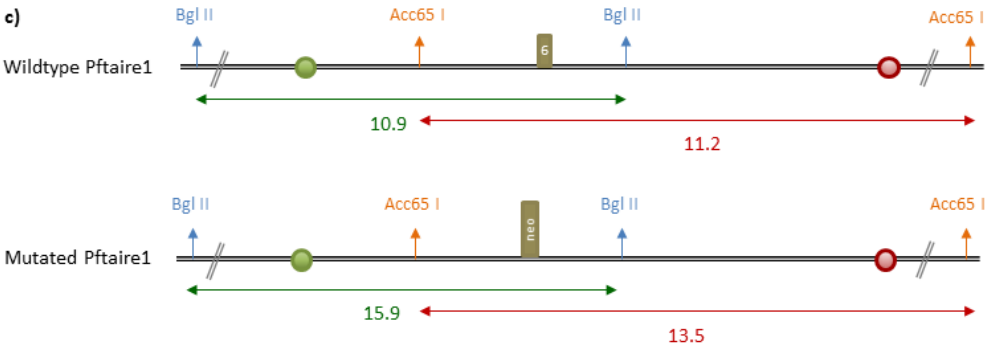

5'probe (644 bp)
A: 5' – CATACATCAGGCATCCAGGGTA
B: 5' – GGCTGGACTCCTGACTTCACCA

3'probe(684 bp)
C: 5' – CTTAGGAGAATTTGACATCCTCA
D: 5' – CAGTGAGTTCCGGAGCTAGTCT

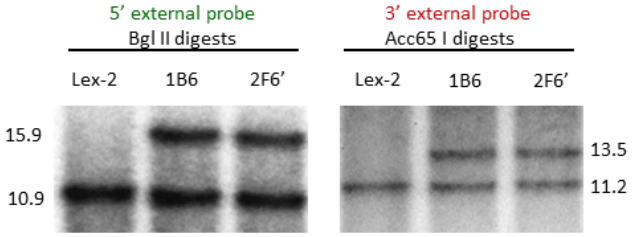

d)

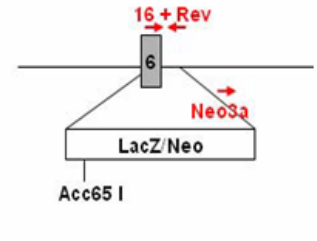

418 bp
341 bp

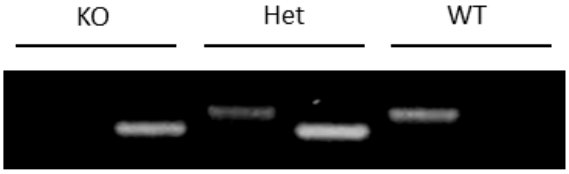

primers

WT	Fwd	5' – TGACCCTTGTCTTTGAATACGTG
KO	Fwd	5' – GCAGCGCATCGCCTTCTATC
WT/KO	Rev	5' – GGAAGCCTAAATTGTAAGGATCAGG

Figure 3-2 Generation of Pftaire1 knockout mice

a) Sequence deleted from mutant line, **b)** Schematic drawing illustrating the targeted deletion of exon 6 and the following intronic sequence to disrupt Pftaire1 gene. Exon 6 is replaced by βgal-neo cassette via homologous recombination in 129SvEvBrd/ES cells. Exons are depicted by **x**, domains likely to have kinase activity **x***. ES cells were injected into C57BL/6 blastocysts to obtain Heterozygous Pftaire1 mice. Pfaire1 heterozygotes were crossed to obtain Pftaire1 knockouts, followed by backcrossing for 10 generations to obtain a pure background. **c)** Following digestion by Bgl II and Acc 65 I, southern blot was performed using ^{32}P labeled probes outside the targeting vector, at 5' and 3' terminals, respectively. 5' terminal probe of 644 bp produces WT band: 10.9 kb, mutant band: 15.9 kb and 3' terminal probe of 684 bp produces: WT band: 11.2 kb, mutant band: 13.5 kb bands. **d)** PCR forward genotyping primers were designed within the deleted/replacing regions to ensure successful differentiation between wild type and knockout alleles; whereas a common reverse primer was designed with the conserved area of intron 6-7 for both alleles. Polymerization of wild type and knockout bands produces oligomers of 418 bp and 341 bp, respectively.

Successful removal of exon 6 and its replacement with the neo cassette in the Pftaire1 gene of Pftaire1 knockouts was confirmed by PCR genotyping on mouse tail genomic DNA at the time of weaning (P21). To ensure primer specificity, forward primers were designed specifically within the deletion cassette of exon 6 (the last 23 nucleotides of exon 6) and within the Neo cassette, for wild type and knockout, respectively. Also, Reverse primer was designed within a conserved area of intron 6-7 (Figure 3-2). Pftaire1 wild type and knockout mice, respectively, produced bands of 418 bp or 341 bp. Heterozygote mice were identified by the presence of PCR bands from both wild type and knockout alleles (Figure 3-2 d).

Subsequently, to determine if the translation of full length Pftaire1 is abolished in the Pftaire1 knockout mice, we examined for the presence of the full Pftaire1 product by western blot analysis of whole brain lysates from mouse embryos at E13.5-14.5 and adult mice, as well. Protein was extracted from brains of individual mice from each genotype and resolved on 12 % SDS-PAGE gels and then probed for Pftaire1 rabbit polyclonal antibody. Wild type, heterozygote mutants or homozygote mutants of Pftaire1 were compared for Pftaire1 protein expression. When processing embryonic samples, a band was detected for wild type Pftaire1 at about 48 kDa; the intensity of the signal was lower in heterozygote mice. No band was detected when blotting for Pftaire1 in the knockout (Figure 3-3 d). Previous reports by Lazzaro et al. (Lazzaro, Albert et al. 1997) and Besset et al. (Besset, Rhee et al. 1998), confirm that Pftaire1 protein migrates at 47.5 (Lazzaro, Albert et al. 1997) to 53 kDa (Besset, Rhee et al. 1998). However, Besset et al. detected an extra band at 39 kDa in brain extracts (Besset, Rhee et al. 1998). In our case, when we

processed adult and pups samples, we observed a double band for Pftaire1 in wild type and the heterozygote mutant of Pftaire1 but none in Pftaire1 homozygote mutants (Figure 3-3 d). This observation is consistent with the splice forms reported for Pftaire1, Cdk14-002 (ENSMUST00000030763) and Cdk14-09 (ENSMUST00000115452), which translate into a protein product with 469 and 451 residues, respectively. As discussed previously, the transgenic mutation produced in Pftaire1 gene results in a frame shift mutation and a premature stop codon. Next, we examined whether disruption of Pftaire1 affects the protein levels of any of its close family members. We did not observe any difference in the levels of Pftaire2, Pctaire1, and Cdk5 among wild type and knockout Pftaire1 mice pups at P21 (Figure 3-4). The equal level of these Pftaire1 family members in the knockout mice suggests that they may not be compensating for any Pftaire1 deficits at the expression level. However, their kinase activity needs to be determined.

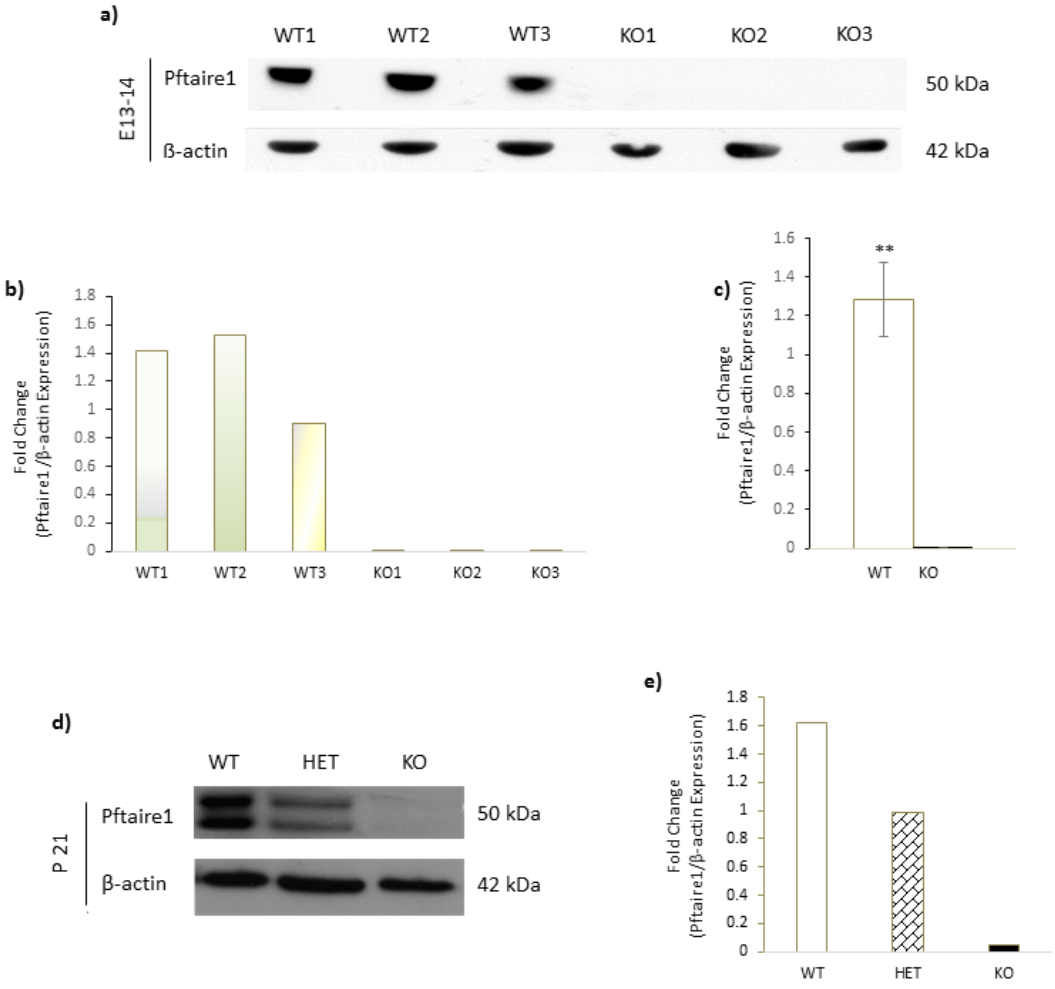
a)
WT1
WT2
WT3
KO1
KO2
KO3
E13-14
Pftaire1
ß-actin
50 kDa
42 kDa
b)
Fold Change
(Pftaire1/β-actin Expression)
1.8
1.6
1.4
1.2
1
0.8
0.6
0.4
0.2
0
WT1
WT2
WT3
KO1
KO2
KO3
c)
Fold Change
(Pftaire1/β-actin Expression)
**
1.6
1.4
1.2
1
0.8
0.6
0.4
0.2
0
WT
KO
d)
WT
HET
KO
P 21
Pftaire1
β-actin
50 kDa
42 kDa
e)
Fold Change
(Pftaire1/β-actin Expression)
1.8
1.6
1.4
1.2
1
0.8
0.6
0.4
0.2
0
WT
HET
KO

Figure 3-3 Pftaire1 protein expression is successfully disrupted in Pftaire1 homozygote mutant mice

Disruption of Pftaire1 in knockout mice in comparison to wild type mice observed. Equal loading was confirmed by β-actin probing. **a)** Western blot of Pftaire1 extracted from whole brain lysates from the progeny of a Het x Het intercross. Whole brain lysates were prepared from mouse embryos E13.5-14.5. Pftaire1 was probed with Pftaire1 rabbit polyclonal antibody (SantaCruz). **b)** Column graph illustrating quantification of Western blot by densitometry analysis for representative blot shown above in section a, **c)** Column graph representing quantification of signal for western blot b, columns represent (Mean ± SEM), n=3 for wild type and knockout quantification s p=0.003 ** denotes significant at p<0.01. **d)** Western blot of Pftaire1 extracted from whole brain lysates from the progeny of a Het x Het intercross. Whole brain lysates were prepared from mouse pups at P21, respectively. Pftaire1 was probed with Pftaire1 rabbit polyclonal antibody (SantaCruz). **e)** Quantification of Western blot by densitometry analysis for representative blot shown beside in section d. Columns represent fold changes of Pftaire1 expression in wild type, heterozygote and homozygote mutants of Pftaire1 normalized to β-actin.

a)

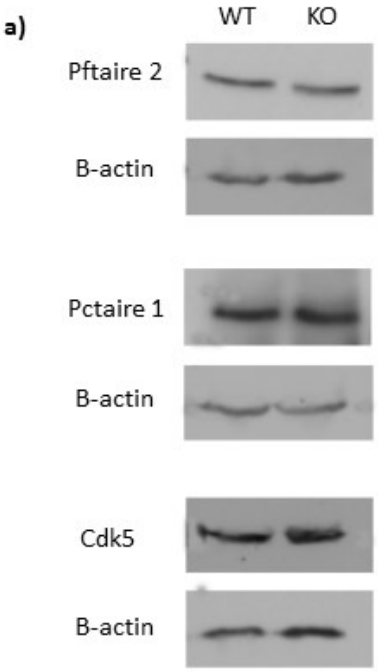
WT
KO
Pftaire 2
B-actin
Pctaire 1
B-actin
Cdk5
B-actin

b)

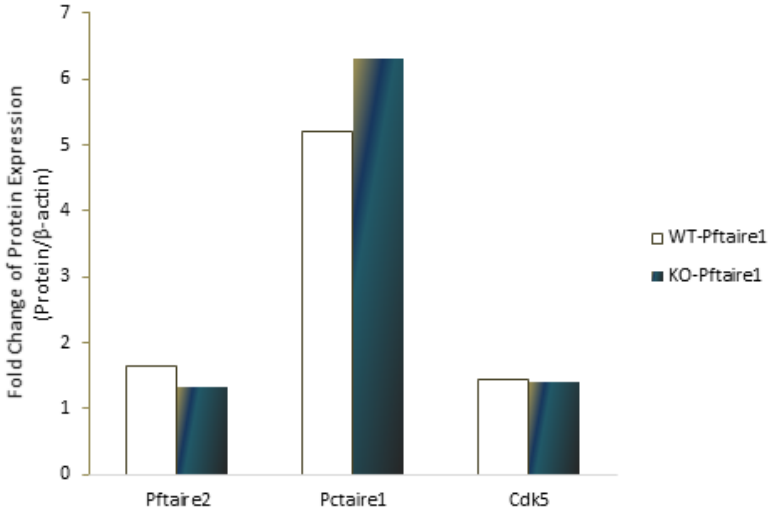
Fold Change of Protein Expression (Protein/β-actin)
0
1
2
3
4
5
6
7
Pftaire2
Pctaire1
Cdk5
WT-Pftaire1
KO-Pftaire1

Figure 3-4 Expression level of Pftaire1 homologues is not affected by Pftaire1 deficiency

Western blot of total protein extracted from whole brain lysates of the progeny of a Het x Het cross in mouse embryos at P21 and immunolabelling for Pftaire2, Pctaire1, and Cdk5 proteins with related antibodies. Disruption of Pftaire1 in knockout mice does not appear to affect the levels of Pftaire2, Pctaire1, and Cdk5 as revealed by western blot. This indicates neither of these genes compensate for the loss of Pftaire1. Equal loading was confirmed by β-actin probing. **b)** Column graph illustrating quantification of Western blot by densitometry analysis for representative blot shown beside in section **a**. Columns represent fold changes of Pftaire2, Pctaire1, and Cdk5 expression, respectively, in wild type, and Pftaire1 knockouts normalized to β-actin.

Since, the Pftaire1 allele is mutated in the germ cells we determined the survival of Pftaire1-knockout mice by evaluating the Mendelian ratios. The mice were genotyped

by PCR as described earlier and Mendelian ratios were obtained using the chi^2-test (p<0.05). We evaluated a total of F1: n=21 (Het x Het) breeding crosses that were backcrossed with C57Bl6, at least for a minimum of 9 times (Table 3-1). Heterozygote intercrossing of Pftaire1 mice F1: (Het x Het) produces F2 offspring of wild type, heterozygote, and homozygote mutant that do not differ significantly from the expected 1:2:1 Mendelian ratios.

At the approximate age of E13.5-14.5, from a total of F1: (Het x Het) of 15 breeding pairs, F2 produced a total of 132 mice, of which 28% (n=37) were knockout mice, which is not significantly different from expected Mendelian ratios (χ^2 = 5.8, p = 0.055) (Table 3-1 a). At the approximate age of P21 (time of weaning), from the total of F1: (Het x Het) of 6 breeding pairs, F2 produced a total of 37 mice of which 24.3% (n=9) were knockout mice, which is not significantly different from expected Mendelian ratios (χ^2 = 0.46, p = 0.79) (Table 3-1 b). Also among another 18 breeding pairs that were not fully backcrossed were compared, F1: (Het x Het) of 18 breeding pairs, F2 produced a total of 128 mice of which 18.8% (n=24) were knockout mice, which is not significantly different from expected Mendelian ratios (χ^2 = 3.3, p = 0.2) (Table 3-1 c) (Figure 3-5). Moreover, within our observations the Pftaire1-knockout mice seem to survive to adulthood and be normally fertile. Four Pftaire1-knockout animals (n=4) were maintained for over eighteen months. These mice were mated as two individual breeding pairs (n=2), which remained fertile up to 13 months and 18 months of age, respectively. The aged mice were humanely culled at the age of 18 months. To conclude a normal lifespan within Pftaire1- knockout

mice, investigation is required upon completion of backcrossing into C57BL6 background, with higher number of mice.

Table 3-1 The number of Pftaire1 homozygote mutant mice does not differ significantly from Mendelian ratios.

a)

Genotype	HET	WT	KO	Expected KO	Total mice
Number of mice	74	21	37	33	132
Total percent	56.0%	15.9%	28.0%	25%	100

b)

Genotype	HET	WT	KO	Expected KO	Total mice
Number of mice	17	11	9	9.2	37
Total percent	45.9%	29.7%	24.3%	25%	100

c)

Genotype	HET	WT	KO	Expected KO	Total mice
Number of mice	73	31	24	32	128
Total percent	57.0%	24.2%	18.8%	25%	100

Table 3-1 summarizes the PCR results of the F2 offspring. F2 offspring from F1 intercrossed (HET x HET) mice were genotyped for Pftaire1 gene by PCR. A total of 39 breeding crosses were evaluated which were subsequently divided into 3 categories. Percentage of knockout mice does not differ from Mendelian ratios, significantly ($p > 0.05$). **a)** Mouse embryos at E13.5-14.5, backcrossed with C57Bl6 for a minimum of 9 times, **b)** Mouse pups at P21, backcrossed with C57Bl6 for a minimum of 9 times, and **c)** Mouse pups at P21, not fully backcrossed to C57Bl6.

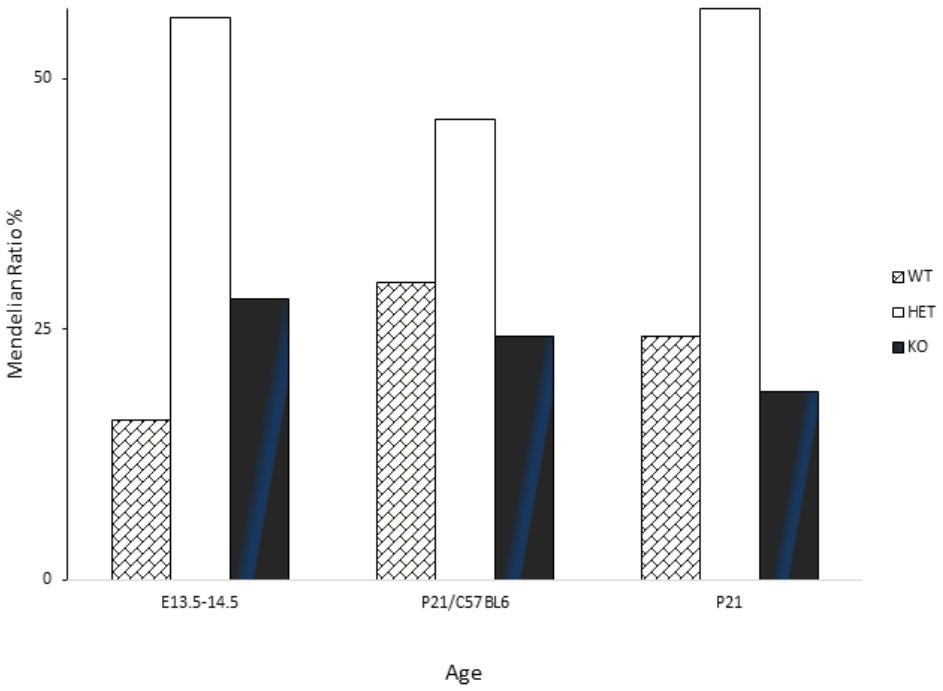
50
25
0
Mendelian Ratio %
E13.5-14.5
P21/C57BL6
P21
Age
WT
HET
KO

Figure 3-5 Survival percent of Pftaire1 homozygote mutant mice does not differ significantly from Mendelian ratios.

Column graph representing Mendelian ratios in F2 progeny. Effect of genotype on percent of survival of progeny resulted from heterozygous intercrossing of Pftaire1 mice plotted on a chart. Significance determined by χ^2 test ($p > 0.05$).

3.1.2. No abnormal phenotype detected in Pftaire1 null mice

Since PFTAIRE deficiency leads to embryonic lethality in fruit flies (Stowers, Garza et al. 2000); we questioned whether loss of Pftaire1 could have a significant impact on mouse development. Macroscopic and morphological examination of Pftaire1 knockout mice, in comparison to their wild type littermates revealed no abnormal phenotype within our observations to date: the pups are viable, age normally and do not show any obvious morphological defects during their life span. We did not detect any obvious alterations in brain morphology within our observations.

3.1.3. Microscopic Analysis of Brain Section

3.1.3.1. Brains of adult Knockout Pftaire1 mice did not show any gross anatomical abnormality by cresyl violet staining

Microscopic analysis of coronal sections of the adult mice brain on a mixed C57Bl6 background revealed no major abnormalities upon cresyl violet staining. Brain sections of two month old, adult wild-type (n=3) and Pftaire1 null mice (n=3), were collected starting at the frontal cortex at bregma: ~ 2.710 mm up through the 4th ventricle at bregma: ~-4.20 mm. The structure of the cortex, septostriatal region, the organization of the hippocampus, shape of the dentate gyrus, diencephalon, mesencephalon, all follow the normal gross anatomy of the brain. Sections representing bregma 1.98, 1.70, 0.74, 1.00, 1.64, and 2.75 mm are presented, respectively, in section “a-f” and “g-l” (Figure 3-6). These results suggest that Pftaire1 loss, alone, in mice, might not have the same effects observed with L63E deficiency in the fly (Rodríguez González and S. 2011). However, the effect of Pftaire1 on development of the brains needs to be examined during younger

ages including the embryonic period using different methods. For instance, silver staining could give us a better idea with regards to the structure of the brain.

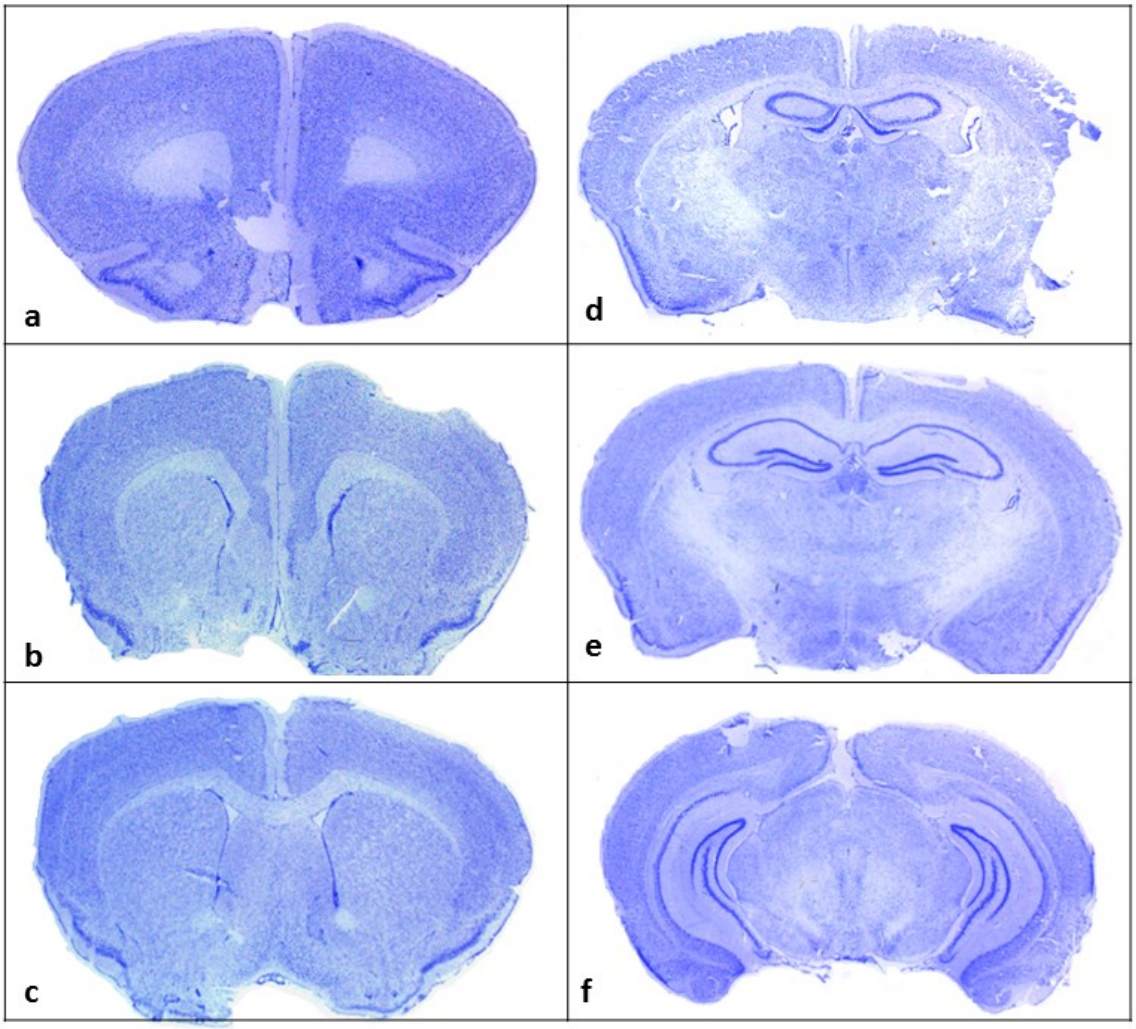
a
d
b
e
c
f

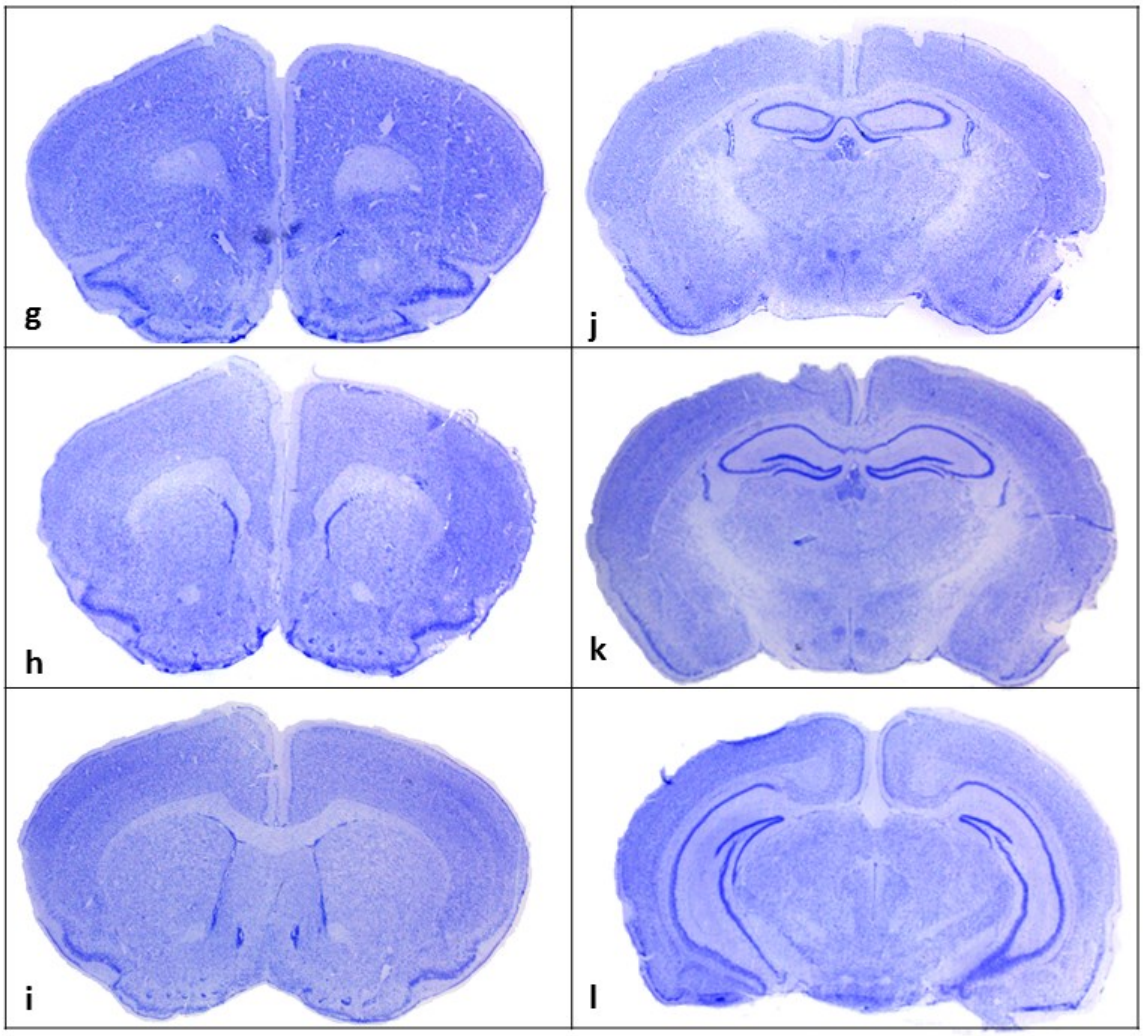
g
j
h
k
i
l

Figure 3-6 Cresyl violet stained sections from Pftaire1 knockout mice reveals no gross abnormality in comparison to wild type mice

Sections representing bregmas: 1.98, 1.70, 0.74, 1.00, 1.64, and 2.75 mm are presented, respectively, in section “a-f” for wild type (n=3) and “g-l” for knockout (n=3). Brains were collected from three month old adult mice, perfused and fixed for sectioning. 14μm sections were collected from cryopreserved samples, sections were collected starting from the cortex at bregma: ~ 2.710 mm up through the 4th ventricle at bregma: ~-4.20 mm. Sections were then stained with cresyl violet to examine the gross anatomy of the brain. Histological examination following cresyl violet staining of Pftaire1 knockout mice brain, reveals no abnormality in the structure of the cortex, septostriatal region, hippocampal organization, shape of the dentate gyrus, diencephalon, and mesencephalon.

3.1.4. Disruption in Pftaire1 does not lead to any difference in basal survival in primary cortical cultures

We investigated whether manipulating Pftaire1 activity has any effect on its basal cell survival or it acts in a manner similar to Cdk5 (O'Hare, Kushwaha et al. 2005). To determine cell viability upon disruption of Pftaire1 activity, we co-infected primary cortical neurons (MOI=100) with GFP along with WT Pftaire1 or the dominant negative form of Pftaire1, (D228N), in which the highly conserved aspartic acid residue of Pftaire1 at residue 228 was mutated to asparagine, by a point mutation (Lazzaro, Albert et al. 1997) as a kinase inactive control for transient transfections. This residue is highly conserved among all protein kinases, and inhibits the endogenous kinase activity of cdc2 kinases in its mutated form upon ectopic expression (Taylor, Knighton et al. 1993, van den Heuvel and Harlow 1993). Neurons were cultured for 12, 16, and 24 hours post-infection, then fixed and stained with Hoechst for detection of morphologically intact healthy nuclei. GFP expressing neurons with viable nuclei were counted. We did not observe a difference in basal survival rate among neurons expressing GFP with Pftaire1 or D228N-Pftaire1 and GFP alone (Table 3-2), (Figure 3-7). From a total of n=1602, (77.1 ± 1.8%), of n=2293, (77.8 ± 1.0%), of n=4533, (92.9 ± 0.6%)of D228N expressing neurons survived at 12, 16, and 24 hours, respectively, which does not significantly differ (p>0.05) from GFP control and WT (Table 3-2), (Figure 3-7). Our result, suggests that Pftaire1 and its dominant negative form D228N do not affect cell viability under normal circumstances.

Table 3-2 Pftaire1 overexpression or disruption does not affect basal survival rates of cortical neurons *in vitro*.

Mean ±SEM			
Time-point	GFP	WT	DN
12 hrs	79.4±1.5	78.3±2.7	77.1±1.8
16 hrs	78.2±1.0	76.0±1.0	76.8±1.0
24 hrs	93.5±0.2	94.5±0.4	92.9±0.6

Table 3-2 represents survival of cortical neurons as (Mean ± SEM), n=3 and 3 replicas per treatment. Basal survival rates of Pftaire1 wild type and D228N vs control is not significant as per ANOVA and Newman-Keuls for means $p>0.05$.

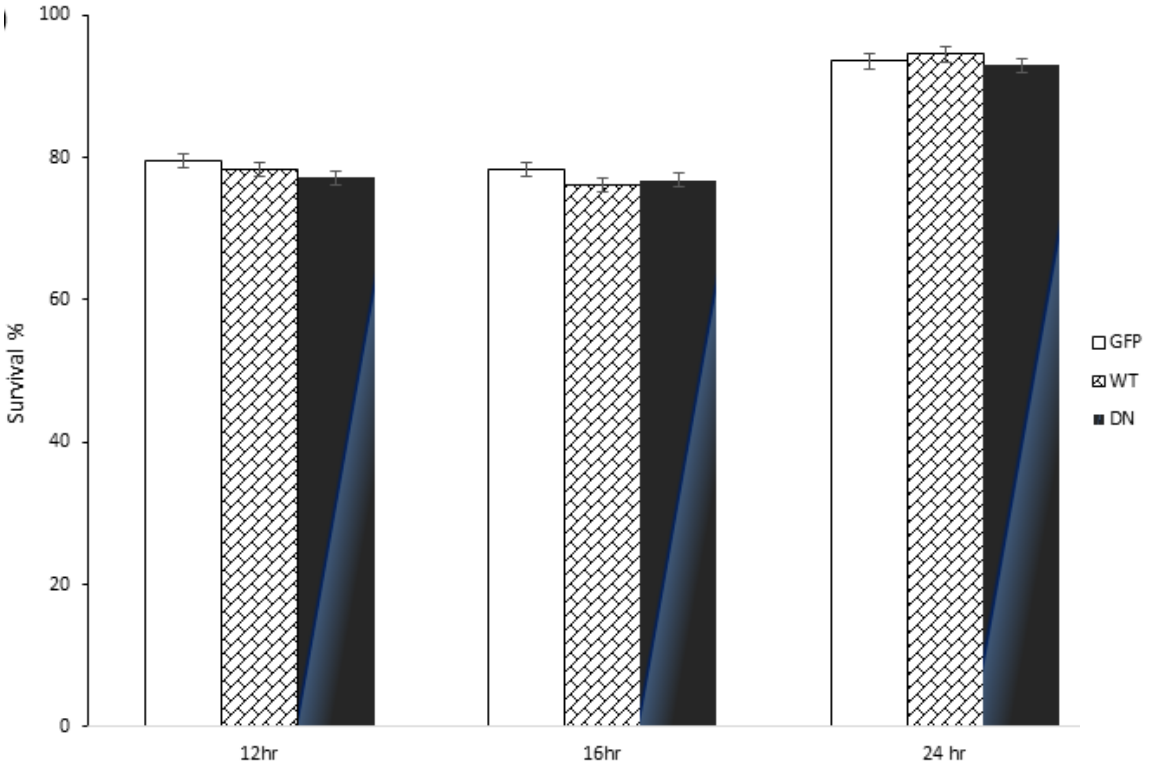
100
80
60
40
20
0
Survival %
12hr
16hr
24 hr
GFP
WT
DN

Figure 3-7 Pftaire1 overexpression or disruption does not affect basal survival rates.

Column Graph representing percent of survival for each treatment with relation to its incubation period. Primary cortical neurons derived from CD1 mice were infected with GFP alone, or co-infected with GFP and WT-Pftaire1 or D228N-Pftaire1 (MOI=100), incubated for 12, 16, and 24 hours, followed by fixation, and Hoechst 33258 staining. Percentage of survival was calculated as percentage of morphologically intact live nuclei over total GFP-expressing neurons. Data/columns represent the (Mean ± SEM), n=3 and 3 replicas per treatment. $p>0.05$ ANOVA, t-Test: paired two sample for means is N.S., no significant difference is observed in basal survival rates of Pftaire1 wild type and D228N vs control.

3.2. Pftaire1 negatively regulates axon length in primary cortical cultures of mouse embryos at E13.5-14.5

3.2.1. Dominant Negative D228N-Pftaire1 expression *in vitro* increases axonal length in cortical cultures

Previous research indicates that Cdk5 inactivation leads to inhibition of axonal growth (Nikolic, Dudek et al. 1996, Nikolic, Chou et al. 1998). In addition, Pctaire1-3 negatively regulates neurite outgrowth (Cole 2009). We speculated whether manipulation of Pftaire1 activity would also have an impact on axon outgrowth. To test this notion, primary cortical cultures were prepared from CD1 mouse embryos at E 13.5-14.5 days and subjected to adenoviral infection with GFP tagged-D228N Pftaire1, GFP tagged-wild type Pftaire1 or GFP control alone, at the time of plating. After allowing cultured neurons to grow and differentiate, they were fixed at subsequent time points: 12, 24, and 48 hours post-infection (Figure 3-8). Neurites were then stained with GFP for an enhanced infection signal and reliable tracing. Also, Hoechst 33258 staining was performed to assess viability of neurons (Figure 3-8 a). Digital images were acquired with Zeiss Axioskop 2 Mot microscope. The total length of neurites was measured on digitally acquired images utilizing Stereo-investigator (version 6; MicroBrightField, Williston, VT) software using the contour mapping mode and tracing the length of axons. Lengths were determined measuring at the 40X objective magnification and diameter of field of view was 575 µm. Measurements were commenced from the edge of the GFP expression in the cell body to the distal terminal of the neurite using the longest neurite for comparative purposes. Each experiment was repeated for a minimum of 3 times and each

treatment was replicated in triplets. The change in axon length is represented and the significance is determined by one way-ANOVA followed by Student-Newman-Keuls post–hoc test and Bonferroni. At 12 hours, a total of 372 neurites were measured. For D228N-Pftaire1 infected neurons, n=124 and (Mean ± SEM) was (14.5 ± 0.6) was statistically significant, as confirmed by one way ANOVA (p<0.001) followed by Student-Newman-Keuls method, from GFP control (10.9 ± 0.7 µm) (p=8.2E-06) and WT-Pftaire1 (10.16 ± 0.5 µm) (p=2.9E-07) but not WT relative to GFP (p=0.3) (Figure 3-8 b). At 16 hours, a total of 1408 neurites were measured and for D228N-Pftaire1 infected neurons, n=509, (Mean ± SEM) was (33.0 ± 0.8 µm) that was statistically significant by one way ANOVA (p<0.001) with Student-Newman-Keuls method from GFP control (24.5±0.7 µm) (p=7E-13) and WT-Pftaire1 (24.6±0.8 µm) (p=3E-11) but WT relative to GFP (p=0.9) (Figure 3-8 b). At 24 hours, a total of 891 neurites were measured. For D228N-Pftaire1 infected neurons, n=241 (Mean ± SEM) was (129.6 ± 3.6 µm) that was statistically significant (p<0.001, ANOVA) with Student-Newman-Keuls method from GFP control (97.9 ± 3.9 µm) (p=6.4E-09) and WT-Pftaire1 (89.5 ± 2.6 µm) (p=3.4E-18) but not WT relative to GFP (p=0.07) (Figure 3-8 b). At 48 hours, a total of 724 neurites were measured. For D228N-Pftaire1 infected neurons, n=283, (Mean ± SEM) was (253.6 ± 9.1 µm) that was not statistically significant (p > 0.05, ANOVA) with Student-Newman-Keuls method from GFP control (275.0 ± 10 µm) (p=0.1) and WT-Pftaire1 (241.3 ± 12.4 µm) (p=0.4); also, GFP and WT (p=0.03) were not significant (Figure 3-8 b). According to our data the D228N-Pftaire1 expressing neurons, showed an enhanced ability to elongate when they were compared to wild type and GFP control expressing neurons, at early time-points (12-24 hours);

however, later at 48 hours, they do not show any difference with GFP control or wild type mice (Figure 3-8 b, c, and d). Also, we show that the percentage of difference to GFP control, in mean neurite length, is higher in D228N expressing neurons. At 12, 16, and 24 hours, we observe a 32.4%, 34.7%, and 32.3% increase in mean neurite length compared to GFP which significantly differs from GFP but not WT in comparison to GFP (Figure 3-8 c). Also, average of log10 of axon measurements of D228N expressing neurons, revealed a linear distribution with higher measures as compared to wild type, at 12, 16, and 24 hours (Figure3-8 d). Furthermore, classifying axons into groups based on their length, reveals a significant difference ($p < 0.0001$) between the GFP, wild-type and the D228N-Pftaire1 group, as determined by chi-square test. We classified neurons into three groups based on the length of their neurites. To classify, average and median were calculated for each time-point. The maximum and minimum numbers related to average and median were considered as average range for that time-point and neurites diverting were from this range were considered as either short or long, relatively. In neurons expressing D228N-Pftaire1, a significantly higher percent of neurons, had longer axons at early time-points 12 (p= 7E-09), 16 (p= 1.6E-12), and 24 hours (p= 1.9E-14) but this difference became insignificant at 48 hours (p= 0.07) (Figure 3-8 d, e). Our data suggests that there is an increase in neurite length *in vitro* upon ectopic expression of D228N-Pftaire1. Previous studies report that loss of Cdk5 results in a decrease in axon length (Nikolic, Dudek et al. 1996). Our observations, suggest that D228N might have an effect that is opposite to that of Cdk5 on axon growth *in vitro.* Thus, we postulate that Pftaire1 might have a role opposite to Cdk5 in regulating axon growth.

a)

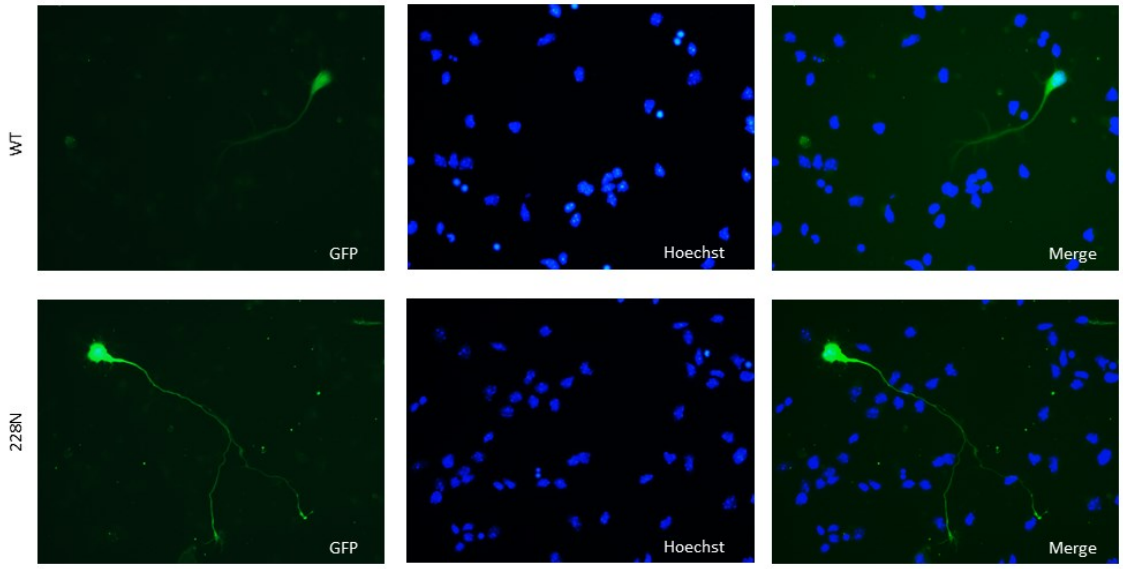
WT
228N
GFP
Hoechst
Merge
GFP
Hoechst
Merge

b)

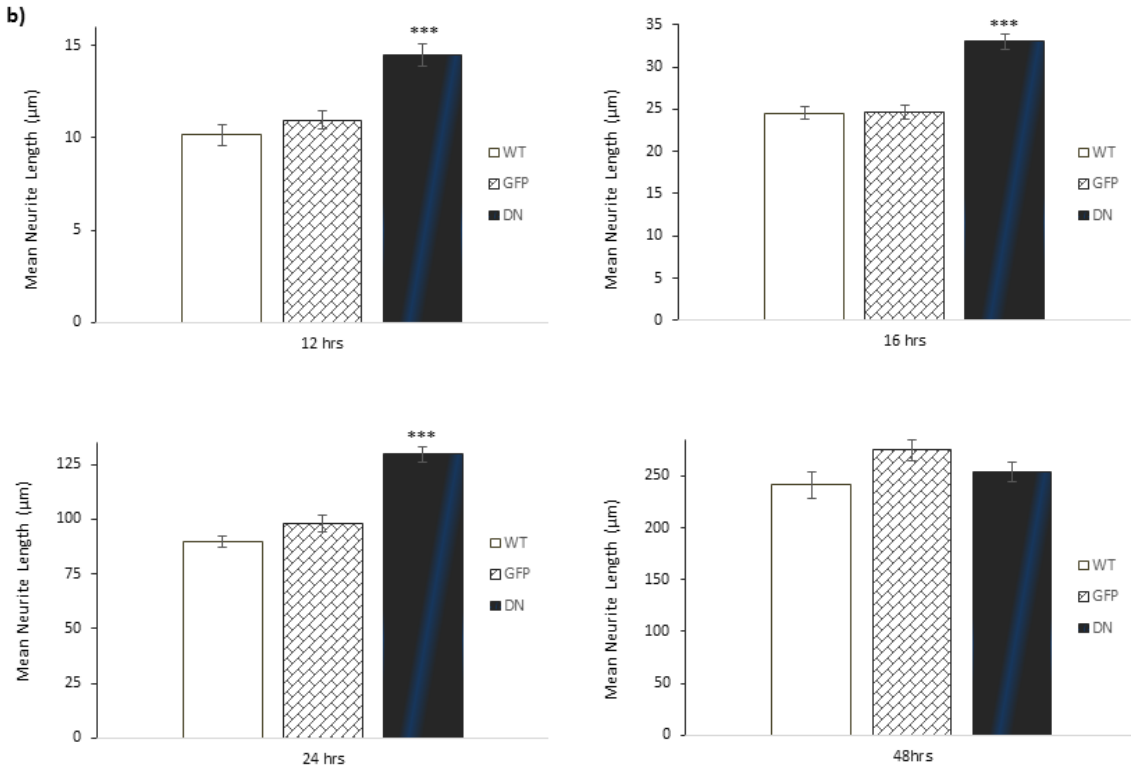
Mean Neurite Length (µm)
***
WT
GFP
DN
12 hrs
16 hrs
24 hrs
48hrs

c)

e)

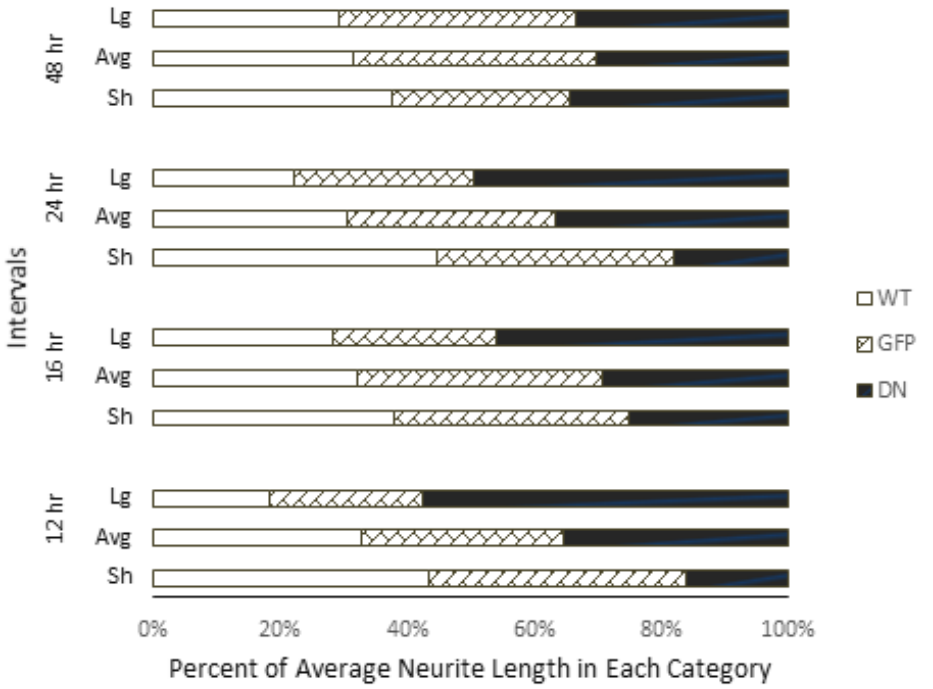
Intervals
48 hr
24 hr
16 hr
12 hr
Lg
Avg
Sh
WT
GFP
DN
0%
20%
40%
60%
80%
100%
Percent of Average Neurite Length in Each Category

d)

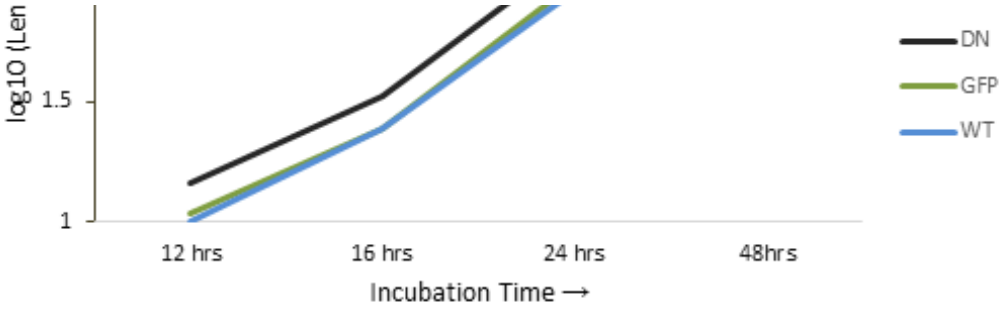
log10 (Len
1.5
1
12 hrs
16 hrs
24 hrs
48hrs
Incubation Time →
DN
GFP
WT

Figure 3-8 Overexpression of dominant negative Pftaire1, enhances axon outgrowth in primary cortical cultures

Image, representing immunostaining of infected neurons with GFP, Hoechst, and merged. Staining was performed to enhance GFP signal for reliable neurite tracing and to determine the viability of neurons assessed. **b)** Column graphs, representing (Mean ± SEM) at different time points (12, 16, 24, and 48 hours post infection. **c)** Column graph, representing percent of difference in mean neurite length of WT and D228N neurites in relation with GFP control. **d)** Same data, represented as log10 of neurites at different time points to homogenize the different distribution pattern over time for easier comparison. **e)** Also, classification of axons into different group based on their lengths (Sh: short, Avg: average, and L: long. Cut off values for each category are 9-14.4; 23.3-33; 85.4-129.5; and 201-275 μm at 12, 16, 24, 48 hrs respectively) reveals more neurons with longer axons especially at earlier time points in the D228N-Pftaire1 cultures, as opposed to, GFP control and WT. Primary cortical cultures were prepared from mouse embryos at E13.5-14.5, infected with AV-virus expressing Pftaire1, D228N-Pftaire1 and GFP (MOI=100), and fixed

at different time points post infection, stained with GFP and Hoechst to enhance signal strength to determine cell viability, respectively. Each experiment was performed for a minimum of three times (n=3) and each treatment was replicated three times. Fluorescent pictures were taken and measurements were done using stereoinvestigator software, as described earlier. The measurements were statistically tested with one way ANOVA ($p < 0.05$) followed by student Newman-Keuls test to determine significance.

3.2.2. Primary neuronal cultures of Pftaire1 null mice produce longer axons

Ectopic expression of dominant negative Pftaire1 *in vitro,* resulted in enhanced axon length in cortical cultures (Figure 3-9). To investigate, whether the effects of D228N overexpression on axon outgrowth could be replicated by Pftaire1 deficiency, we studied populations of axons in primary cortical cultures from Pftaire1 deficient mice. We crossed heterozygote Pftaire1 mice to obtain littermates that were either Pftaire1 wild types or homozygote mutants. Cultures were prepared from mouse embryos at gestation days 13.5-14.5 from generation 6 backcrossed animals. To detect the genotype of the littermates, samples were taken from each embryo at the time of dissection but all further processing of axon assessment was done in a blind manner. The cells were plated and fixed and stained at 16 and 24 hours after seeding (Figure 3-9 a). At both time points, the axon length of Pftaire1-knockout neurons was found to be significantly longer than WT cultures ($p < 0.0001$, upon student's paired two tailed t-test) (Figure 3-9). At 16 hours, axons from primary cortical cultures prepared from 3 different Het x Het crosses (litters) were compared, in 3 replicates, and a total n=15 (wild type n=6, knockout n=9) mice were

examined. Axons were detected using Tau-1 microtubule marker and viability of neurons was assessed using Hoechst 33258 (Figure 3-9 a). Length of axons was measured, on digitally acquired fluorescent images at the 40X objective magnification with a diameter of field of view of 575 µm using Northern Eclipse Zeiss on Zeiss Axioskop 2 Mot fluorescent microscope, utilizing Stereo-investigator (version 6; MicroBrightField, Williston, VT) software using the contour mapping mode. Measurements were commenced from the edge of the Tau-1 expression in the cell body to the distal terminal of the axon. We observed a significant increase in the length of axons of KO-Pftaire1 neurons when compared to WT-Pftaire1. (Mean ± SEM) was (131.2 ± 1.9) µm (n= 2510) for KO axons and (90.0 ± 1.6) µm (n=1738) for WT axons (*p*=2E-37) (Figure 3-9 b). The same trend was observed at 24 hours while fluorescent Digital images were acquired with Zeiss Axioskop 2 Mot fluorescent microscope at objective 20 x magnification with a field of view diameter of 1150 µm. For measuring, axons were traced on digitally acquired images using Stereo-investigator (version 6; MicroBrightField, Williston, VT) software utilizing the contour mapping mode. At 24 hours, among two different litters n=6 (wild type n=3, knockout n=3), (Mean ± SEM) was (204.0 ± 3.3) µm (n= 1499) for KO axons and (158.68 ± 3.0) µm (n=1272) for WT axons (*p* = 2E-37) (Figure 3-9 b). In other words, KO axons revealed a 45.6% and 28.5% increase in relative axonal length in comparison to WT axons, prepared from the progeny of Het x Het crosses primary cortical neurons, at 16 and 24 hours, respectively (Figure 3-9 c). Also, average of log10 of axon measurements of knockout Pftaire1 axon lengths revealed a linear distribution with higher measures, as compared to wild type, both at 16 and 24 hours (Figure 3-9 d). Next, axons were binned according to

their lengths into short, average, and long ranges, as explained previously. The maximum and minimum numbers related to average and median were considered as average range for that time-point and neurites diverting were from this range were considered as either short or long, relatively and statistical significance was determined by chi-square (p < 0.001). At 16 hours, KO and WT neurons consisted of 40.8% and 25% long axons (p = 2.12E-64), respectively. At 24 hours, the KO and WT neurons consisted of 41.8 % and 28.3 % longer axons (p= 9.58E-15), respectively (Figure 3-9 e).

a)

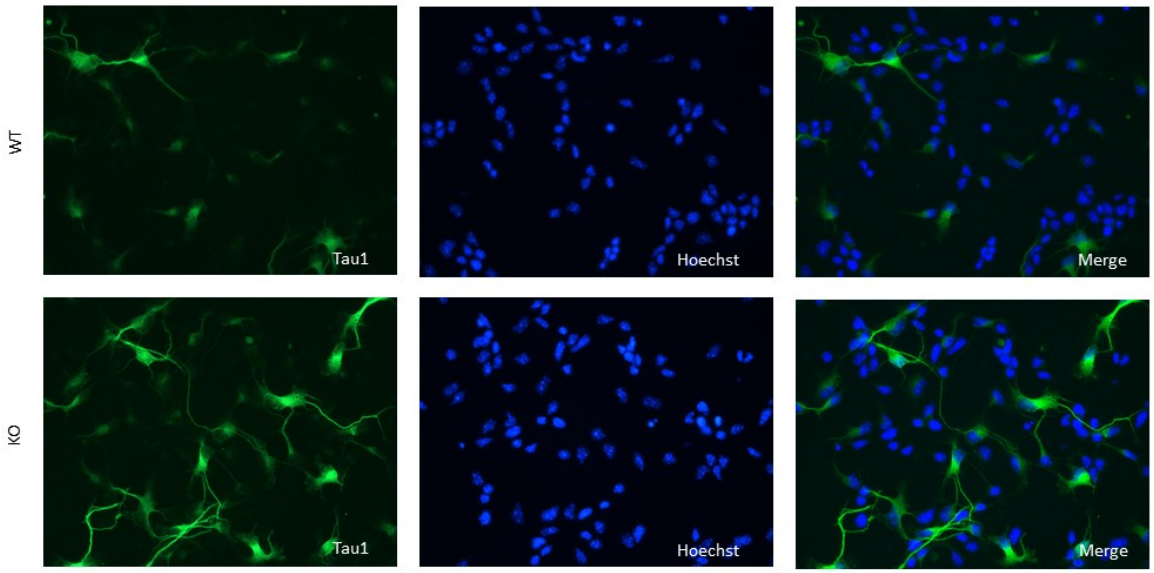
WT
KO
Tau1
Hoechst
Merge
Tau1
Hoechst
Merge

b)

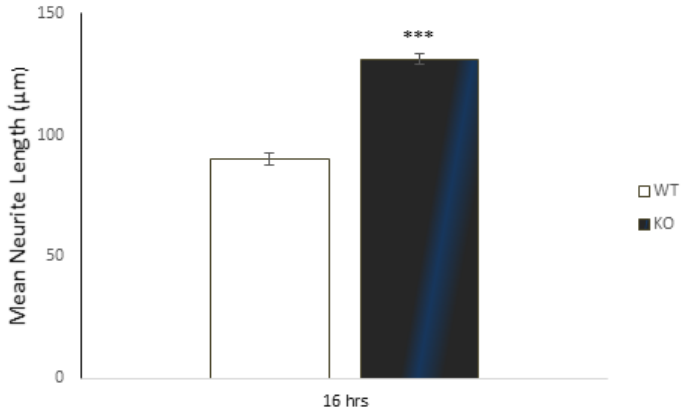
Mean Neurite Length (µm)
150
100
50
0
***
16 hrs
WT
KO

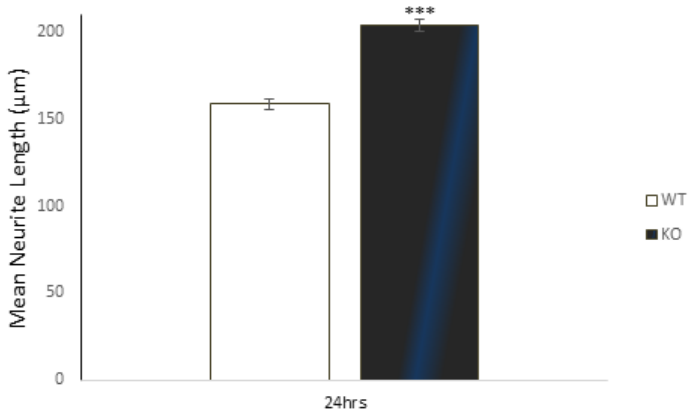
Mean Neurite Length (µm)
200
150
100
50
0
***
24hrs
WT
KO

c)

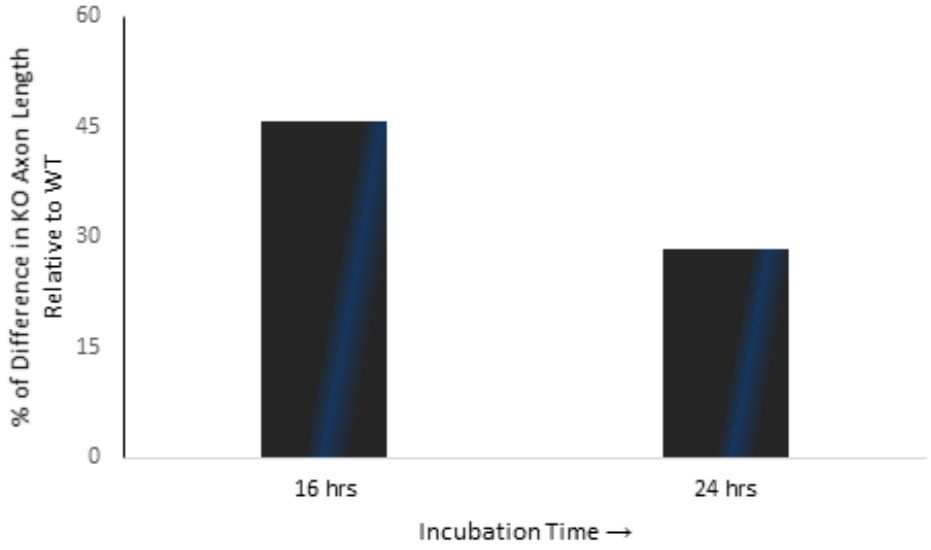
60
45
30
15
0
% of Difference in KO Axon Length Relative to WT
16 hrs
24 hrs
Incubation Time ⟶

d)

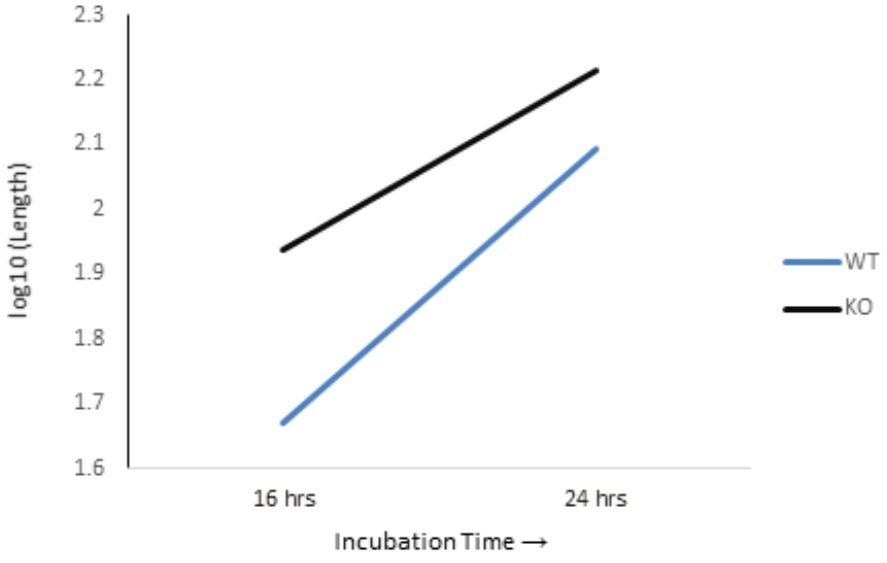
2.3
2.2
2.1
2
1.9
1.8
1.7
1.6
log10 (Length)
16 hrs
24 hrs
Incubation Time ⟶
WT
KO

e)

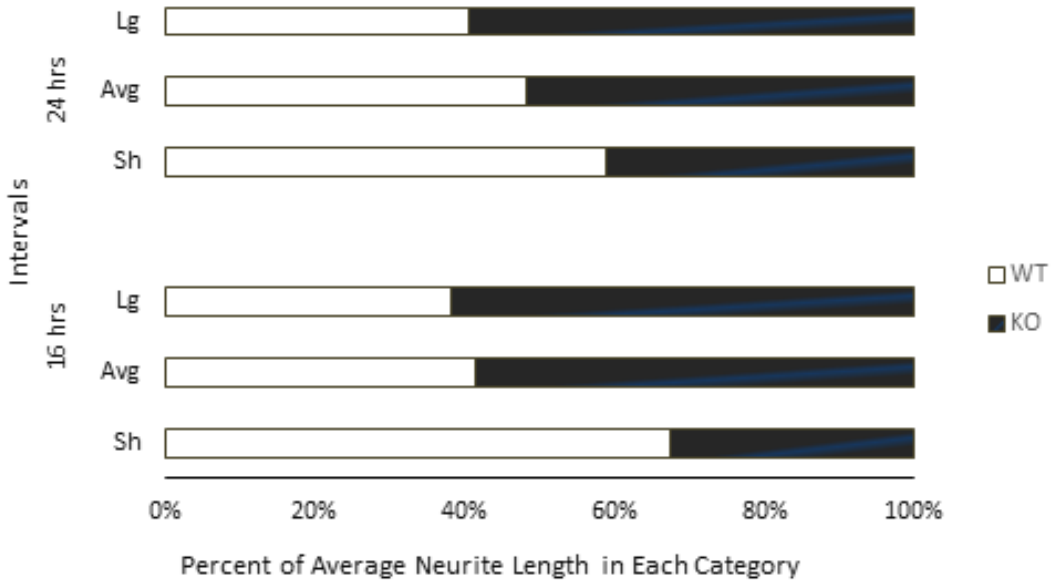
Lg
Avg
Sh
24 hrs
Intervals
Lg
Avg
Sh
16 hrs
WT
KO
0%
20%
40%
60%
80%
100%
Percent of Average Neurite Length in Each Category

Figure 3-9 Knockout of Pftaire1 results in enhanced axonal growth, at 16 and 24 hours *in vitro*

a) Image, representing immunostaining of neurons with Tau-1, Hoechst, and merged. Staining was performed to immunolabel axon for tracing and to determine viability of neurons measured. **b)** Column graphs, representing (Mean ± SEM) for different time points. At 16 and 24 hours, the knockout neurons have significantly longer axons in comparison to the WT (p<0.001) groups. **c)** Column graphs representing percent of difference in axonal length in knockout relative to wild type **d)** Linear graph, represents log10 of axons to simplify comparison at different time points due to changes in length. **e)** Also, classification of axons into different groups based on their lengths (Sh: short, Avg: average, and L: long) reveals more neurons with longer axons KO-Pftaire1 cultures as opposed to WT as determined by chi square (p < 0.001). Primary cortical cultures were prepared from mouse embryos at E13.5-14.5 from Pftaire1 Het x Het crosses and fixed at different time points. Fluorescent pictures were taken and measurements were done using stereo-investigator software as described earlier. Statistical significance of the measurements were determined with student's paired two tail t-test (p < 0.001).

3.3. Pftaire1 regulates axon outgrowth through RhoA GTPase

3.3.1. Identification of RhoA as a Pftaire1 interacting protein

PFTAIRE may affect signals known to regulate neurite outgrowth including the small Rho GTPase proteins. Rho GTPases are important regulators of neurite outgrowth (Jalink, van Corven et al. 1994, Luo, Hensch et al. 1996). Cdk5, indirectly interacts with Rac1 to regulate neurite outgrowth (Nikolic, Dudek et al. 1996, Nikolic, Chou et al. 1998, Rashid, Banerjee et al. 2001). Based on the similarities in the expression pattern, and sequence of Pftaire1 and Cdk5, in this study, we investigated the possibility of a physical interaction between Pftaire1 and the Rho GTPases. To determine whether Pftaire1 physically interacts with Rho GTPases and if that interaction depends on the ability of Pftaire1 to act as a kinase; we transfected HEK293T cells with dominant negative D228N-Pftaire1, as well as, the wild type form of the Rho GTPases utilizing lipofectamine2000. As mentioned earlier, the dominant negative form of Pftaire1, D228N, in which the aspartic acid is altered to asparagine, is suggested to diminish the phosphorylation capacity of Pftaire1 in interaction with its endogenous effectors (Lazzaro, Albert et al. 1997). We show that expression of GST-Rac1/Cdc42 and Myc-RhoA but not a GST and Myc control plasmid immunoprecipitate with Pftaire1. We, initially, confirmed the physical interaction between D228N-Pftaire1 and wild type Rac1 (Figure 3-10 a), Cdc42 (Figure 3-10 b) and/or RhoA (Figure 3-10 c). To ensure the specificity of Pftaire1 interaction with each Rho GTPase and impede the possibility of interaction with other members of the family, we investigated whether their constitutively active form is able to interact with Pftaire1. The substitution of the glycine at amino acid 12 with a valine, and glutamine at position 63

with leucine, respectively, in constitutively active (G12V-Rac1), (G12V-Cdc42), and (Q63L-RhoA) inhibits endogenous and GAP-stimulated GTPase activity; thus, Rac1, Cdc42, and RhoA retain a permanent active GTP-bound state and signal constitutively to their effector proteins. The physical interaction of D228N-Pftaire1 with (G12V-Rac1) (Figure 3-10 a), (G12V-Cdc42) (Figure 3-10 b) and, (Q63L-RhoA) (Figure 3-10 c) was confirmed, once again. Furthermore, to test whether interaction of Pftaire1 with Rho GTPases depends on their activation, we used inactive forms (S17N-Rac1), (S17N-Cdc42), and (L19N-RhoA) in which serine and leucine were, respectively, mutated to asparagine. Upon ectopic expression of D228N-Pftaire1 with dominant negative forms of either Rac1, (S17N-Rac1) (Figure 3-10 a) or Cdc42 (S17N-Cdc42)(Figure 3-10 b) we were able to detect a physical interaction between D228N-Pftaire1 and (S17N-Rac1) (Figure 3-10 a) and (S17N-Cdc42) (Figure 3-10 b), suggesting that their physical interaction is independent of the activity of Pftaire1 and Rac1 or Cdc42. Interestingly, the interaction was abolished between the dominant negative form of RhoA (L19N-RhoA) and the dominant negative Pftaire1 (D228N-Pftaire1)(Figure 3-10 c) whereas, wild type and constitutively active RhoA (Q63L-RhoA) both interacted with dominant negative Pftaire1 (D228N-Pftaire1). This may suggest that the interaction of Pftaire1 and RhoA occurs only when RhoA has the ability to become activated. In summary, our data suggests that Pftaire1 physically interacts with small Rho GTPase proteins including RhoA. We decided to focus our study on RhoA as the level of Rac1 and Cdc42 remained the same in WT and KO Pftaire1. This could also give us a better understanding of the reason that Pftaire1 discriminates between different forms

of RhoA. We next decided to examine the level of RhoA in Pftaire1 deficient mice and investigate the possibility of an endogenous interaction between Pftaire1 and RhoA.

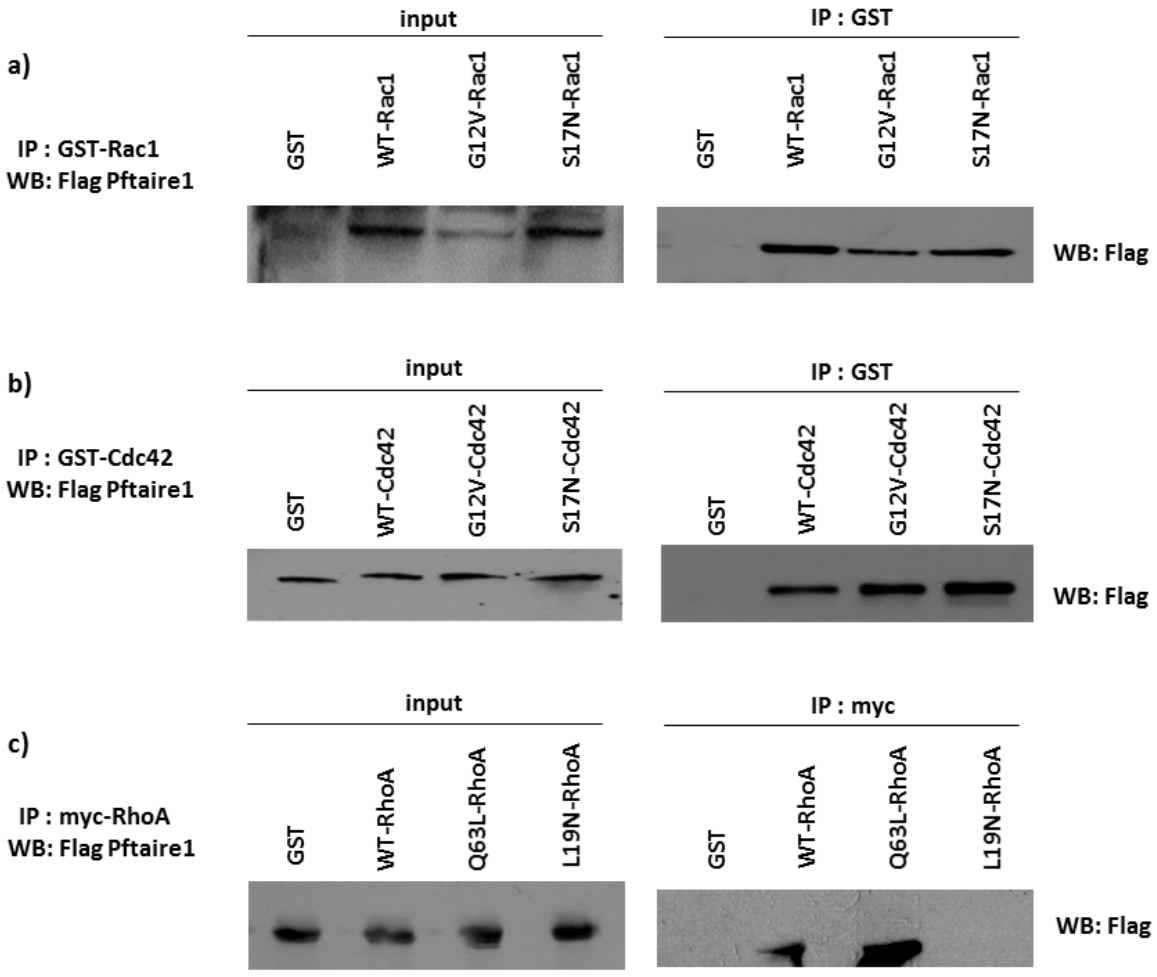
a)
IP : GST-Rac1
WB: Flag Pftaire1
input
IP : GST
GST
WT-Rac1
G12V-Rac1
S17N-Rac1
WB: Flag
b)
IP : GST-Cdc42
WB: Flag Pftaire1
input
IP : GST
GST
WT-Cdc42
G12V-Cdc42
S17N-Cdc42
WB: Flag
c)
IP : myc-RhoA
WB: Flag Pftaire1
input
IP : myc
GST
WT-RhoA
Q63L-RhoA
L19N-RhoA
WB: Flag

Figure 3-10 Pftaire1 physically interacts with Rho GTPase proteins *in vitro*

Western blots representing **a)** physical interaction of D228N-Pftaire1 with Rac1, wild type (WT-Rac1), constitutively active (G12V-Rac1) and dominant negative (S17N-Rac1). **b)** D228N-Pftaire1 also interacts with wild type (WT-Cdc42), constitutively active (G12V-Cdc42) and dominant negative (S17N-Cdc42), **c)** D228N-Pftaire1 interacts with both wild type RhoA and constitutively active (Q63L-RhoA) but not with dominant negative (L19N-RhoA). Ectopic expression of Flag-D228N-Pftaire and GST-Rac1, GST-Cdc42 or Myc-RhoA in HEK293T cell line via lipofectamine transfection. 24 hours post transfection cells were collected and lysed for pull down assay. Pftaire1, input samples were collected and GST tagged Rac1 and Cdc42 were precipitated using GST glutathione sepharose beads. In case of RhoA samples were immunoprecipitated using myc antibody and mouse –IgG True blot beads. Protein complexes were then resolved on a 12% SDS-gel followed by western blotting. Membranes were probed for Flag protein.

3.3.2. RhoA protein is upregulated in the cortex of Pftaire1 knockout mice

We next examined whether Pftaire1 levels had an effect on RhoA expression, *in vivo.* Upon, examination of endogenous levels of RhoA protein, by western blot analysis of cortical neuronal lysates from wild type and knockout Pftaire1 mice at E13.5-14.5 days, we observed significantly higher levels of RhoA in Pftaire1 knockout mice in comparison to wild type mice (Figure3-11 a and b). To explore whether Pftaire1 regulates RhoA gene expression at transcriptional level, we assessed the RhoA mRNA levels in wild type and Pftaire1 knockouts, utilizing reverse transcription polymerase chain reaction (RT-PCR) analysis, and no difference in RhoA levels were observed among wild type and knockout Pftaire1 mice (Figure 3-11 c and d). This indicates Pftaire1 deficiency increases the expression of RhoA protein.

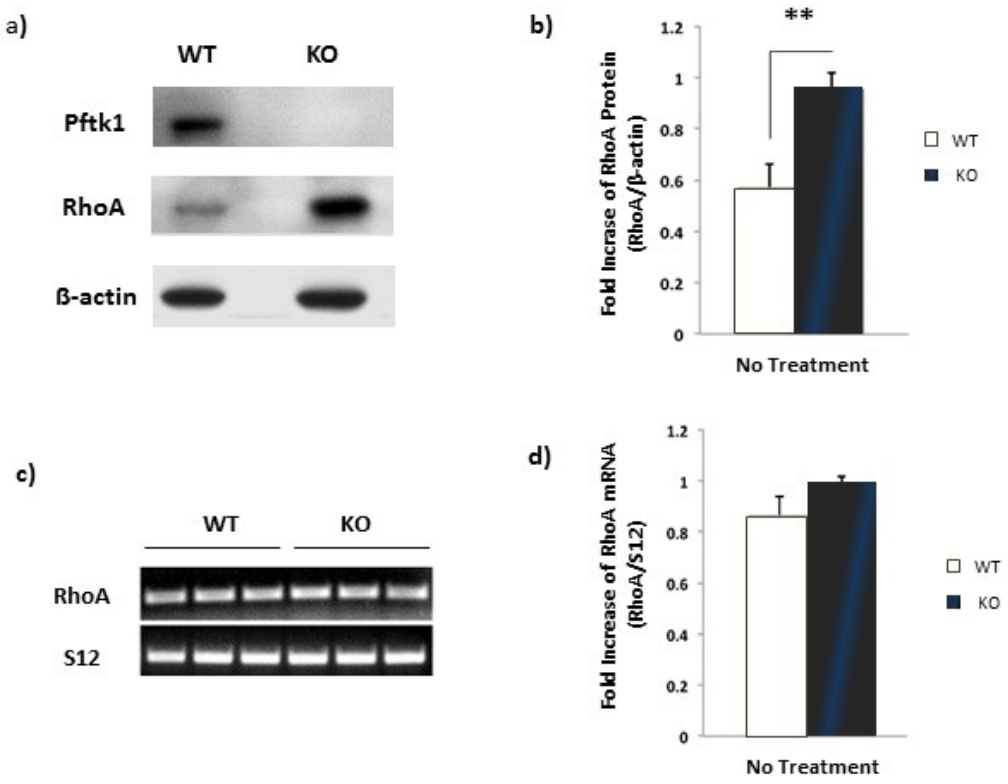
a)
WT
KO
Pftk1
RhoA
ß-actin
b)
**
Fold Increase of RhoA Protein (RhoA/β-actin)
1.2
1
0.8
0.6
0.4
0.2
0
No Treatment
WT
KO
c)
WT
KO
RhoA
S12
d)
Fold Increase of RhoA mRNA (RhoA/S12)
1.2
1
0.8
0.6
0.4
0.2
0
No Treatment
WT
KO

Figure 3-11 Pftaire1 knockout mice exhibit higher levels of basal RhoA protein

a) Western blot assessment using RhoA antibody, representing basal levels of RhoA protein in cortical neuronal extracts of E13.5-14.5 d of wild type and knock out Pftaire1 mice. **b)** Basal levels of RhoA protein expression are quantified by densitometry analysis, (n=7), p= 0.005, ** denotes p<0.001. **c)** Basal levels of RhoA mRNA detected by RT-PCR extracted from cortical neuronal extracts of E13.5-14.5 d wild type and knockout Pftaire1 mice. **d)** Basal levels of RhoA mRNA quantified by densitometry analysis, (n=3), N.S. Significance is determined by paired two tail t-Test. Mean is N.S., no significant difference is observed in basal levels of Pftaire1 expression levels of wild type and knockout Pftaire1 neurons.

3.3.3. RhoA interacts with Pftaire1 in mice brain

Next, we examined the possibility of an endogenous interaction between Pftaire1 and Rho GTPase. The endogenous expression level of RhoA GTPase is low and it is rapidly subject to hydrolysis. Thus, for immunoprecipitation purposes high amounts of protein (approximately 2000 μg of total protein) was required per reaction. Moreover, due to high sensitivity of Rho GTPases to temperature, all steps were performed at 4˚C using ice cold solutions to ensure the stability of reactions. Protein lysates were extracted from embryonic mouse brains at E13.5-14.5. We immunoprecipitated endogenous Pftaire1 utilizing rabbit polyclonal Pftaire1 (H-140) antibody from SantaCruz and used rabbit polyclonal IgG as control antibody. Our result indicates physical interaction of Pftaire1 and RhoA at an endogenous level (Figure 3-12).

To determine whether the activity of RhoA has any effect on this interaction we added GTPγS to stabilize the active form. Both the endogenous form of RhoA and GTP bound RhoA interacted with Pftaire1 (Figure 3-12).

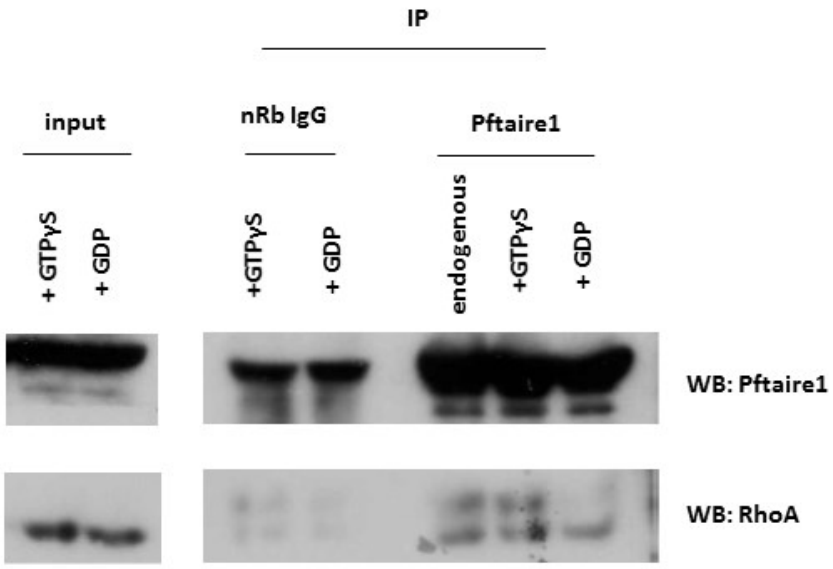
IP
input
nRb IgG
Pftaire1
+ GTPγS
+ GDP
+GTPγS
+ GDP
endogenous
+GTPγS
+ GDP
WB: Pftaire1
WB: RhoA

Figure 3-12 Pftaire1 and GTPase protein Rho A interact at an endogenous level

Western blot representing physical interaction of Pftaire1 and RhoA *in vivo*, on whole brain extracts from wild type CD1 mouse embryo at E13.5-14.5 d**.** Inputs and immunoprecipitated proteins were separated on 12% SDS gel, followed by western blot. Immune complexes were detected using RhoA antibody. Pftaire1 antibody and RhoA antibody were used for western blotting. To immunoprecipitate, lysates were collected and incubated with Pftaire1 antibody and true blot rabbit IgG beads. GTPγS was loaded with the interactions to determine the effect of GTP bound RhoA on interaction with Pftaire1.

3.3.4. RhoA activity could not be detected in Pftaire1 deficient neurons by GTPase assay *in vitro*

Our data revealed an increase in levels of RhoA protein in primary cortical cultures of Pftaire1 knockout mice, p=0.005 (Figure 3-11 a). To further investigate the relationship between the activity of RhoA and Pftaire1; the GTPase activity of RhoA was examined under conditions where Pftaire1 was absent. The activation level of RhoA was determined by Rho GTPase activity assay utilizing GTPase activation kit from Cell Biolabs, on cell lysates as described earlier in methodology. Briefly, cell extracts were prepared from cortical cultures of Pftaire1 wild type and knockout littermates at E13.5-14.5 and then incubated with Rho-binding domain (RBD) of Rhotekin PBD beads provided with the kit which exclusively pull down the active form of RhoA from the endogenous cell lysate. We immunoprecipitated rhotekin /active RhoA complex with the provided PBD beads. Active RhoA levels were revealed by western blotting probing with RhoA specific antibody. The detected signal would correlate with the activity level of RhoA. Interestingly, in spite of RhoA protein upregulation in Pftaire1 knockout mice, we did not detect RhoA activity in the KO extracts (Figure 3-13).

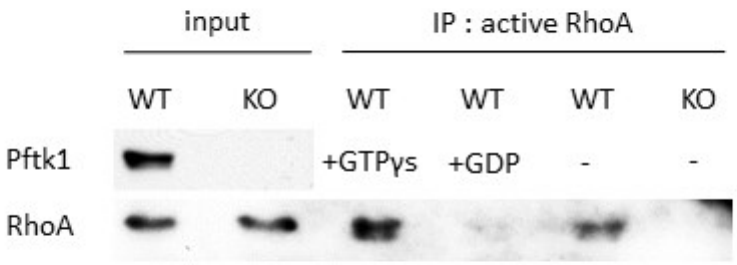
input
IP : active RhoA
WT
KO
WT
WT
WT
KO
Pftk1
+GTPγs
+GDP
-
-
RhoA

Figure 3-13 RhoA activity was undetectable in the absence of Pftaire1

Western blot representing RhoA activity as a function of Pftaire1. The activity of RhoA seems to be disrupted in Pftaire1 knockouts as opposed to wild type mice in primary cortical cultures from mouse embryos at E13.5-14.5 d. Rho GTPase activity assay was performed on cell lysates as described earlier. Active RhoA binds to its downstream target Rhotekin, and regulates signaling of downstream effectors. Rho-binding domain (RBD) of Rhotekin PBD beads exclusively pulls down the active form of RhoA of the endogenous cell lysate. Image represents of experimental replicates (n=4).

3.3.5. Pftaire1 phosphorylates RhoA on a Serine residue *in vitro*

Since according to our results, RhoA activity was undetectable in Pftaire1 knockout cortical neurons in spite of its upregulation (Figure 3-11 a, 3-13), we decided to investigate whether Pftaire1 has direct kinase activity over RhoA *in vitro*. We performed an *in vitro* kinase assay using immunoprecipitated Pftaire1. Briefly, we immunoprecipitated Pftaire1 from mouse embryonic cortical neurons at E13.5-14.5, as described in methods section. Immunoprecipitated Pftaire1 was incubated overnight with human recombinant RhoA substrate for kinase assay. The reaction was then resolved on a 12% SDS gel and subjected to western blotting. Phosphorylated RhoA was detected using phosphoserine antibody. Our results revealed Pftaire1 mediated the phosphorylation of RhoA but IgG control had no effect (Figure 3-13a). We next examined the ability of Pftaire1 to phosphorylate the GDP bound form of RhoA. Upon adding GDP to our reactions we observed increased phosphorylation of RhoA-GDP as opposed to RhoA alone. Our results suggest RhoA as a direct *in vitro* substrate of Pftaire1 (Figure 3-14 a).

3.3.6. Pftaire1 mediated RhoA phosphorylation leads to RhoA activation

To investigate the effects of pftaire1 mediated phosphorylation over RhoA activity more accurately, we analyzed RhoA activity following kinase activity utilizing an absorbance based G-LISA assay biochem kit from Cytoskeleton as described by the manufacturer. We performed the *in vitro* Kinase Assay as described earlier, with or without GDP in the reaction mix followed by the G-LISA reaction. A significant increase in RhoA activity was detected as a function of Pftaire1 versus IgG control, as determined by

two-way ANOVA (p= 0.046). Post-hoc Bonfferoni's test, revealed that the highest difference was associated with the presence of GDP, suggesting that RhoA-GDP is the most efficient target for Pftaire1 phosphorylation (p= 0.033). In summary, in the presence of GDP, Pftaire1-RhoA reveals significantly higher activity when compared to IgG-RhoA (Figure 3-14 b).

a)

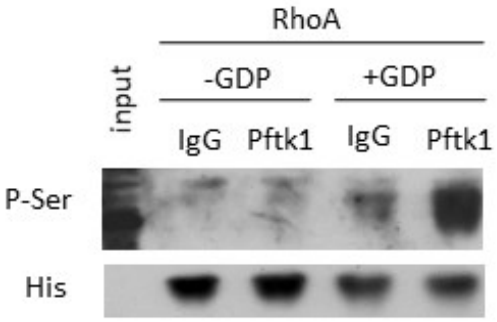
RhoA
-GDP
+GDP
input
IgG
Pftk1
IgG
Pftk1
P-Ser
His

b)

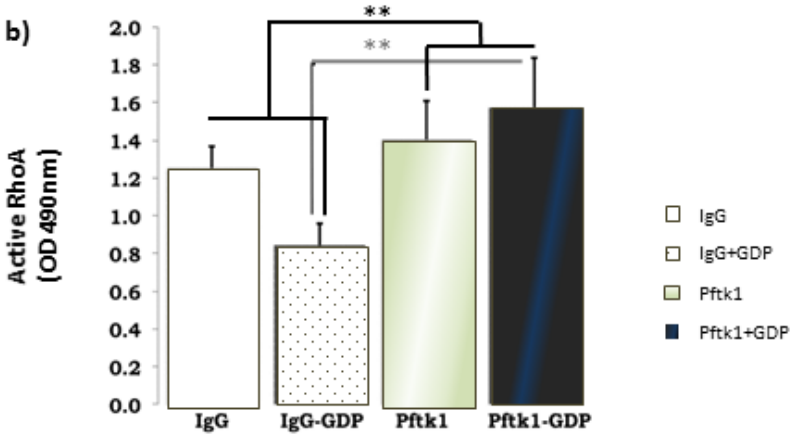
**
**
Active RhoA (OD 490nm)
2.0
1.8
1.6
1.4
1.2
1.0
0.8
0.6
0.4
0.2
0.0
IgG
IgG-GDP
Pftk1
Pftk1-GDP
IgG
IgG+GDP
Pftk1
Pftk1+GDP

Figure 3-14 Pftaire1 phosphorylates RhoA and activates RhoA *in vitro*

a) Western blot analysis, representing *in vitro* kinase assay using IP-Pftaire1 or IP-IgG from wild type mouse embryonic cortical neurons at E13.5-14.5. Human recombinant RhoA was used as substrate. Beads were incubated with RhoA O/N at 4 ˚C and then reactions were separated on a 12% SDS-PAGE gel followed by western blotting. Blots were probed with polyclonal rabbit phosphoserine antibody to detect RhoA phosphorylation. Pftaire1 but not control IgG phosphorylates RhoA. GDP bound RhoA reveals a significantly stronger phosphorylation pattern as compared to RhoA alone as detected by phosphoserine antibody. **b)** RhoA activity assay following *in vitro* kinase assay. Reactions were prepared in the presence and absence of GDP and analyzed by G-LISA as described earlier. A significant difference was observed following GDP treatment of the Pftaire1 reaction with IgG control p= 0.046 between Pftaire1 and control groups, as determined by two-way ANOVA. Post-hoc Bonfferoni's test suggests significant difference between GDP-RhoA is the most significant target for Pftaire1 (p=0.033).

CHAPTER 4

DISCUSSION

4. DISCUSSION

4.1. Summary

Neurodegenerative diseases result from disturbed function and structure of neurons that lead to progressive damage in the CNS and PNS. Presently, much focus has been directed on developing therapies and strategies to prevent or reverse these conditions. Success in developing therapeutic protocols, depends on a profound understanding of the function of the nervous system. Cdks have a crucial role in cell cycle regulation and neurogenesis. Numerous studies, including work done in our laboratory, support the indispensable role of Cdks especially postmitotic Cdks, including Cdk5 in the regulation of the nervous system. In the work presented here, we focus on a novel postmitotic Cdk family member, Pftaire1 (Cdk14), and we explore its effect on axon outgrowth during the development of CNS.

Pftaire1, is a novel serine/threonine protein kinase that was identified when cloning for cdc2 related kinases (Lazzaro, Albert et al. 1997). Our lab, described the effect of Pftaire (Eip63E) deficiency on CNS development in *Drosophila,* for the first time (Rodríguez González and S. 2011). Eip63E deficiency results in concerted defects in axons and neurons of the *Drosophila* ventral nerve cord (VNC). Premature axonal outgrowth, as well as, defasciculation and misguidance of the commissural and longitudinal axon tracks at the ventral nerve cord (VNC) were among the phenotypic features detected in Eip63 deficient embryos. This suggested a role for Eip63E in the regulation of axon development in *Drosophila* (Rodríguez González and S. 2011). Furthermore, Stowers et al. had previously shown that Eip63E deficient flies die mainly during larval development and

only a few that survive to pupae are smaller in size (Stowers, Garza et al. 2000). We speculate that the smaller size of Eip63E mutants could be due to loss of functionality in the nervous system. Considering the severe effects of Eip63E deficiency in *Drosophila*, and the high degree of similarity (about 75 %) with the mammalian homologue, one could infer that Pftaire1 has an important role in the development of axons in the mammalian system, as well. Taking this into consideration, in addition to the high expression of Pftaire1 in the central nervous system (Lazzaro, Albert et al. 1997, Besset, Rhee et al. 1998, Yang and Chen 2001), we anticipated defects in the mouse system with Pftaire1 deficiency. While this is complicated by the presence of two Pftaire genes (Pftaire 1 and 2) in the mammalian system; we nonetheless, focused on evaluating the effects of Pftaire1, in of Pftaire1 deficient mice. In our study, presented in "Chapter Three" of this thesis, we developed[3] Pftaire1 homozygous deficient mice, for the first time, to explore the role and function of Pftaire1 in the CNS. We initially focused on obtaining and characterizing Pftaire1 homozygous mice. Then, we examined the effects of Pftaire1 deficiency on axon length*, in vitro;* and finally we investigated the possible mechanism of action of Pftaire1. Our study, provides evidence that Pftaire1 deficiency results in premature axon outgrowth, *in vitro*; and interacts physically with RhoA by phosphorylating it, *in vitro*.

4.2. Overview

4.2.1. Pftaire1: A Novel Protein and newly generated knockout mice

[3] Pftaire1 was commercially obtained from TIGM (Texas A&M Institute for Genomic Medicine)

In the first part of this thesis, we report, for the first time, the design of a standard germline Pftaire1 knockout mouse model, specifically for our study. We hypothesized that Pftaire1 is critical for neuronal development. In this knockout line, the 6th exon (out of a total 15) was replaced by the IRES / bGeo / PolyA cassette via homologous recombination and successful replacement was confirmed by PCR genotyping of the DNA samples (Figure 3-1, and 3-2). This replacement interferes with the coding sequence and results in a frameshift that translates into a truncated protein. Loss of full length Pftaire1 protein in the 48 kDa was confirmed by western blot (Figure 3-3). It is unlikely that the produced truncated protein (about 18 kDa) could have any kinase activity. In their tertiary structure, Cdks form a bilobal fold which includes a large carboxy-terminal lobe, a small amino-terminal lobe and a flexible hinge that connects the two lobes to each other and acts as the ATP binding domain or the catalytic cleft. This mutated protein lacks the carboxy terminal and the majority of the subkinase domains except subdomains I-III. It also does not have the flexible threonine-loop (T-loop) that binds to the substrate. Taking into consideration, the structural and functional characteristics of Cdk family members; we speculate that the truncated protein lacks the L12 helix, which contributes to the structural modification and reorientation of amino acids site in the ATP binding site though it likely contains the conserved glycine-rich loop (G-loop), which facilitates the binding and alignment of γ-phosphate of ATP for transfer(Dhavan and Tsai 2001, Bartova, Otyepka et al. 2005, Morgan 2007).

The Pftaire1 deficient mice that were designed for the purpose of this study, followed normal Mendelian ratios (Table 3-1, Figure 3-5) and no gross abnormalities were

detected in their morphology, fertility, or life span at early mix background generations. Also, upon cresyl violet staining of brain sections collected from Bregma: ~ 2.710 to 4.20 no gross abnormality was detected in the anatomical structure of the brain within our observations (Figure 3-6). However, the possibility of abnormal structure cannot be ruled out until more specific methods, for instance Golgi staining, are utilized to examine the structure of the brain further. Additionally, axonal guidance during development of the nervous system is an important feature to further study considering that Pftaire (Eip63E) deficiency results in concerted defects in axons and neurons of the *Drosophila* VNC (Rodríguez González and S. 2011). Although, the lack of gross developmental defects is not inconsistent with effects on axon length since the latter might not be readily observable by gross analyses due to the presence of other post-mitotic Cdk genes. For instance, Pftaire2, Pctaire1-3, and Cdk5 thus more careful observation of Pftaire1 and detection of the kinase activity of other genes is required.

The question that arises is why does there appear to be a lack of apparent gross CNS phenotype with Pftaire1 loss in comparison to the fly? One possible explanation could be the methods and the age of the mice in our study. In this study, we examined the structure of the brain in 2 month old adult mice and E17.5-18.5 embryos using cresyl violet (Figure 3-6). The defects in axons of Eip63E flies appeared as early as stage 11 of embryonic development (Rodríguez González and S. 2011). Although, this might not be a major problem due to survival of the mouse embryos to adulthood. It would be interesting to have a closer investigation. Furthermore, the adult Pftaire1 null mice were still on a mixed background as opposed to a pure C57BL6 background. To rule out any

possible differences, the gross structure of the brains need to be examined at younger ages, during embryonic period, on fully backcrossed mice. Another, obvious explanation is that *Drosophila* merely possess the Pftaire1 homologue Eip63L but not Pftaire2 and PCTAIRE kinases. In comparison, mammals contain two highly similar Pftaire kinase proteins, Pftaire1 and 2 that are about 68 % similar, as well as, three Pctaire kinases, Pctaire 1-3, which are about 61 % similar to Pftaire1 and are all highly expressed in the mouse brain (Okuda, Cleveland et al. 1992, Hirose, Kawabuchi et al. 2000, Cole 2009, Mikolcevic, Sigl et al. 2012). The presence of these highly similar genes in the mammalian system could compensate for the lack of Pftaire1 and result in a lower level of abnormalities in the knockout mice. This concern was taken into consideration by examining levels of Pftaire2, Pctaire1 and Cdk5 proteins in Pftaire1 knockouts. No increase was observed in the level of these proteins in wild type mice versus Pftaire1 knockouts (Figure 3-4 a, b), yet, this does not rule out the possibility of functional redundancy between any of them and pftaire1. Nevertheless, we have already generated a Pftarie2 deficient mouse line and it would be critical to determine the phenotype of this mouse, as well as, a double Pftaire1/2 knock out mouse. Finally, although Pftaire1 deficiency did not affect basal cell survival levels of cortical cell cultures at E13.5-14.5 (Figure 3-7), there is the possibility that loss of Pftaire1 may result in abnormal features under stress. There is precedence for this. Cdk5, another neuronal Cdk member has been shown to be associated with the degenerative process in animal models of CNS disease (Patrick, Zhou et al. 1998, Dhavan and Tsai 2001, Cruz and Tsai 2004, Rashidian, Iyirhiaro

et al. 2005, Smith, Mount et al. 2006). It would be interesting to determine whether this is true for Pftaire1.

4.2.2. Axon outgrowth *in vitro* and Biological Relevance of Pftaire1

Our studies indicate that Pftaire-1 plays a role in regulating axon length. Cdk5 and Pctaire, two close family members of Pftaire1 have been implicated in axon outgrowth. For instance, Cdk5 inactivation leads to inhibition of axonal growth (Nikolic, Dudek et al. 1996, Nikolic, Chou et al. 1998), while Pctaire1 negatively regulates neurite outgrowth (Graeser, Gannon et al. 2002, Cole 2009). Ectopic expression of dominant negative Pctaire1 (K194R) in Neuro-2A neuroblastoma cells resulted in a 5 % increase in neurite outgrowth of Pctaire1 mutants, as opposed to their wild type counterparts (Graeser, Gannon et al. 2002). Likewise, our data suggests a role for Pftaire1 in regulation of axonal length. A significant increase, about 32.4%, 34.7%, and 32.3%, change in axonal length relative to GFP control was observed upon ectopic expression of dominant negative D228N-Pftaire1 in cortical neurons at 12, 16, and 24 hours, respectively (Figure 3-8 c). Also, a 45.6% and 28.5% increase in relative axonal length is observed in cultures prepared from primary cortical neurons of Pftaire1 knockout mice, at 16 and 24 hours, respectively (Figure 3-9 c). The higher percent of change at earlier time-points might indicate that Pftaire1 is more important in regulating the initiation of axon outgrowth rather than being involved in the growth of axon afterwards. Interestingly, categorizing the axons to different ranges, based on their lengths, reveals that in Pftaire1 deficient mice, the percent of neurons with longer axons are higher at 16 hours 40.8% and 48.3%; in comparison to at 24 hours 43.1% and 43.3%, in D228N infected and knockout cortical

cultures, respectively (Figure 3-8 e, 3-9 e). Furthermore, at 48 hours D228N infected neurons do not differ significantly from wild type and GFP (Figure 3-8 e). This indicates that the rate of axonal outgrowth as a function of time decreases in Pftaire1 deficient cortical cultures and supports the notion that Pftaire1 negatively regulates the initiation of axon growth and later on this effect is diminished. The rate of axon outgrowth as an effect of Pftaire1 could be easily assessed using special gridded glass bottom culture dishes that sustain CO_2 and facilitate tracing individual cells at different time points. Another interesting observation is that not all cultures obtained from Pftaire1 deficient embryos showed increased axonal length when compared to wild type cultures (although collectively the data shows a difference). This could indicate a partial penetrance phenotype, which requires further investigation. In this regard, epigenetic control of gene expression results in diversity of phenotypes within a population independent of their genotype. Epigenetic inheritance occurs in multiple kingdoms of life including: plants, fungi (Henderson and Jacobsen 2007, Jablonka and Raz 2009), flies, mice and humans (Roemer, Reik et al. 1997, Cavalli and Paro 1998, Morgan, Sutherland et al. 1999, Hitchins, Wong et al. 2007, Cropley, Dang et al. 2012) and it may be an explanation for observing different phenotypes among the knockouts of a same litter; specifically, given the fact that the assessments were done in generation 6^{th} embryos.

4.2.3. Pftaire1: Possible Mechanism of Action

How Pftaire1 regulates axon outgrowth is still unknown. In line with our data, we suggest that it does so through regulation of RhoA. In this thesis, we revealed a physical interaction between Pftaire1 and RhoA both upon ectopic expression and at endogenous

state. To test if pftaire1, like its family members, would interact with molecules known to regulate axon development, we performed a biased investigation focusing on Rho GTPases. We hypothesized that Pftaire1 interacts with known regulators of growth cone machinery, Rho GTPases specifically RhoA. Rho GTPases are implicated in neurite outgrowth, the activation and inactivation of the Rho GTPases controls downstream signaling cascades which in return regulate outgrowth and guidance of an axon (Nikolic 2002, Jaffe and Hall 2005). Furthermore, the Rac signaling pathway is shown to be modulated by Cdk5. Cdk5 inactivation leads to inhibition of axonal growth (Nikolic, Dudek et al. 1996, Nikolic, Chou et al. 1998). In *Xenopus,* neuronal morphology of retinal ganglion cells (RGCs) is regulated by Rac via Cdk5/p35 (Ruchhoeft, Ohnuma et al. 1999). Cdk5 interacts with Rac1 via p35 in a GTP dependent manner (Nikolic, Chou et al. 1998, Rashid, Banerjee et al. 2001). Our investigations indicate that RhoA interacts with Pftaire1 both under expressed (Figure 3-10 c) and endogenous (Figure 3-12) conditions. In HEK293T cells, L19N-RhoA inactivates the endogenous RhoA and disrupts the interaction (Figure 3-10 c). We initially, interpreted that this interaction depends upon the ability of RhoA to become activated but not on the kinase activity of Pftaire1. Interestingly, RhoA activity was undetectable in the absence of Pftaire1 (Figure 3-13), whereas, RhoA basal levels were higher in Pftaire1 knockouts (Figure 3-11).

These results in conjunction with the observed effects of Pftaire1 deficiency on axon length is suggestive of a model by which Pftaire1 regulates outgrowth through its effects on RhoA. This infers that GTP-RhoA impedes excessive axon outgrowth; thus, regulates axon phenotype. We speculate that the inactive or not activated RhoA becomes

upregulated or does not get eliminated in the absence of Pftaire1. In spite of the interaction of active RhoA with Pftaire1, our *in vitro* kinase assay results suggest that GDP increases phosphorylation of RhoA by Pftaire1 (Figure 3-14 a). Furthermore, our GLISA assay results suggest the kinase activity of Pftaire1, results in a significant increase in the activity of RhoA bound GDP (Figure 3-14 b). How might this occur? One possibility is that under basal circumstances Pftaire1 interacts with active RhoA and regulates its function. We show that Pftaire1 phosphorylates GDP-RhoA on a serine residue. We speculate that Pftaire1 may directly phosphorylate RhoA, *in vivo,* in cortical neurons, as well. We propose that this leads to an increase in RhoA activity (Figure 3-13), which in turn controls axon outgrowth. Alternatively, we speculate in Pftaire1 deficient cortical neurons, upregulation of basal RhoA levels might be in an attempt to compensate for the low basal activity of RhoA. We speculate that hyperextention of axons in D228N and Pftaire1 knockouts *in vitro* (Figure 3-8 and 3-9) is due to impediment of the negative regulation of RhoA on axon outgrowth (Sebok, Nusser et al. 1999). However, we need to further investigate this by determining whether RhoA function can be modulated in the absence of Pftaire1 to reverse the axon effects of Pftaire1 loss. Also, it is necessary to determine if RhoA is able to rescue the phenotype of knockout-Pftaire1 cortical neurons.

We have shown that *in vitro*, Pftaire1 phosphorylation of RhoA leads to an increase in RhoA activity. Nevertheless, this neither does rule out the possibility of Pftaire1 regulating the pathway of axon outgrowth at different levels nor suggest RhoA as the universal target for Pftaire1. At the moment, we cannot explain how phosphorylation of RhoA leads to increased activity. Could it be due to a conformational

change? This is hard to test at this point. One possibility is that *in vivo* Pftaire1 may phosphorylate other targets in addition to RhoA, which in turn could affect RhoA activity. For instance, we have not tested whether Rho regulating proteins, like GDI or GEFs, are Pftaire1 targets. Moreover, we have shown that other Rho GTPase proteins like Cdc42 and Rac1 physically interact with Pftaire1 *in vitro* (Figure 3-10 a and b). However, we do not know, yet, if any of the Rho GTPase proteins are Pftaire1 targets. That is important because any changes in their activity levels could affect RhoA activity due to the fact that they share most of their regulators.

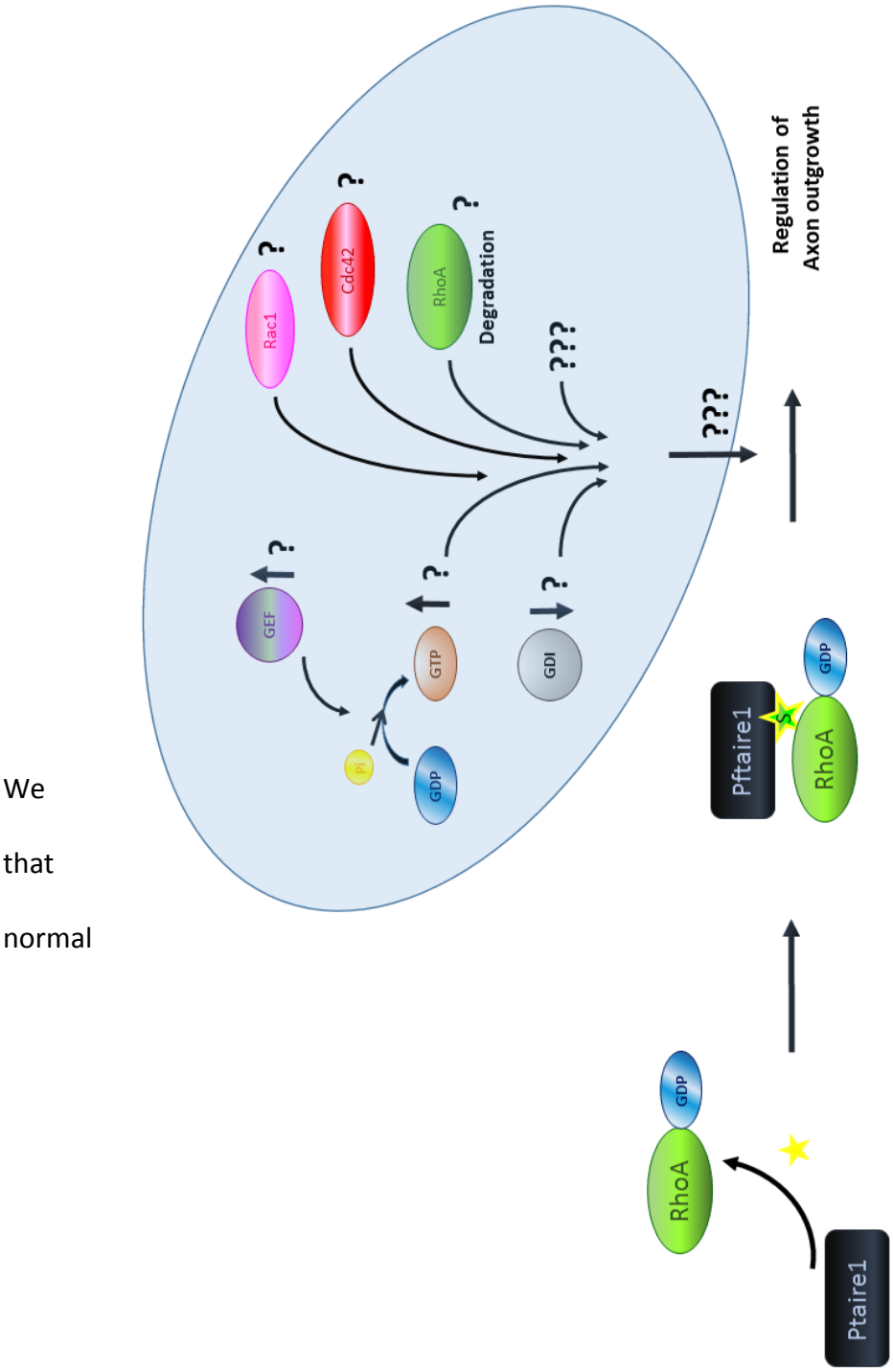

We propose that under normal

Figure 4-1 A proposed model for the mechanism of action of Pftaire1

circumstances, Pftaire1 (black) and RhoA (green) physically interact. Pftaire1 phosphorylates (yellow star), GDP-RhoA on a serine residue (yellow-green star), activates it and regulates axon outgrowth in a negative manner. Potential factors that may be involved include but are not limited to, are exemplified and demonstrated by question marks (?) in the blue background. pi (yellow), GDIs (gray), GEFs (purple), other Rho GTPase proteins, , Cdc42 (red), Rac1 (pink), GDP to GTP (brown) exchange, also other unknown factors (**???**).

4.3. Conclusion

The role of Pftaire1 in the development of the CNS is virtually unknown. We are the first to develop / obtain Pftaire1 deficient mice and study its effect on axon outgrowth. Our *in vitro* data, suggests a role for mammalian Pftaire1 in axogenesis from a phenotypic aspect, revealing a hyperextension in axonal length upon inhibition or absence of Pftaire1. Furthermore, our study, confirms a physical interaction between Pftaire1 and the small GTPase proteins Rac1, Cdc42, and **RhoA**. RhoA, is known to negatively regulate axon outgrowth (Sebok, Nusser et al. 1999). Importantly, we showed that Pftaire1 phosphorylates GDP-RhoA on a serine residue. We propose that this leads to an increase in RhoA activity, which in turn controls axon outgrowth.

REFERENCES

Adams, N. C., T. Tomoda, M. Cooper, G. Dietz and M. E. Hatten (2002). "Mice that lack astrotactin have slowed neuronal migration." Development **129**(4): 965-972.

Adra, C. N., D. Manor, J. L. Ko, S. Zhu, T. Horiuchi, L. Van Aelst, R. A. Cerione and B. Lim (1997). "RhoGDIgamma: a GDP-dissociation inhibitor for Rho proteins with preferential expression in brain and pancreas." Proc Natl Acad Sci U S A **94**(9): 4279-4284.

Amano, M., K. Chihara, N. Nakamura, T. Kaneko, Y. Matsuura and K. Kaibuchi (1999). "The COOH terminus of Rho-kinase negatively regulates rho-kinase activity." J Biol Chem **274**(45): 32418-32424.

Amano, T., K. Tanabe, T. Eto, S. Narumiya and K. Mizuno (2001). "LIM-kinase 2 induces formation of stress fibres, focal adhesions and membrane blebs, dependent on its activation by Rho-associated kinase-catalysed phosphorylation at threonine-505." Biochem J **354**(Pt 1): 149-159.

Anton, E. S., J. A. Kreidberg and P. Rakic (1999). "Distinct functions of alpha3 and alpha(v) integrin receptors in neuronal migration and laminar organization of the cerebral cortex." Neuron **22**(2): 277-289.

Anton, E. S., M. A. Marchionni, K. F. Lee and P. Rakic (1997). "Role of GGF/neuregulin signaling in interactions between migrating neurons and radial glia in the developing cerebral cortex." Development **124**(18): 3501-3510.

Aoki, K., T. Nakamura and M. Matsuda (2004). "Spatio-temporal regulation of Rac1 and Cdc42 activity during nerve growth factor-induced neurite outgrowth in PC12 cells." J Biol Chem **279**(1): 713-719.

Arber, S., F. A. Barbayannis, H. Hanser, C. Schneider, C. A. Stanyon, O. Bernard and P. Caroni (1998). "Regulation of actin dynamics through phosphorylation of cofilin by LIM-kinase." Nature **393**(6687): 805-809.

Arimura, N., N. Inagaki, K. Chihara, C. Menager, N. Nakamura, M. Amano, A. Iwamatsu, Y. Goshima and K. Kaibuchi (2000). "Phosphorylation of collapsin response mediator protein-2 by Rho-kinase. Evidence for two separate signaling pathways for growth cone collapse." J Biol Chem **275**(31): 23973-23980.

Arozarena, I., D. Matallanas and P. Crespo (2001). "Maintenance of CDC42 GDP-bound state by Rho-GDI inhibits MAP kinase activation by the exchange factor Ras-GRF. evidence for Ras-GRF function being inhibited by Cdc42-GDP but unaffected by CDC42-GTP." J Biol Chem **276**(24): 21878-21884.

Asada, A., N. Yamamoto, M. Gohda, T. Saito, N. Hayashi and S. Hisanaga (2008). "Myristoylation of p39 and p35 is a determinant of cytoplasmic or nuclear localization of active cyclin-dependent kinase 5 complexes." J Neurochem **106**(3): 1325-1336.

Ball, H. J., A. Melnick, R. Shaknovich, R. A. Kohanski and J. D. Licht (1999). "The promyelocytic leukemia zinc finger (PLZF) protein binds DNA in a high molecular weight complex associated with cdc2 kinase." Nucleic Acids Res **27**(20): 4106-4113.

Bartkova, J., B. Gron, E. Dabelsteen and J. Bartek (2003). "Cell-cycle regulatory proteins in human wound healing." Arch Oral Biol **48**(2): 125-132.

Bartova, I., M. Otyepka, Z. Kriz and J. Koca (2005). "The mechanism of inhibition of the cyclin-dependent kinase-2 as revealed by the molecular dynamics study on the complex CDK2 with the peptide substrate HHASPRK." Protein Sci **14**(2): 445-451.

Baumli, S., G. Lolli, E. D. Lowe, S. Troiani, L. Rusconi, A. N. Bullock, J. E. Debreczeni, S. Knapp and L. N. Johnson (2008). "The structure of P-TEFb (CDK9/cyclin T1), its complex with flavopiridol and regulation by phosphorylation." EMBO J **27**(13): 1907-1918.

Bear, J. E., T. M. Svitkina, M. Krause, D. A. Schafer, J. J. Loureiro, G. A. Strasser, I. V. Maly, O. Y. Chaga, J. A. Cooper, G. G. Borisy and F. B. Gertler (2002). "Antagonism between Ena/VASP proteins and actin filament capping regulates fibroblast motility." Cell **109**(4): 509-521.

Bernard, O. (2007). "Lim kinases, regulators of actin dynamics." Int J Biochem Cell Biol **39**(6): 1071-1076.

Bernards, A. and J. Settleman (2004). "GAP control: regulating the regulators of small GTPases." Trends Cell Biol **14**(7): 377-385.

Besset, V., K. Rhee and D. J. Wolgemuth (1998). "The identification and characterization of expression of Pftaire-1, a novel Cdk family member, suggest its function in the mouse testis and nervous system." Mol Reprod Dev **50**(1): 18-29.

Besset, V., K. Rhee and D. J. Wolgemuth (1999). "The cellular distribution and kinase activity of the Cdk family member Pctaire1 in the adult mouse brain and testis suggest functions in differentiation." Cell Growth Differ **10**(3): 173-181.

Bibb, J. A., G. L. Snyder, A. Nishi, Z. Yan, L. Meijer, A. A. Fienberg, L. H. Tsai, Y. T. Kwon, J. A. Girault, A. J. Czernik, R. L. Huganir, H. C. Hemmings, Jr., A. C. Nairn and P. Greengard (1999). "Phosphorylation of DARPP-32 by Cdk5 modulates dopamine signalling in neurons." Nature **402**(6762): 669-671.

Billuart, P., T. Bienvenu, N. Ronce, V. des Portes, M. C. Vinet, R. Zemni, H. Roest Crollius, A. Carrie, F. Fauchereau, M. Cherry, S. Briault, B. Hamel, J. P. Fryns, C. Beldjord, A. Kahn, C. Moraine and J. Chelly (1998). "Oligophrenin-1 encodes a rhoGAP protein involved in X-linked mental retardation." Nature **392**(6679): 923-926.

Biswas, S. C., Y. Zhang, G. Iyirhiaro, R. T. Willett, Y. Rodriguez Gonzalez, S. P. Cregan, R. S. Slack, D. S. Park and L. A. Greene (2010). "Sertad1 plays an essential role in developmental and pathological neuron death." J Neurosci **30**(11): 3973-3982.

Borrell, V. and O. Marin (2006). "Meninges control tangential migration of hem-derived Cajal-Retzius cells via CXCL12/CXCR4 signaling." Nat Neurosci **9**(10): 1284-1293.

Brambilla, R. and G. Draetta (1994). "Molecular cloning of PISSLRE, a novel putative member of the cdk family of protein serine/threonine kinases." Oncogene **9**(10): 3037-3041.

Brouns, M. R., S. F. Matheson and J. Settleman (2001). "p190 RhoGAP is the principal Src substrate in brain and regulates axon outgrowth, guidance and fasciculation." Nat Cell Biol **3**(4): 361-367.

Bu, B., J. Li, P. Davies and I. Vincent (2002). "Deregulation of cdk5, hyperphosphorylation, and cytoskeletal pathology in the Niemann-Pick type C murine model." J Neurosci **22**(15): 6515-6525.

Burbelo, P. D., D. Drechsel and A. Hall (1995). "A conserved binding motif defines numerous candidate target proteins for both Cdc42 and Rac GTPases." J Biol Chem **270**(49): 29071-29074.

Burridge, K. and K. Wennerberg (2004). "Rho and Rac take center stage." Cell **116**(2): 167-179.

Butler, S. J. and J. Dodd (2003). "A role for BMP heterodimers in roof plate-mediated repulsion of commissural axons." Neuron **38**(3): 389-401.

Cafferty, W. B., P. Duffy, E. Huebner and S. M. Strittmatter (2010). "MAG and OMgp synergize with Nogo-A to restrict axonal growth and neurological recovery after spinal cord trauma." J Neurosci **30**(20): 6825-6837.

Cajal, S. R. y. (1906). "The structure and connexions of neurons." Nobel Lecture.

Campbell, K. and M. Gotz (2002). "Radial glia: multi-purpose cells for vertebrate brain development." Trends Neurosci **25**(5): 235-238.

Carbonetto, S., D. Evans and P. Cochard (1987). "Nerve fiber growth in culture on tissue substrata from central and peripheral nervous systems." J Neurosci **7**(2): 610-620.

Caroni, P. and M. E. Schwab (1988). "Two membrane protein fractions from rat central myelin with inhibitory properties for neurite growth and fibroblast spreading." J Cell Biol **106**(4): 1281-1288.

Cavalli, G. and R. Paro (1998). "The Drosophila Fab-7 chromosomal element conveys epigenetic inheritance during mitosis and meiosis." Cell **93**(4): 505-518.

Chae, T., Y. T. Kwon, R. Bronson, P. Dikkes, E. Li and L. H. Tsai (1997). "Mice lacking p35, a neuronal specific activator of Cdk5, display cortical lamination defects, seizures, and adult lethality." Neuron **18**(1): 29-42.

Charron, F., E. Stein, J. Jeong, A. P. McMahon and M. Tessier-Lavigne (2003). "The morphogen sonic hedgehog is an axonal chemoattractant that collaborates with netrin-1 in midline axon guidance." Cell **113**(1): 11-23.

Cheng, Q., Y. Sasaki, M. Shoji, Y. Sugiyama, H. Tanaka, T. Nakayama, N. Mizuki, F. Nakamura, K. Takei and Y. Goshima (2003). "Cdk5/p35 and Rho-kinase mediate ephrin-A5-induced signaling in retinal ganglion cells." Mol Cell Neurosci **24**(3): 632-645.

Cherfils, J. and M. Zeghouf (2013). "Regulation of small GTPases by GEFs, GAPs, and GDIs." Physiol Rev **93**(1): 269-309.

Cheung, Z. H., W. H. Chin, Y. Chen, Y. P. Ng and N. Y. Ip (2007). "Cdk5 is involved in BDNF-stimulated dendritic growth in hippocampal neurons." PLoS Biol **5**(4): e63.

Cheung, Z. H., A. K. Fu and N. Y. Ip (2006). "Synaptic roles of Cdk5: implications in higher cognitive functions and neurodegenerative diseases." Neuron **50**(1): 13-18.

Cheung, Z. H. and N. Y. Ip (2004). "Cdk5: mediator of neuronal death and survival." Neurosci Lett **361**(1-3): 47-51.

Ciccolini, F., T. J. Collins, J. Sudhoelter, P. Lipp, M. J. Berridge and M. D. Bootman (2003). "Local and global spontaneous calcium events regulate neurite outgrowth and onset of GABAergic phenotype during neural precursor differentiation." J Neurosci **23**(1): 103-111.

Cicero, S. and K. Herrup (2005). "Cyclin-dependent kinase 5 is essential for neuronal cell cycle arrest and differentiation." J Neurosci **25**(42): 9658-9668.

Coelho, C. M. and S. J. Leevers (2000). "Do growth and cell division rates determine cell size in multicellular organisms?" J Cell Sci **113 (Pt 17)**: 2927-2934.

Cole, A. R. (2009). "PCTK proteins: the forgotten brain kinases?" Neurosignals **17**(4): 288-297.

Condeelis, J. (1993). "Life at the leading edge: the formation of cell protrusions." Annu Rev Cell Biol **9**: 411-444.

Connell-Crowley, L., D. Vo, L. Luke and E. Giniger (2007). "Drosophila lacking the Cdk5 activator, p35, display defective axon guidance, age-dependent behavioral deficits and reduced lifespan." Mech Dev **124**(5): 341-349.

Cook, M., A. Gould, N. Brand, J. Davies, P. Strutt, R. Shaknovich, J. Licht, S. Waxman, Z. Chen, S. Gluecksohn-Waelsch and et al. (1995). "Expression of the zinc-finger gene PLZF at rhombomere boundaries in the vertebrate hindbrain." Proc Natl Acad Sci U S A **92**(6): 2249-2253.

Corbin, J. G., S. Nery and G. Fishell (2001). "Telencephalic cells take a tangent: non-radial migration in the mammalian forebrain." Nat Neurosci **4 Suppl**: 1177-1182.

Cropley, J. E., T. H. Dang, D. I. Martin and C. M. Suter (2012). "The penetrance of an epigenetic trait in mice is progressively yet reversibly increased by selection and environment." Proc Biol Sci **279**(1737): 2347-2353.

Cruz, J. C. and L. H. Tsai (2004). "Cdk5 deregulation in the pathogenesis of Alzheimer's disease." Trends Mol Med **10**(9): 452-458.

Cunningham, J. J. and M. F. Roussel (2001). "Cyclin-dependent kinase inhibitors in the development of the central nervous system." Cell Growth Differ **12**(8): 387-396.

Cutforth, T. and C. J. Harrison (2002). "Ephs and ephrins close ranks." Trends Neurosci **25**(7): 332-334.

da Silva, J. S. and C. G. Dotti (2002). "Breaking the neuronal sphere: regulation of the actin cytoskeleton in neuritogenesis." Nat Rev Neurosci **3**(9): 694-704.

Da Silva, J. S., M. Medina, C. Zuliani, A. Di Nardo, W. Witke and C. G. Dotti (2003). "RhoA/ROCK regulation of neuritogenesis via profilin IIa-mediated control of actin stability." J Cell Biol **162**(7): 1267-1279.

Dancause, N. (2006). "Vicarious function of remote cortex following stroke: recent evidence from human and animal studies." Neuroscientist **12**(6): 489-499.

Daniels, R. H. and G. M. Bokoch (1999). "p21-activated protein kinase: a crucial component of morphological signaling?" Trends Biochem Sci **24**(9): 350-355.

Das, S. K., T. Hashimoto, K. Shimizu, T. Yoshida, T. Sakai, Y. Sowa, A. Komoto and K. Kanazawa (2005). "Fucoxanthin induces cell cycle arrest at G0/G1 phase in human colon carcinoma cells through up-regulation of p21WAF1/Cip1." Biochim Biophys Acta **1726**(3): 328-335.

Daub, H., K. Gevaert, J. Vandekerckhove, A. Sobel and A. Hall (2001). "Rac/Cdc42 and p65PAK regulate the microtubule-destabilizing protein stathmin through phosphorylation at serine 16." J Biol Chem **276**(3): 1677-1680.

Davidson, G., J. Shen, Y. L. Huang, Y. Su, E. Karaulanov, K. Bartscherer, C. Hassler, P. Stannek, M. Boutros and C. Niehrs (2009). "Cell cycle control of wnt receptor activation." Dev Cell **17**(6): 788-799.

De Bondt, H. L., J. Rosenblatt, J. Jancarik, H. D. Jones, D. O. Morgan and S. H. Kim (1993). "Crystal structure of cyclin-dependent kinase 2." Nature **363**(6430): 595-602.

Dehay, C. and H. Kennedy (2007). "Cell-cycle control and cortical development." Nat Rev Neurosci **8**(6): 438-450.

Del Rio, J. A., C. Gonzalez-Billault, J. M. Urena, E. M. Jimenez, M. J. Barallobre, M. Pascual, L. Pujadas, S. Simo, A. La Torre, F. Wandosell, J. Avila and E. Soriano (2004). "MAP1B is required for Netrin 1 signaling in neuronal migration and axonal guidance." Curr Biol **14**(10): 840-850.

Denicourt, C. and S. F. Dowdy (2004). "Cip/Kip proteins: more than just CDKs inhibitors." Genes Dev **18**(8): 851-855.

Dhavan, R. and L. H. Tsai (2001). "A decade of CDK5." Nat Rev Mol Cell Biol **2**(10): 749-759.

Dickson, B. J. (2002). "Molecular mechanisms of axon guidance." Science **298**(5600): 1959-1964.

Dotti, C. G., C. A. Sullivan and G. A. Banker (1988). "The establishment of polarity by hippocampal neurons in culture." J Neurosci **8**(4): 1454-1468.

Dvorsky, R. and M. R. Ahmadian (2004). "Always look on the bright site of Rho: structural implications for a conserved intermolecular interface." EMBO Rep **5**(12): 1130-1136.

Dvorsky, R., L. Blumenstein, I. R. Vetter and M. R. Ahmadian (2004). "Structural insights into the interaction of ROCKI with the switch regions of RhoA." J Biol Chem **279**(8): 7098-7104.

Echalier, A., J. A. Endicott and M. E. Noble (2010). "Recent developments in cyclin-dependent kinase biochemical and structural studies." Biochim Biophys Acta **1804**(3): 511-519.

Ehler, E., F. van Leeuwen, J. G. Collard and P. C. Salinas (1997). "Expression of Tiam-1 in the developing brain suggests a role for the Tiam-1-Rac signaling pathway in cell migration and neurite outgrowth." Mol Cell Neurosci **9**(1): 1-12.

Etienne-Manneville, S. and A. Hall (2002). "Rho GTPases in cell biology." Nature **420**(6916): 629-635.

Fan, X., J. P. Labrador, H. Hing and G. J. Bashaw (2003). "Slit stimulation recruits Dock and Pak to the roundabout receptor and increases Rac activity to regulate axon repulsion at the CNS midline." Neuron **40**(1): 113-127.

Fawcett, J. W. (1992). "Intrinsic neuronal determinants of regeneration." Trends Neurosci **15**(1): 5-8.

Filbin, M. T. (2003). "Myelin-associated inhibitors of axonal regeneration in the adult mammalian CNS." Nat Rev Neurosci **4**(9): 703-713.

Font, M. A., A. Arboix and J. Krupinski (2010). "Angiogenesis, neurogenesis and neuroplasticity in ischemic stroke." Curr Cardiol Rev **6**(3): 238-244.

Freeman, R. S., S. Estus and E. M. Johnson, Jr. (1994). "Analysis of cell cycle-related gene expression in postmitotic neurons: selective induction of Cyclin D1 during programmed cell death." Neuron **12**(2): 343-355.

Fu, H., R. R. Subramanian and S. C. Masters (2000). "14-3-3 proteins: structure, function, and regulation." Annu Rev Pharmacol Toxicol **40**: 617-647.

Fu, W. Y., Y. Chen, M. Sahin, X. S. Zhao, L. Shi, J. B. Bikoff, K. O. Lai, W. H. Yung, A. K. Fu, M. E. Greenberg and N. Y. Ip (2007). "Cdk5 regulates EphA4-mediated dendritic spine retraction through an ephexin1-dependent mechanism." Nat Neurosci **10**(1): 67-76.

Fu, W. Y., K. Cheng, A. K. Fu and N. Y. Ip (2011). "Cyclin-dependent kinase 5-dependent phosphorylation of Pctaire1 regulates dendrite development." Neuroscience **180**: 353-359.

Fujita Y, Y. T. (2014). "Axon growth inhibition by RhoA/ROCK in the central nervous system." Front Neurosci. **8**: 338.

Futatsugi, A., E. Utreras, P. Rudrabhatla, H. Jaffe, H. C. Pant and A. B. Kulkarni (2012). "Cyclin-dependent kinase 5 regulates E2F transcription factor through phosphorylation of Rb protein in neurons." Cell Cycle **11**(8): 1603-1610.

Galbraith, M. D., A. J. Donner and J. M. Espinosa (2010). "CDK8: a positive regulator of transcription." Transcription **1**(1): 4-12.

Galderisi, U., F. P. Jori and A. Giordano (2003). "Cell cycle regulation and neural differentiation." Oncogene **22**(33): 5208-5219.

Gao, Y., M. Jiang, T. Yang, J. Ni and J. Chen (2006). "A Cdc2-related protein kinase hPFTAIRE1 from human brain interacting with 14-3-3 proteins." Cell Res **16**(6): 539-547.

Gao, Y. K., M. Jiang, T. Yang and J. Y. Chen (2006). "Analysis of the interaction between hPFTAIRE1 and PLZF in a yeast two-hybrid system." Acta Biochim Biophys Sin (Shanghai) **38**(3): 164-170.

Georgiev, D., H. Taniura, Y. Kambe, T. Takarada and Y. Yoneda (2008). "A critical importance of polyamine site in NMDA receptors for neurite outgrowth and fasciculation at early stages of P19 neuronal differentiation." Exp Cell Res **314**(14): 2603-2617.

Gilmore, E. C., T. Ohshima, A. M. Goffinet, A. B. Kulkarni and K. Herrup (1998). "Cyclin-dependent kinase 5-deficient mice demonstrate novel developmental arrest in cerebral cortex." J Neurosci **18**(16): 6370-6377.

Giovanni, A., E. Keramaris, E. J. Morris, S. T. Hou, M. O'Hare, N. Dyson, G. S. Robertson, R. S. Slack and D. S. Park (2000). "E2F1 mediates death of B-amyloid-treated cortical neurons in a manner independent of p53 and dependent on Bax and caspase 3." J Biol Chem **275**(16): 11553-11560.

Giovanni, A., F. Wirtz-Brugger, E. Keramaris, R. Slack and D. S. Park (1999). "Involvement of cell cycle elements, cyclin-dependent kinases, pRb, and E2F x DP, in B-amyloid-induced neuronal death." J Biol Chem **274**(27): 19011-19016.

Golestaneh, N., E. Beauchamp, S. Fallen, M. Kokkinaki, A. Uren and M. Dym (2009). "Wnt signaling promotes proliferation and stemness regulation of spermatogonial stem/progenitor cells." Reproduction **138**(1): 151-162.

Gomez, T. M. and N. C. Spitzer (1999). "In vivo regulation of axon extension and pathfinding by growth-cone calcium transients." Nature **397**(6717): 350-355.

Gonzalez, Y. R., Y. Zhang, D. Behzadpoor, S. Cregan, S. Bamforth, R. S. Slack and D. S. Park (2008). "CITED2 signals through peroxisome proliferator-activated receptor-gamma to regulate death of cortical neurons after DNA damage." J Neurosci **28**(21): 5559-5569.

Govek, E. E., S. E. Newey and L. Van Aelst (2005). "The role of the Rho GTPases in neuronal development." Genes Dev **19**(1): 1-49.

Graeser, R., J. Gannon, R. Y. Poon, T. Dubois, A. Aitken and T. Hunt (2002). "Regulation of the CDK-related protein kinase PCTAIRE-1 and its possible role in neurite outgrowth in Neuro-2A cells." J Cell Sci **115**(Pt 17): 3479-3490.

Grana, X., A. De Luca, N. Sang, Y. Fu, P. P. Claudio, J. Rosenblatt, D. O. Morgan and A. Giordano (1994). "PITALRE, a nuclear CDC2-related protein kinase that phosphorylates the retinoblastoma protein in vitro." Proc Natl Acad Sci U S A **91**(9): 3834-3838.

Grigoryan, T., P. Wend, A. Klaus and W. Birchmeier (2008). "Deciphering the function of canonical Wnt signals in development and disease: conditional loss- and gain-of-function mutations of beta-catenin in mice." Genes Dev **22**(17): 2308-2341.

Gu, X., E. C. Olson and N. C. Spitzer (1994). "Spontaneous neuronal calcium spikes and waves during early differentiation." J Neurosci **14**(11 Pt 1): 6325-6335.

Gu, X. and N. C. Spitzer (1995). "Distinct aspects of neuronal differentiation encoded by frequency of spontaneous Ca2+ transients." Nature **375**(6534): 784-787.

Gu, Y., J. Rosenblatt and D. O. Morgan (1992). "Cell cycle regulation of CDK2 activity by phosphorylation of Thr160 and Tyr15." EMBO J **11**(11): 3995-4005.

Gurdon, J. B. and P. Y. Bourillot (2001). "Morphogen gradient interpretation." Nature **413**(6858): 797-803.

Hakeda-Suzuki, S., J. Ng, J. Tzu, G. Dietzl, Y. Sun, M. Harms, T. Nardine, L. Luo and B. J. Dickson (2002). "Rac function and regulation during Drosophila development." Nature **416**(6879): 438-442.

Hall, A. (1998). "Rho GTPases and the actin cytoskeleton." Science **279**(5350): 509-514.

Hall, A. and G. Lalli (2010). "Rho and Ras GTPases in axon growth, guidance, and branching." Cold Spring Harb Perspect Biol **2**(2): a001818.

Hall, C., M. Brown, T. Jacobs, G. Ferrari, N. Cann, M. Teo, C. Monfries and L. Lim (2001). "Collapsin response mediator protein switches RhoA and Rac1 morphology in N1E-115 neuroblastoma cells and is regulated by Rho kinase." J Biol Chem **276**(46): 43482-43486.

Hall, C., G. J. Michael, N. Cann, G. Ferrari, M. Teo, T. Jacobs, C. Monfries and L. Lim (2001). "alpha2-chimaerin, a Cdc42/Rac1 regulator, is selectively expressed in the rat embryonic nervous system and is involved in neuritogenesis in N1E-115 neuroblastoma cells." J Neurosci **21**(14): 5191-5202.

Hansen, S. M., V. Berezin and E. Bock (2008). "Signaling mechanisms of neurite outgrowth induced by the cell adhesion molecules NCAM and N-cadherin." Cell Mol Life Sci **65**(23): 3809-3821.

Harada, T., T. Morooka, S. Ogawa and E. Nishida (2001). "ERK induces p35, a neuron-specific activator of Cdk5, through induction of Egr1." Nat Cell Biol **3**(5): 453-459.

Hartwell, L. H. (1974). "Saccharomyces cerevisiae cell cycle." Bacteriol Rev **38**(2): 164-198.

Hashida, T., M. Yamada, K. Hashimoto, N. Shibusawa, T. Monden, T. Satoh and M. Mori (2002). "A novel TRH-PFTAIRE protein kinase 1 pathway in the cerebellum: subtractive hybridization analysis of TRH-deficient mice." Endocrinology **143**(7): 2808-2811.

Hawasli, A. H. and J. A. Bibb (2007). "Alternative roles for Cdk5 in learning and synaptic plasticity." Biotechnol J **2**(8): 941-948.

Hellmich, M. R., H. C. Pant, E. Wada and J. F. Battey (1992). "Neuronal cdc2-like kinase: a cdc2-related protein kinase with predominantly neuronal expression." Proc Natl Acad Sci U S A **89**(22): 10867-10871.

Henderson, I. R. and S. E. Jacobsen (2007). "Epigenetic inheritance in plants." Nature **447**(7143): 418-424.

Higgs, H. N. and T. D. Pollard (2001). "Regulation of actin filament network formation through ARP2/3 complex: activation by a diverse array of proteins." Annu Rev Biochem **70**: 649-676.

Hindley, C. and A. Philpott (2012). "Co-ordination of cell cycle and differentiation in the developing nervous system." Biochem J **444**(3): 375-382.

Hirose, T., M. Kawabuchi, T. Tamaru, N. Okumura, K. Nagai and M. Okada (2000). "Identification of tudor repeat associator with PCTAIRE 2 (Trap). A novel protein that interacts with the N-terminal domain of PCTAIRE 2 in rat brain." Eur J Biochem **267**(7): 2113-2121.

Hitchins, M. P., J. J. Wong, G. Suthers, C. M. Suter, D. I. Martin, N. J. Hawkins and R. L. Ward (2007). "Inheritance of a cancer-associated MLH1 germ-line epimutation." N Engl J Med **356**(7): 697-705.

Hoffman, G. R., N. Nassar and R. A. Cerione (2000). "Structure of the Rho family GTP-binding protein Cdc42 in complex with the multifunctional regulator RhoGDI." Cell **100**(3): 345-356.

Horii, Y., J. F. Beeler, K. Sakaguchi, M. Tachibana and T. Miki (1994). "A novel oncogene, ost, encodes a guanine nucleotide exchange factor that potentially links Rho and Rac signaling pathways." EMBO J **13**(20): 4776-4786.

Hoshino, M., M. Sone, M. Fukata, S. Kuroda, K. Kaibuchi, Y. Nabeshima and C. Hama (1999). "Identification of the stef gene that encodes a novel guanine nucleotide exchange factor specific for Rac1." J Biol Chem **274**(25): 17837-17844.

Huang, E. J. and L. F. Reichardt (2003). "Trk receptors: roles in neuronal signal transduction." Annu Rev Biochem **72**: 609-642.

Huber, A. B., A. L. Kolodkin, D. D. Ginty and J. F. Cloutier (2003). "Signaling at the growth cone: ligand-receptor complexes and the control of axon growth and guidance." Annu Rev Neurosci **26**: 509-563.

Ille, F., S. Atanasoski, S. Falk, L. M. Ittner, D. Marki, S. Buchmann-Moller, H. Wurdak, U. Suter, M. M. Taketo and L. Sommer (2007). "Wnt/BMP signal integration regulates the balance between

proliferation and differentiation of neuroepithelial cells in the dorsal spinal cord." Dev Biol **304**(1): 394-408.

Ishiguro, K., M. Takamatsu, K. Tomizawa, A. Omori, M. Takahashi, M. Arioka, T. Uchida and K. Imahori (1992). "Tau protein kinase I converts normal tau protein into A68-like component of paired helical filaments." J Biol Chem **267**(15): 10897-10901.

Ishizaki, T., M. Maekawa, K. Fujisawa, K. Okawa, A. Iwamatsu, A. Fujita, N. Watanabe, Y. Saito, A. Kakizuka, N. Morii and S. Narumiya (1996). "The small GTP-binding protein Rho binds to and activates a 160 kDa Ser/Thr protein kinase homologous to myotonic dystrophy kinase." EMBO J **15**(8): 1885-1893.

Itoh, Y., N. Masuyama, K. Nakayama, K. I. Nakayama and Y. Gotoh (2007). "The cyclin-dependent kinase inhibitors p57 and p27 regulate neuronal migration in the developing mouse neocortex." J Biol Chem **282**(1): 390-396.

Jablonka, E. and G. Raz (2009). "Transgenerational epigenetic inheritance: prevalence, mechanisms, and implications for the study of heredity and evolution." Q Rev Biol **84**(2): 131-176.

Jablonska, B., A. Aguirre, R. Vandenbosch, S. Belachew, C. Berthet, P. Kaldis and V. Gallo (2007). "Cdk2 is critical for proliferation and self-renewal of neural progenitor cells in the adult subventricular zone." J Cell Biol **179**(6): 1231-1245.

Jaffe, A. B. and A. Hall (2005). "Rho GTPases: biochemistry and biology." Annu Rev Cell Dev Biol **21**: 247-269.

Jalink, K., E. J. van Corven, T. Hengeveld, N. Morii, S. Narumiya and W. H. Moolenaar (1994). "Inhibition of lysophosphatidate- and thrombin-induced neurite retraction and neuronal cell rounding by ADP ribosylation of the small GTP-binding protein Rho." J Cell Biol **126**(3): 801-810.

Jeffrey, P. D., A. A. Russo, K. Polyak, E. Gibbs, J. Hurwitz, J. Massague and N. P. Pavletich (1995). "Mechanism of CDK activation revealed by the structure of a cyclinA-CDK2 complex." Nature **376**(6538): 313-320.

Jiang, M., Y. Gao, T. Yang, X. Zhu and J. Chen (2009). "Cyclin Y, a novel membrane-associated cyclin, interacts with PFTK1." FEBS Lett **583**(13): 2171-2178.

Johansson, J. U., L. Lilja, X. L. Chen, H. Higashida, B. Meister, M. Noda, Z. G. Zhong, S. Yokoyama, P. O. Berggren and C. Bark (2005). "Cyclin-dependent kinase 5 activators p35 and p39 facilitate formation of functional synapses." Brain Res Mol Brain Res **138**(2): 215-227.

John, P. C., M. Mews and R. Moore (2001). "Cyclin/Cdk complexes: their involvement in cell cycle progression and mitotic division." Protoplasma **216**(3-4): 119-142.

Kaldis, P. (1999). "The cdk-activating kinase (CAK): from yeast to mammals." Cell Mol Life Sci **55**(2): 284-296.

Kast, D. J., C. Yang, A. Disanza, M. Boczkowska, Y. Madasu, G. Scita, T. Svitkina and R. Dominguez (2014). "Mechanism of IRSp53 inhibition and combinatorial activation by Cdc42 and downstream effectors." Nat Struct Mol Biol **21**(4): 413-422.

Kawauchi, T. (2014). "Cdk5 regulates multiple cellular events in neural development, function and disease." Dev Growth Differ **56**(5): 335-348.

Kawauchi, T., K. Chihama, Y. Nabeshima and M. Hoshino (2006). "Cdk5 phosphorylates and stabilizes p27kip1 contributing to actin organization and cortical neuronal migration." Nat Cell Biol **8**(1): 17-26.

Kawauchi, T. and M. Hoshino (2008). "Molecular pathways regulating cytoskeletal organization and morphological changes in migrating neurons." Dev Neurosci **30**(1-3): 36-46.

Kawauchi, T., M. Shikanai and Y. Kosodo (2013). "Extra-cell cycle regulatory functions of cyclin-dependent kinases (CDK) and CDK inhibitor proteins contribute to brain development and neurological disorders." Genes Cells **18**(3): 176-194.

Kemphues, K. (2000). "PARsing embryonic polarity." Cell **101**(4): 345-348.

Kerr, G. E., J. C. Young, K. Horvay, H. E. Abud and K. L. Loveland (2014). "Regulated Wnt/beta-catenin signaling sustains adult spermatogenesis in mice." Biol Reprod **90**(1): 3.

Kesavapany, S., N. Amin, Y. L. Zheng, R. Nijhara, H. Jaffe, R. Sihag, J. S. Gutkind, S. Takahashi, A. Kulkarni, P. Grant and H. C. Pant (2004). "p35/cyclin-dependent kinase 5 phosphorylation of ras guanine nucleotide releasing factor 2 (RasGRF2) mediates Rac-dependent Extracellular Signal-regulated kinase 1/2 activity, altering RasGRF2 and microtubule-associated protein 1b distribution in neurons." J Neurosci **24**(18): 4421-4431.

Kesavapany, S., T. K. Pareek, Y. L. Zheng, N. Amin, J. S. Gutkind, W. Ma, A. B. Kulkarni, P. Grant and H. C. Pant (2006). "Neuronal nuclear organization is controlled by cyclin-dependent kinase 5 phosphorylation of Ras Guanine nucleotide releasing factor-1." Neurosignals **15**(4): 157-173.

Kim, Y. T. and M. Zhao (2005). "Aberrant cell cycle regulation in cervical carcinoma." Yonsei Med J **46**(5): 597-613.

Ko, J., S. Humbert, R. T. Bronson, S. Takahashi, A. B. Kulkarni, E. Li and L. H. Tsai (2001). "p35 and p39 are essential for cyclin-dependent kinase 5 function during neurodevelopment." J Neurosci **21**(17): 6758-6771.

Konishi, Y. and A. Bonni (2003). "The E2F-Cdc2 cell-cycle pathway specifically mediates activity deprivation-induced apoptosis of postmitotic neurons." J Neurosci **23**(5): 1649-1658.

Konishi, Y., M. Lehtinen, N. Donovan and A. Bonni (2002). "Cdc2 phosphorylation of BAD links the cell cycle to the cell death machinery." Mol Cell **9**(5): 1005-1016.

Korenjak, M. and A. Brehm (2005). "E2F-Rb complexes regulating transcription of genes important for differentiation and development." Curr Opin Genet Dev **15**(5): 520-527.

Kruman, II, R. P. Wersto, F. Cardozo-Pelaez, L. Smilenov, S. L. Chan, F. J. Chrest, R. Emokpae, Jr., M. Gorospe and M. P. Mattson (2004). "Cell cycle activation linked to neuronal cell death initiated by DNA damage." Neuron **41**(4): 549-561.

Kubo, T., A. Yamaguchi, N. Iwata and T. Yamashita (2008). "The therapeutic effects of Rho-ROCK inhibitors on CNS disorders." Ther Clin Risk Manag **4**(3): 605-615.

Kunda, P., G. Paglini, S. Quiroga, K. Kosik and A. Caceres (2001). "Evidence for the involvement of Tiam1 in axon formation." J Neurosci **21**(7): 2361-2372.

Kusakawa, G., T. Saito, R. Onuki, K. Ishiguro, T. Kishimoto and S. Hisanaga (2000). "Calpain-dependent proteolytic cleavage of the p35 cyclin-dependent kinase 5 activator to p25." J Biol Chem **275**(22): 17166-17172.

Kwon, Y. T. and L. H. Tsai (2000). "The role of the p35/cdk5 kinase in cortical development." Results Probl Cell Differ **30**: 241-253.

Lange, C., W. B. Huttner and F. Calegari (2009). "Cdk4/cyclinD1 overexpression in neural stem cells shortens G1, delays neurogenesis, and promotes the generation and expansion of basal progenitors." Cell Stem Cell **5**(3): 320-331.

Langhorst, M. F., F. A. Jaeger, S. Mueller, L. Sven Hartmann, G. Luxenhofer and C. A. Stuermer (2008). "Reggies/flotillins regulate cytoskeletal remodeling during neuronal differentiation via CAP/ponsin and Rho GTPases." Eur J Cell Biol **87**(12): 921-931.

Lanier, L. M., M. A. Gates, W. Witke, A. S. Menzies, A. M. Wehman, J. D. Macklis, D. Kwiatkowski, P. Soriano and F. B. Gertler (1999). "Mena is required for neurulation and commissure formation." Neuron **22**(2): 313-325.

Lazzaro, M. A., P. R. Albert and J. P. Julien (1997). "A novel cdc2-related protein kinase expressed in the nervous system." J Neurochem **69**(1): 348-364.

Lazzaro, M. A. and J. P. Julien (1997). "Chromosomal mapping of the PFTAIRE gene, Pftk1, a cdc2-related kinase expressed predominantly in the mouse nervous system." Genomics **42**(3): 536-537.

Lee, T., C. Winter, S. S. Marticke, A. Lee and L. Luo (2000). "Essential roles of Drosophila RhoA in the regulation of neuroblast proliferation and dendritic but not axonal morphogenesis." Neuron **25**(2): 307-316.

Leung, W. K., A. K. Ching, A. W. Chan, T. C. Poon, H. Mian, A. S. Wong, K. F. To and N. Wong (2011). "A novel interplay between oncogenic PFTK1 protein kinase and tumor suppressor TAGLN2 in the control of liver cancer cell motility." Oncogene **30**(44): 4464-4475.

Leung, W. K., A. K. Ching and N. Wong (2011). "Phosphorylation of Caldesmon by PFTAIRE1 kinase promotes actin binding and formation of stress fibers." Mol Cell Biochem **350**(1-2): 201-206.

Lew, J., Q. Q. Huang, Z. Qi, R. J. Winkfein, R. Aebersold, T. Hunt and J. H. Wang (1994). "A brain-specific activator of cyclin-dependent kinase 5." Nature **371**(6496): 423-426.

Lew, J., R. J. Winkfein, H. K. Paudel and J. H. Wang (1992). "Brain proline-directed protein kinase is a neurofilament kinase which displays high sequence homology to p34cdc2." J Biol Chem **267**(36): 25922-25926.

Li, B. and E. DiCicco-Bloom (2004). "Basic fibroblast growth factor exhibits dual and rapid regulation of cyclin D1 and p27 to stimulate proliferation of rat cerebral cortical precursors." Dev Neurosci **26**(2-4): 197-207.

Li, J. Y., M. A. English, H. J. Ball, P. L. Yeyati, S. Waxman and J. D. Licht (1997). "Sequence-specific DNA binding and transcriptional regulation by the promyelocytic leukemia zinc finger protein." J Biol Chem **272**(36): 22447-22455.

Lim, S. and P. Kaldis (2013). "Cdks, cyclins and CKIs: roles beyond cell cycle regulation." Development **140**(15): 3079-3093.

Lin, S., J. Wang, Z. Ye, N. Y. Ip and S. C. Lin (2008). "CDK5 activator p35 downregulates E-cadherin precursor independently of CDK5." FEBS Lett **582**(8): 1197-1202.

Liu, D. X., S. C. Biswas and L. A. Greene (2004). "B-myb and C-myb play required roles in neuronal apoptosis evoked by nerve growth factor deprivation and DNA damage." J Neurosci **24**(40): 8720-8725.

Liu, H., T. Nakazawa, T. Tezuka and T. Yamamoto (2006). "Physical and functional interaction of Fyn tyrosine kinase with a brain-enriched Rho GTPase-activating protein TCGAP." J Biol Chem **281**(33): 23611-23619.

Liu, J. and E. T. Kipreos (2000). "Evolution of cyclin-dependent kinases (CDKs) and CDK-activating kinases (CAKs): differential conservation of CAKs in yeast and metazoa." Mol Biol Evol **17**(7): 1061-1074.

Liu, Y., K. Cheng, K. Gong, A. K. Fu and N. Y. Ip (2006). "Pctaire1 phosphorylates N-ethylmaleimide-sensitive fusion protein: implications in the regulation of its hexamerization and exocytosis." J Biol Chem **281**(15): 9852-9858.

Longenecker, K., P. Read, U. Derewenda, Z. Dauter, X. Liu, S. Garrard, L. Walker, A. V. Somlyo, R. K. Nakamoto, A. P. Somlyo and Z. S. Derewenda (1999). "How RhoGDI binds Rho." Acta Crystallogr D Biol Crystallogr **55**(Pt 9): 1503-1515.

Lopes, J. P., C. R. Oliveira and P. Agostinho (2009). "Cdk5 acts as a mediator of neuronal cell cycle re-entry triggered by amyloid-beta and prion peptides." Cell Cycle **8**(1): 97-104.

Lowery, L. A. and D. Van Vactor (2009). "The trip of the tip: understanding the growth cone machinery." Nat Rev Mol Cell Biol **10**(5): 332-343.

Loyer, P., J. H. Trembley, J. A. Grenet, A. Busson, A. Corlu, W. Zhao, M. Kocak, V. J. Kidd and J. M. Lahti (2008). "Characterization of cyclin L1 and L2 interactions with CDK11 and splicing factors: influence of cyclin L isoforms on splice site selection." J Biol Chem **283**(12): 7721-7732.

Loyer, P., J. H. Trembley, R. Katona, V. J. Kidd and J. M. Lahti (2005). "Role of CDK/cyclin complexes in transcription and RNA splicing." Cell Signal **17**(9): 1033-1051.

Lucking, C. B., A. Durr, V. Bonifati, J. Vaughan, G. De Michele, T. Gasser, B. S. Harhangi, G. Meco, P. Denefle, N. W. Wood, Y. Agid and A. Brice (2000). "Association between early-onset Parkinson's disease and mutations in the parkin gene." N Engl J Med **342**(21): 1560-1567.

Luo, L., T. K. Hensch, L. Ackerman, S. Barbel, L. Y. Jan and Y. N. Jan (1996). "Differential effects of the Rac GTPase on Purkinje cell axons and dendritic trunks and spines." Nature **379**(6568): 837-840.

Ma, X. M., R. C. Johnson, R. E. Mains and B. A. Eipper (2001). "Expression of kalirin, a neuronal GDP/GTP exchange factor of the trio family, in the central nervous system of the adult rat." J Comp Neurol **429**(3): 388-402.

Machesky, L. M., R. D. Mullins, H. N. Higgs, D. A. Kaiser, L. Blanchoin, R. C. May, M. E. Hall and T. D. Pollard (1999). "Scar, a WASp-related protein, activates nucleation of actin filaments by the Arp2/3 complex." Proc Natl Acad Sci U S A **96**(7): 3739-3744.

Madaule, P. and R. Axel (1985). "A novel ras-related gene family." Cell **41**(1): 31-40.

Maekawa, M., T. Ishizaki, S. Boku, N. Watanabe, A. Fujita, A. Iwamatsu, T. Obinata, K. Ohashi, K. Mizuno and S. Narumiya (1999). "Signaling from Rho to the actin cytoskeleton through protein kinases ROCK and LIM-kinase." Science **285**(5429): 895-898.

Malumbres, M. (2011). "Physiological relevance of cell cycle kinases." Physiol Rev **91**(3): 973-1007.

Malumbres, M. (2014). "Cyclin-dependent kinases." Genome Biol **15**(6): 122.

Malumbres, M. and M. Barbacid (2005). "Mammalian cyclin-dependent kinases." Trends Biochem Sci **30**(11): 630-641.

Malumbres, M., E. Harlow, T. Hunt, T. Hunter, J. M. Lahti, G. Manning, D. O. Morgan, L. H. Tsai and D. J. Wolgemuth (2009). "Cyclin-dependent kinases: a family portrait." Nat Cell Biol **11**(11): 1275-1276.

Manser, E., T. Leung, H. Salihuddin, Z. S. Zhao and L. Lim (1994). "A brain serine/threonine protein kinase activated by Cdc42 and Rac1." Nature **367**(6458): 40-46.

Marchler-Bauer, A., C. Zheng, F. Chitsaz, M. K. Derbyshire, L. Y. Geer, R. C. Geer, N. R. Gonzales, M. Gwadz, D. I. Hurwitz, C. J. Lanczycki, F. Lu, S. Lu, G. H. Marchler, J. S. Song, N. Thanki, R. A. Yamashita, D. Zhang and S. H. Bryant (2013). "CDD: conserved domains and protein three-dimensional structure." Nucleic Acids Res **41**(Database issue): D348-352.

Marin, O. and J. L. Rubenstein (2001). "A long, remarkable journey: tangential migration in the telencephalon." Nat Rev Neurosci **2**(11): 780-790.

Marin, O., M. Valiente, X. Ge and L. H. Tsai (2010). "Guiding neuronal cell migrations." Cold Spring Harb Perspect Biol **2**(2): a001834.

Martini, F. J., M. Valiente, G. Lopez Bendito, G. Szabo, F. Moya, M. Valdeolmillos and O. Marin (2009). "Biased selection of leading process branches mediates chemotaxis during tangential neuronal migration." Development **136**(1): 41-50.

May, V., M. R. Schiller, B. A. Eipper and R. E. Mains (2002). "Kalirin Dbl-homology guanine nucleotide exchange factor 1 domain initiates new axon outgrowths via RhoG-mediated mechanisms." J Neurosci **22**(16): 6980-6990.

Mazzarello, P. (1999). "The Hidden Structure. Translated from Cajal's Histologie du Systeme Nerveux, describing a first view of the results of the Golgi-staining method.".

McKerracher, L., S. David, D. L. Jackson, V. Kottis, R. J. Dunn and P. E. Braun (1994). "Identification of myelin-associated glycoprotein as a major myelin-derived inhibitor of neurite growth." Neuron **13**(4): 805-811.

Meyerson, M., G. H. Enders, C. L. Wu, L. K. Su, C. Gorka, C. Nelson, E. Harlow and L. H. Tsai (1992). "A family of human cdc2-related protein kinases." EMBO J **11**(8): 2909-2917.

Mikolcevic, P., R. Sigl, V. Rauch, M. W. Hess, K. Pfaller, M. Barisic, L. J. Pelliniemi, M. Boesl and S. Geley (2012). "Cyclin-dependent kinase 16/PCTAIRE kinase 1 is activated by cyclin Y and is essential for spermatogenesis." Mol Cell Biol **32**(4): 868-879.

Miyajima, M., H. O. Nornes and T. Neuman (1995). "Cyclin E is expressed in neurons and forms complexes with cdk5." Neuroreport **6**(8): 1130-1132.

Miyata, T., A. Kawaguchi, H. Okano and M. Ogawa (2001). "Asymmetric inheritance of radial glial fibers by cortical neurons." Neuron **31**(5): 727-741.

Miyata, T. and M. Ogawa (2007). "Twisting of neocortical progenitor cells underlies a spring-like mechanism for daughter-cell migration." Curr Biol **17**(2): 146-151.

Morgan, D. O. (1995). "Principles of CDK regulation." Nature **374**(6518): 131-134.

Morgan, D. O. (2007). "The Cell Cycle: Principles of Control. ." London: New Science Press, 1st ed.

Morgan, H. D., H. G. Sutherland, D. I. Martin and E. Whitelaw (1999). "Epigenetic inheritance at the agouti locus in the mouse." Nat Genet **23**(3): 314-318.

Morris, E. J., E. Keramaris, H. J. Rideout, R. S. Slack, N. J. Dyson, L. Stefanis and D. S. Park (2001). "Cyclin-dependent kinases and P53 pathways are activated independently and mediate Bax activation in neurons after DNA damage." J Neurosci **21**(14): 5017-5026.

Mukhopadhyay, G., P. Doherty, F. S. Walsh, P. R. Crocker and M. T. Filbin (1994). "A novel role for myelin-associated glycoprotein as an inhibitor of axonal regeneration." Neuron **13**(3): 757-767.

Munger, K. and P. M. Howley (2002). "Human papillomavirus immortalization and transformation functions." Virus Res **89**(2): 213-228.

Muslin, A. J. and H. Xing (2000). "14-3-3 proteins: regulation of subcellular localization by molecular interference." Cell Signal **12**(11-12): 703-709.

Nadarajah, B., J. E. Brunstrom, J. Grutzendler, R. O. Wong and A. L. Pearlman (2001). "Two modes of radial migration in early development of the cerebral cortex." Nat Neurosci **4**(2): 143-150.

Nadarajah, B. and J. G. Parnavelas (2002). "Modes of neuronal migration in the developing cerebral cortex." Nat Rev Neurosci **3**(6): 423-432.

Nagy, Z., M. M. Esiri, A. M. Cato and A. D. Smith (1997). "Cell cycle markers in the hippocampus in Alzheimer's disease." Acta Neuropathol **94**(1): 6-15.

Negishi, M. and H. Katoh (2002). "Rho family GTPases as key regulators for neuronal network formation." J Biochem **132**(2): 157-166.

Ng, J. and L. Luo (2004). "Rho GTPases regulate axon growth through convergent and divergent signaling pathways." Neuron **44**(5): 779-793.

Ng, J., T. Nardine, M. Harms, J. Tzu, A. Goldstein, Y. Sun, G. Dietzl, B. J. Dickson and L. Luo (2002). "Rac GTPases control axon growth, guidance and branching." Nature **416**(6879): 442-447.

Nguyen, M. D., M. Boudreau, J. Kriz, S. Couillard-Despres, D. R. Kaplan and J. P. Julien (2003). "Cell cycle regulators in the neuronal death pathway of amyotrophic lateral sclerosis caused by mutant superoxide dismutase 1." J Neurosci **23**(6): 2131-2140.

Nguyen, M. D. and J. P. Julien (2003). "Cyclin-dependent kinase 5 in amyotrophic lateral sclerosis." Neurosignals **12**(4-5): 215-220.

Nikolic, M. (2002). "The role of Rho GTPases and associated kinases in regulating neurite outgrowth." Int J Biochem Cell Biol **34**(7): 731-745.

Nikolic, M., M. M. Chou, W. Lu, B. J. Mayer and L. H. Tsai (1998). "The p35/Cdk5 kinase is a neuron-specific Rac effector that inhibits Pak1 activity." Nature **395**(6698): 194-198.

Nikolic, M., H. Dudek, Y. T. Kwon, Y. F. Ramos and L. H. Tsai (1996). "The cdk5/p35 kinase is essential for neurite outgrowth during neuronal differentiation." Genes Dev **10**(7): 816-825.

Nobes, C. D. and A. Hall (1995). "Rho, rac, and cdc42 GTPases regulate the assembly of multimolecular focal complexes associated with actin stress fibers, lamellipodia, and filopodia." Cell **81**(1): 53-62.

Nusser, N., E. Gosmanova, Y. Zheng and G. Tigyi (2002). "Nerve growth factor signals through TrkA, phosphatidylinositol 3-kinase, and Rac1 to inactivate RhoA during the initiation of neuronal differentiation of PC12 cells." J Biol Chem **277**(39): 35840-35846.

O'Hare, M. J., S. T. Hou, E. J. Morris, S. P. Cregan, Q. Xu, R. S. Slack and D. S. Park (2000). "Induction and modulation of cerebellar granule neuron death by E2F-1." J Biol Chem **275**(33): 25358-25364.

O'Hare, M. J., N. Kushwaha, Y. Zhang, H. Aleyasin, S. M. Callaghan, R. S. Slack, P. R. Albert, I. Vincent and D. S. Park (2005). "Differential roles of nuclear and cytoplasmic cyclin-dependent kinase 5 in apoptotic and excitotoxic neuronal death." J Neurosci **25**(39): 8954-8966.

Odajima, J., Z. P. Wills, Y. M. Ndassa, M. Terunuma, K. Kretschmannova, T. Z. Deeb, Y. Geng, S. Gawrzak, I. M. Quadros, J. Newman, M. Das, M. E. Jecrois, Q. Yu, N. Li, F. Bienvenu, S. J. Moss,

M. E. Greenberg, J. A. Marto and P. Sicinski (2011). "Cyclin E constrains Cdk5 activity to regulate synaptic plasticity and memory formation." Dev Cell **21**(4): 655-668.

Ohno, S. (2001). "Intercellular junctions and cellular polarity: the PAR-aPKC complex, a conserved core cassette playing fundamental roles in cell polarity." Curr Opin Cell Biol **13**(5): 641-648.

Ohshima, T., M. Hirasawa, H. Tabata, T. Mutoh, T. Adachi, H. Suzuki, K. Saruta, T. Iwasato, S. Itohara, M. Hashimoto, K. Nakajima, M. Ogawa, A. B. Kulkarni and K. Mikoshiba (2007). "Cdk5 is required for multipolar-to-bipolar transition during radial neuronal migration and proper dendrite development of pyramidal neurons in the cerebral cortex." Development **134**(12): 2273-2282.

Ohshima, T., J. M. Ward, C. G. Huh, G. Longenecker, Veeranna, H. C. Pant, R. O. Brady, L. J. Martin and A. B. Kulkarni (1996). "Targeted disruption of the cyclin-dependent kinase 5 gene results in abnormal corticogenesis, neuronal pathology and perinatal death." Proc Natl Acad Sci U S A **93**(20): 11173-11178.

Okuda, T., J. L. Cleveland and J. R. Downing (1992). "PCTAIRE-1 and PCTAIRE-3, two members of a novel cdc2/CDC28-related protein kinase gene family." Oncogene **7**(11): 2249-2258.

Osuga, H., S. Osuga, F. Wang, R. Fetni, M. J. Hogan, R. S. Slack, A. M. Hakim, J. E. Ikeda and D. S. Park (2000). "Cyclin-dependent kinases as a therapeutic target for stroke." Proc Natl Acad Sci U S A **97**(18): 10254-10259.

Otsuka, Y., T. Tanaka, D. Uchida, Y. Noguchi, N. Saeki, Y. Saito and I. Tatsuno (2004). "Roles of cyclin-dependent kinase 4 and p53 in neuronal cell death induced by doxorubicin on cerebellar granule neurons in mouse." Neurosci Lett **365**(3): 180-185.

Padmanabhan, J., D. S. Park, L. A. Greene and M. L. Shelanski (1999). "Role of cell cycle regulatory proteins in cerebellar granule neuron apoptosis." J Neurosci **19**(20): 8747-8756.

Pang, E. Y., A. H. Bai, K. F. To, S. M. Sy, N. L. Wong, P. B. Lai, J. A. Squire and N. Wong (2007). "Identification of PFTAIRE protein kinase 1, a novel cell division cycle-2 related gene, in the motile phenotype of hepatocellular carcinoma cells." Hepatology **46**(2): 436-445.

Park, D. S., S. E. Farinelli and L. A. Greene (1996). "Inhibitors of cyclin-dependent kinases promote survival of post-mitotic neuronally differentiated PC12 cells and sympathetic neurons." J Biol Chem **271**(14): 8161-8169.

Park, D. S., B. Levine, G. Ferrari and L. A. Greene (1997). "Cyclin dependent kinase inhibitors and dominant negative cyclin dependent kinase 4 and 6 promote survival of NGF-deprived sympathetic neurons." J Neurosci **17**(23): 8975-8983.

Park, D. S., E. J. Morris, L. A. Greene and H. M. Geller (1997). "G1/S cell cycle blockers and inhibitors of cyclin-dependent kinases suppress camptothecin-induced neuronal apoptosis." J Neurosci **17**(4): 1256-1270.

Park, D. S., E. J. Morris, J. Padmanabhan, M. L. Shelanski, H. M. Geller and L. A. Greene (1998). "Cyclin-dependent kinases participate in death of neurons evoked by DNA-damaging agents." J Cell Biol **143**(2): 457-467.

Park, D. S., E. J. Morris, L. Stefanis, C. M. Troy, M. L. Shelanski, H. M. Geller and L. A. Greene (1998). "Multiple pathways of neuronal death induced by DNA-damaging agents, NGF deprivation, and oxidative stress." J Neurosci **18**(3): 830-840.

Park, D. S., A. Obeidat, A. Giovanni and L. A. Greene (2000). "Cell cycle regulators in neuronal death evoked by excitotoxic stress: implications for neurodegeneration and its treatment." Neurobiol Aging **21**(6): 771-781.

Patrick, G. N., P. Zhou, Y. T. Kwon, P. M. Howley and L. H. Tsai (1998). "p35, the neuronal-specific activator of cyclin-dependent kinase 5 (Cdk5) is degraded by the ubiquitin-proteasome pathway." J Biol Chem **273**(37): 24057-24064.

Patrick, G. N., L. Zukerberg, M. Nikolic, S. de la Monte, P. Dikkes and L. H. Tsai (1999). "Conversion of p35 to p25 deregulates Cdk5 activity and promotes neurodegeneration." Nature **402**(6762): 615-622.

Pei, J. J., I. Grundke-Iqbal, K. Iqbal, N. Bogdanovic, B. Winblad and R. F. Cowburn (1998). "Accumulation of cyclin-dependent kinase 5 (cdk5) in neurons with early stages of Alzheimer's disease neurofibrillary degeneration." Brain Res **797**(2): 267-277.

Penzes, P., R. C. Johnson, R. Sattler, X. Zhang, R. L. Huganir, V. Kambampati, R. E. Mains and B. A. Eipper (2001). "The neuronal Rho-GEF Kalirin-7 interacts with PDZ domain-containing proteins and regulates dendritic morphogenesis." Neuron **29**(1): 229-242.

Pines, J. (1993). "Cyclins and cyclin-dependent kinases: take your partners." Trends Biochem Sci **18**(6): 195-197.

Pollack, D., Y. Xiao, V. Shrivasatava, A. Levy, M. Andrusier, J. D'Armiento, M. K. Holz and M. Vigodner (2015). "CDK14 expression is down-regulated by cigarette smoke in vivo and in vitro." Toxicol Lett **234**(2): 120-130.

Polleux, F. and W. Snider (2010). "Initiating and growing an axon." Cold Spring Harb Perspect Biol **2**(4): a001925.

Polleux, F., K. L. Whitford, P. A. Dijkhuizen, T. Vitalis and A. Ghosh (2002). "Control of cortical interneuron migration by neurotrophins and PI3-kinase signaling." Development **129**(13): 3147-3160.

Pozas, E. and C. F. Ibanez (2005). "GDNF and GFRalpha1 promote differentiation and tangential migration of cortical GABAergic neurons." Neuron **45**(5): 701-713.

Qu, D., J. Rashidian, M. P. Mount, H. Aleyasin, M. Parsanejad, A. Lira, E. Haque, Y. Zhang, S. Callaghan, M. Daigle, M. W. Rousseaux, R. S. Slack, P. R. Albert, I. Vincent, J. M. Woulfe and D. S. Park (2007). "Role of Cdk5-mediated phosphorylation of Prx2 in MPTP toxicity and Parkinson's disease." Neuron **55**(1): 37-52.

Rakic, P. (1990). "Principles of neural cell migration." Experientia **46**(9): 882-891.

Rashid, T., M. Banerjee and M. Nikolic (2001). "Phosphorylation of Pak1 by the p35/Cdk5 kinase affects neuronal morphology." J Biol Chem **276**(52): 49043-49052.

Rashidian, J., G. Iyirhiaro, H. Aleyasin, M. Rios, I. Vincent, S. Callaghan, R. J. Bland, R. S. Slack, M. J. During and D. S. Park (2005). "Multiple cyclin-dependent kinases signals are critical mediators of ischemia/hypoxic neuronal death in vitro and in vivo." Proc Natl Acad Sci U S A **102**(39): 14080-14085.

Rashidian, J., M. W. Rousseaux, K. Venderova, D. Qu, S. M. Callaghan, M. Phillips, R. J. Bland, M. J. During, Z. Mao, R. S. Slack and D. S. Park (2009). "Essential role of cytoplasmic cdk5 and Prx2 in multiple ischemic injury models, in vivo." J Neurosci **29**(40): 12497-12505.

Revenu, C., R. Athman, S. Robine and D. Louvard (2004). "The co-workers of actin filaments: from cell structures to signals." Nat Rev Mol Cell Biol **5**(8): 635-646.

Rhee, K. and D. J. Wolgemuth (1995). "Cdk family genes are expressed not only in dividing but also in terminally differentiated mouse germ cells, suggesting their possible function during both cell division and differentiation." Dev Dyn **204**(4): 406-420.

Richard-Parpaillon, L., R. A. Cosgrove, C. Devine, A. E. Vernon and A. Philpott (2004). "G1/S phase cyclin-dependent kinase overexpression perturbs early development and delays tissue-specific differentiation in Xenopus." Development **131**(11): 2577-2586.

Rideout, H. J., Q. Wang, D. S. Park and L. Stefanis (2003). "Cyclin-dependent kinase activity is required for apoptotic death but not inclusion formation in cortical neurons after proteasomal inhibition." J Neurosci **23**(4): 1237-1245.

Ridley, A. J. and A. Hall (1992). "The small GTP-binding protein rho regulates the assembly of focal adhesions and actin stress fibers in response to growth factors." Cell **70**(3): 389-399.

Riento, K., R. M. Guasch, R. Garg, B. Jin and A. J. Ridley (2003). "RhoE binds to ROCK I and inhibits downstream signaling." Mol Cell Biol **23**(12): 4219-4229.

Riento, K. and A. J. Ridley (2003). "Rocks: multifunctional kinases in cell behaviour." Nat Rev Mol Cell Biol **4**(6): 446-456.

Rodríguez González, Y. and P. D. S. (2011). "Cited2 and PFTAIRE, two Ways in Which Cyclin Dependent Kinases Impact on Development and Degeneration in the Central Nervous System." Thesis submitted to the Faculty of Graduate and Postdoctoral Studies of University of Ottawa.

Rodriguez, O. C., A. W. Schaefer, C. A. Mandato, P. Forscher, W. M. Bement and C. M. Waterman-Storer (2003). "Conserved microtubule-actin interactions in cell movement and morphogenesis." Nat Cell Biol **5**(7): 599-609.

Roemer, I., W. Reik, W. Dean and J. Klose (1997). "Epigenetic inheritance in the mouse." Curr Biol **7**(4): 277-280.

Rohatgi, R., L. Ma, H. Miki, M. Lopez, T. Kirchhausen, T. Takenawa and M. W. Kirschner (1999). "The interaction between N-WASP and the Arp2/3 complex links Cdc42-dependent signals to actin assembly." Cell **97**(2): 221-231.

Rosales, J. L., M. J. Nodwell, R. N. Johnston and K. Y. Lee (2000). "Cdk5/p25(nck5a) interaction with synaptic proteins in bovine brain." J Cell Biochem **78**(1): 151-159.

Ruchhoeft, M. L., S. Ohnuma, L. McNeill, C. E. Holt and W. A. Harris (1999). "The neuronal architecture of Xenopus retinal ganglion cells is sculpted by rho-family GTPases in vivo." J Neurosci **19**(19): 8454-8463.

Russo, A. A., P. D. Jeffrey, A. K. Patten, J. Massague and N. P. Pavletich (1996). "Crystal structure of the p27Kip1 cyclin-dependent-kinase inhibitor bound to the cyclin A-Cdk2 complex." Nature **382**(6589): 325-331.

Russo, A. A., P. D. Jeffrey and N. P. Pavletich (1996). "Structural basis of cyclin-dependent kinase activation by phosphorylation." Nat Struct Biol **3**(8): 696-700.

Sanchez-Soriano, N. and A. Prokop (2005). "The influence of pioneer neurons on a growing motor nerve in Drosophila requires the neural cell adhesion molecule homolog FasciclinII." J Neurosci **25**(1): 78-87.

Sassa, T., H. Gomi, W. Sun, T. Ikeda, R. F. Thompson and S. Itohara (2000). "Identification of variants and dual promoters of murine serine/threonine kinase KKIAMRE." J Neurochem **74**(5): 1809-1819.

Sauer, K., K. Weigmann, S. Sigrist and C. F. Lehner (1996). "Novel members of the cdc2-related kinase family in Drosophila: cdk4/6, cdk5, PFTAIRE, and PITSLRE kinase." Mol Biol Cell **7**(11): 1759-1769.

Savio, T. and M. E. Schwab (1989). "Rat CNS white matter, but not gray matter, is nonpermissive for neuronal cell adhesion and fiber outgrowth." J Neurosci **9**(4): 1126-1133.

Schaefer, A., N. R. Reinhard and P. L. Hordijk (2014). "Toward understanding RhoGTPase specificity: structure, function and local activation." Small GTPases **5**(2): 6.

Scheffzek, K., I. Stephan, O. N. Jensen, D. Illenberger and P. Gierschik (2000). "The Rac-RhoGDI complex and the structural basis for the regulation of Rho proteins by RhoGDI." Nat Struct Biol **7**(2): 122-126.

Schmidt, A. and A. Hall (2002). "Guanine nucleotide exchange factors for Rho GTPases: turning on the switch." Genes Dev **16**(13): 1587-1609.

Schnorrer, F. and B. J. Dickson (2004). "Axon guidance: morphogens show the way." Curr Biol **14**(1): R19-21.

Schwab, M. E. and H. Thoenen (1985). "Dissociated neurons regenerate into sciatic but not optic nerve explants in culture irrespective of neurotrophic factors." J Neurosci **5**(9): 2415-2423.

Schwamborn, J. C., M. Muller, A. H. Becker and A. W. Puschel (2007). "Ubiquitination of the GTPase Rap1B by the ubiquitin ligase Smurf2 is required for the establishment of neuronal polarity." EMBO J **26**(5): 1410-1422.

Schwamborn, J. C. and A. W. Puschel (2004). "The sequential activity of the GTPases Rap1B and Cdc42 determines neuronal polarity." Nat Neurosci **7**(9): 923-929.

Sebok, A., N. Nusser, B. Debreceni, Z. Guo, M. F. Santos, J. Szeberenyi and G. Tigyi (1999). "Different roles for RhoA during neurite initiation, elongation, and regeneration in PC12 cells." J Neurochem **73**(3): 949-960.

Sepe, M., L. Lignitto, M. Porpora, R. Delle Donne, L. Rinaldi, G. Belgianni, G. Colucci, O. Cuomo, D. Viggiano, A. Scorziello, C. Garbi, L. Annunziato and A. Feliciello (2014). "Proteolytic control of neurite outgrowth inhibitor NOGO-A by the cAMP/PKA pathway." Proc Natl Acad Sci U S A **111**(44): 15729-15734.

Sernagor, E., F. Chabrol, G. Bony and L. Cancedda (2010). "GABAergic control of neurite outgrowth and remodeling during development and adult neurogenesis: general rules and differences in diverse systems." Front Cell Neurosci **4**: 11.

Shaknovich, R., P. L. Yeyati, S. Ivins, A. Melnick, C. Lempert, S. Waxman, A. Zelent and J. D. Licht (1998). "The promyelocytic leukemia zinc finger protein affects myeloid cell growth, differentiation, and apoptosis." Mol Cell Biol **18**(9): 5533-5545.

Sheng, L., I. Leshchyns'ka and V. Sytnyk (2013). "Cell adhesion and intracellular calcium signaling in neurons." Cell Commun Signal **11**: 94.

Sherr, C. J. and J. M. Roberts (1999). "CDK inhibitors: positive and negative regulators of G1-phase progression." Genes Dev **13**(12): 1501-1512.

Shu, F., S. Lv, Y. Qin, X. Ma, X. Wang, X. Peng, Y. Luo, B. E. Xu, X. Sun and J. Wu (2007). "Functional characterization of human PFTK1 as a cyclin-dependent kinase." Proc Natl Acad Sci U S A **104**(22): 9248-9253.

Smith, D. S. and L. H. Tsai (2002). "Cdk5 behind the wheel: a role in trafficking and transport?" Trends Cell Biol **12**(1): 28-36.

Smith, P. D., S. J. Crocker, V. Jackson-Lewis, K. L. Jordan-Sciutto, S. Hayley, M. P. Mount, M. J. O'Hare, S. Callaghan, R. S. Slack, S. Przedborski, H. Anisman and D. S. Park (2003). "Cyclin-dependent kinase 5 is a mediator of dopaminergic neuron loss in a mouse model of Parkinson's disease." Proc Natl Acad Sci U S A **100**(23): 13650-13655.

Smith, P. D., M. P. Mount, R. Shree, S. Callaghan, R. S. Slack, H. Anisman, I. Vincent, X. Wang, Z. Mao and D. S. Park (2006). "Calpain-regulated p35/cdk5 plays a central role in dopaminergic neuron death through modulation of the transcription factor myocyte enhancer factor 2." J Neurosci **26**(2): 440-447.

Sonja Rakić, Y. Y., Kunihiko Obata, Clare Faux,John G. Parnavelas,and Margareta Nikolić (2009). "Cortical Interneurons Require p35/Cdk5 for their Migration and Laminar Organization." Cereb Cortex. **19**(8): 1857-1869.

Staropoli, J. F., C. McDermott, C. Martinat, B. Schulman, E. Demireva and A. Abeliovich (2003). "Parkin is a component of an SCF-like ubiquitin ligase complex and protects postmitotic neurons from kainate excitotoxicity." Neuron **37**(5): 735-749.

Stepanova, D. and J. Chernoff (2008). "PAK1 (p21/Cdc42/Rac1-activated kinase 1 (STE20 homolog, yeast))." Atlas Genet Cytogenet Oncol Haematol. **12**(4): 318-319.

Stevaux, O. and N. J. Dyson (2002). "A revised picture of the E2F transcriptional network and RB function." Curr Opin Cell Biol **14**(6): 684-691.

Stowers, R. S., D. Garza, A. Rascle and D. S. Hogness (2000). "The L63 gene is necessary for the ecdysone-induced 63E late puff and encodes CDK proteins required for Drosophila development." Dev Biol **221**(1): 23-40.

Stuermer, C. A. (2010). "The reggie/flotillin connection to growth." Trends Cell Biol **20**(1): 6-13.

Stuermer, C. A., M. Bastmeyer, M. Bahr, G. Strobel and K. Paschke (1992). "Trying to understand axonal regeneration in the CNS of fish." J Neurobiol **23**(5): 537-550.

Sugimoto, M., T. Nakamura, N. Ohtani, L. Hampson, I. N. Hampson, A. Shimamoto, Y. Furuichi, K. Okumura, S. Niwa, Y. Taya and E. Hara (1999). "Regulation of CDK4 activity by a novel CDK4-binding protein, p34(SEI-1)." Genes Dev **13**(22): 3027-3033.

Sumrejkanchanakij, P., M. Tamamori-Adachi, Y. Matsunaga, K. Eto and M. A. Ikeda (2003). "Role of cyclin D1 cytoplasmic sequestration in the survival of postmitotic neurons." Oncogene **22**(54): 8723-8730.

Sun KLW, C. J., Kennedy, TE (2011). "Netrins: versatile extracellular cues with diverse functions." Development **138**(11): 2153-2169.

Sun, Y., Y. Lim, F. Li, S. Liu, J. J. Lu, R. Haberberger, J. H. Zhong and X. F. Zhou (2012). "ProBDNF collapses neurite outgrowth of primary neurons by activating RhoA." PLoS One **7**(4): e35883.

Tabata, H. and K. Nakajima (2003). "Multipolar migration: the third mode of radial neuronal migration in the developing cerebral cortex." J Neurosci **23**(31): 9996-10001.

Tang, D., J. Yeung, K. Y. Lee, M. Matsushita, H. Matsui, K. Tomizawa, O. Hatase and J. H. Wang (1995). "An isoform of the neuronal cyclin-dependent kinase 5 (Cdk5) activator." J Biol Chem **270**(45): 26897-26903.

Tarricone, C., R. Dhavan, J. Peng, L. B. Areces, L. H. Tsai and A. Musacchio (2001). "Structure and regulation of the CDK5-p25(nck5a) complex." Mol Cell **8**(3): 657-669.

Taylor, S. S., D. R. Knighton, J. Zheng, J. M. Sowadski, C. S. Gibbs and M. J. Zoller (1993). "A template for the protein kinase family." Trends Biochem Sci **18**(3): 84-89.

ten Klooster, J. P. and P. L. Hordijk (2007). "Targeting and localized signalling by small GTPases." Biol Cell **99**(1): 1-12.

Togashi, H., K. Nagata, M. Takagishi, N. Saitoh and M. Inagaki (2000). "Functions of a rho-specific guanine nucleotide exchange factor in neurite retraction. Possible role of a proline-rich motif of KIAA0380 in localization." J Biol Chem **275**(38): 29570-29578.

Totsukawa, G., Y. Yamakita, S. Yamashiro, D. J. Hartshorne, Y. Sasaki and F. Matsumura (2000). "Distinct roles of ROCK (Rho-kinase) and MLCK in spatial regulation of MLC phosphorylation

for assembly of stress fibers and focal adhesions in 3T3 fibroblasts." J Cell Biol **150**(4): 797-806.

Tsai, L. H., I. Delalle, V. S. Caviness, Jr., T. Chae and E. Harlow (1994). "p35 is a neural-specific regulatory subunit of cyclin-dependent kinase 5." Nature **371**(6496): 419-423.

Tsai, L. H., T. Takahashi, V. S. Caviness, Jr. and E. Harlow (1993). "Activity and expression pattern of cyclin-dependent kinase 5 in the embryonic mouse nervous system." Development **119**(4): 1029-1040.

Tu, D., Y. Li, H. K. Song, A. V. Toms, C. J. Gould, S. B. Ficarro, J. A. Marto, B. L. Goode and M. J. Eck (2011). "Crystal structure of a coiled-coil domain from human ROCK I." PLoS One **6**(3): e18080.

Umeshima, H. and M. Kengaku (2013). "Differential roles of cyclin-dependent kinase 5 in tangential and radial migration of cerebellar granule cells." Mol Cell Neurosci **52**: 62-72.

van den Heuvel, S. and E. Harlow (1993). "Distinct roles for cyclin-dependent kinases in cell cycle control." Science **262**(5142): 2050-2054.

Vastrik, I., B. J. Eickholt, F. S. Walsh, A. Ridley and P. Doherty (1999). "Sema3A-induced growth-cone collapse is mediated by Rac1 amino acids 17-32." Curr Biol **9**(18): 991-998.

Vetter, I. R. and A. Wittinghofer (2001). "The guanine nucleotide-binding switch in three dimensions." Science **294**(5545): 1299-1304.

Vincent, I., G. Jicha, M. Rosado and D. W. Dickson (1997). "Aberrant expression of mitotic cdc2/cyclin B1 kinase in degenerating neurons of Alzheimer's disease brain." J Neurosci **17**(10): 3588-3598.

Voigt, J., I. Liebich, J. Wostemeyer, K. H. Adam and O. Marquardt (2000). "Nucleotide sequence, genomic organization and cell-cycle-dependent expression of a Chlamydomonas 14-3-3 gene." Biochim Biophys Acta **1492**(2-3): 395-405.

Walsh, F. S., K. Meiri and P. Doherty (1997). "Cell signalling and CAM-mediated neurite outgrowth." Soc Gen Physiol Ser **52**: 221-226.

Wang, F., D. Corbett, H. Osuga, S. Osuga, J. E. Ikeda, R. S. Slack, M. J. Hogan, A. M. Hakim and D. S. Park (2002). "Inhibition of cyclin-dependent kinases improves CA1 neuronal survival and behavioral performance after global ischemia in the rat." J Cereb Blood Flow Metab **22**(2): 171-182.

Wang, J., S. Liu, Y. Fu, J. H. Wang and Y. Lu (2003). "Cdk5 activation induces hippocampal CA1 cell death by directly phosphorylating NMDA receptors." Nat Neurosci **6**(10): 1039-1047.

Wang, Y., K. J. Addess, J. Chen, L. Y. Geer, J. He, S. He, S. Lu, T. Madej, A. Marchler-Bauer, P. A. Thiessen, N. Zhang and S. H. Bryant (2007). "MMDB: annotating protein sequences with Entrez's 3D-structure database." Nucleic Acids Res **35**(Database issue): D298-300.

Ward, M. E., H. Jiang and Y. Rao (2005). "Regulated formation and selection of neuronal processes underlie directional guidance of neuronal migration." Mol Cell Neurosci **30**(3): 378-387.

Weishaupt, J. H., C. Neusch and M. Bahr (2003). "Cyclin-dependent kinase 5 (CDK5) and neuronal cell death." Cell Tissue Res **312**(1): 1-8.

Wennerberg, K., K. L. Rossman and C. J. Der (2005). "The Ras superfamily at a glance." J Cell Sci **118**(Pt 5): 843-846.

Wherlock, M. and H. Mellor (2002). "The Rho GTPase family: a Racs to Wrchs story." J Cell Sci **115**(Pt 2): 239-240.

Wichterle, H., J. M. Garcia-Verdugo and A. Alvarez-Buylla (1997). "Direct evidence for homotypic, glia-independent neuronal migration." Neuron **18**(5): 779-791.

Wilkinson, D. G. (2001). "Multiple roles of EPH receptors and ephrins in neural development." Nat Rev Neurosci **2**(3): 155-164.

Williams, G., E. J. Williams, P. Maison, M. N. Pangalos, F. S. Walsh and P. Doherty (2005). "Overcoming the inhibitors of myelin with a novel neurotrophin strategy." J Biol Chem **280**(7): 5862-5869.

Wills, Z., J. Bateman, C. A. Korey, A. Comer and D. Van Vactor (1999). "The tyrosine kinase Abl and its substrate enabled collaborate with the receptor phosphatase Dlar to control motor axon guidance." Neuron **22**(2): 301-312.

Witke, W., A. V. Podtelejnikov, A. Di Nardo, J. D. Sutherland, C. B. Gurniak, C. Dotti and M. Mann (1998). "In mouse brain profilin I and profilin II associate with regulators of the endocytic pathway and actin assembly." EMBO J **17**(4): 967-976.

Wittinghofer, A. and I. R. Vetter (2011). "Structure-function relationships of the G domain, a canonical switch motif." Annu Rev Biochem **80**: 943-971.

Wray, S. (2002). "Molecular mechanisms for migration of placodally derived GnRH neurons." Chem Senses **27**(6): 569-572.

Xie, Z., B. A. Samuels and L. H. Tsai (2006). "Cyclin-dependent kinase 5 permits efficient cytoskeletal remodeling--a hypothesis on neuronal migration." Cereb Cortex **16 Suppl 1**: i64-68.

Xin, X., Y. Wang, X. M. Ma, P. Rompolas, H. T. Keutmann, R. E. Mains and B. A. Eipper (2008). "Regulation of Kalirin by Cdk5." J Cell Sci **121**(Pt 15): 2601-2611.

Yang, N., O. Higuchi, K. Ohashi, K. Nagata, A. Wada, K. Kangawa, E. Nishida and K. Mizuno (1998). "Cofilin phosphorylation by LIM-kinase 1 and its role in Rac-mediated actin reorganization." Nature **393**(6687): 809-812.

Yang, T. and J. Y. Chen (2001). "Identification and cellular localization of human PFTAIRE1." Gene **267**(2): 165-172.

Yang, T., Y. K. Gao and J. Y. Chen (2002). "KIAA0202, a human septin family member, interacting with hPFTAIRE1." Sheng Wu Hua Xue Yu Sheng Wu Wu Li Xue Bao (Shanghai) **34**(4): 520-525.

Ye, T., A. K. Fu and N. Y. Ip (2012). "Cyclin-dependent kinase 5 in axon growth and regeneration." Int Rev Neurobiol **105**: 91-115.

Yen, S. H., A. Kenessey, S. C. Lee and D. W. Dickson (1995). "The distribution and biochemical properties of a Cdc2-related kinase, KKIALRE, in normal and Alzheimer brains." J Neurochem **65**(6): 2577-2584.

Yeyati, P. L., R. Shaknovich, S. Boterashvili, J. Li, H. J. Ball, S. Waxman, K. Nason-Burchenal, E. Dmitrovsky, A. Zelent and J. D. Licht (1999). "Leukemia translocation protein PLZF inhibits cell growth and expression of cyclin A." Oncogene **18**(4): 925-934.

Yokota, Y., H. T. Gashghaei, C. Han, H. Watson, K. J. Campbell and E. S. Anton (2007). "Radial glial dependent and independent dynamics of interneuronal migration in the developing cerebral cortex." PLoS One **2**(8): e794.

Yoshikawa, S., R. D. McKinnon, M. Kokel and J. B. Thomas (2003). "Wnt-mediated axon guidance via the Drosophila Derailed receptor." Nature **422**(6932): 583-588.

Yu, D. S., R. Zhao, E. L. Hsu, J. Cayer, F. Ye, Y. Guo, Y. Shyr and D. Cortez (2010). "Cyclin-dependent kinase 9-cyclin K functions in the replication stress response." EMBO Rep **11**(11): 876-882.

Yu, T. W., J. C. Hao, W. Lim, M. Tessier-Lavigne and C. I. Bargmann (2002). "Shared receptors in axon guidance: SAX-3/Robo signals via UNC-34/Enabled and a Netrin-independent UNC-40/DCC function." Nat Neurosci **5**(11): 1147-1154.

Zechner, D., Y. Fujita, J. Hulsken, T. Muller, I. Walther, M. M. Taketo, E. B. Crenshaw, 3rd, W. Birchmeier and C. Birchmeier (2003). "beta-Catenin signals regulate cell growth and the balance between progenitor cell expansion and differentiation in the nervous system." Dev Biol **258**(2): 406-418.

Zhang, B., V. B. Tan, K. M. Lim and T. E. Tay (2007). "The activation and inhibition of cyclin-dependent kinase-5 by phosphorylation." Biochemistry **46**(38): 10841-10851.

Zhang, P., P. C. Yu, A. H. Tsang, Y. Chen, A. K. Fu, W. Y. Fu, K. K. Chung and N. Y. Ip (2010). "S-nitrosylation of cyclin-dependent kinase 5 (cdk5) regulates its kinase activity and dendrite growth during neuronal development." J Neurosci **30**(43): 14366-14370.

Zhao, Z. S. and E. Manser (2005). "PAK and other Rho-associated kinases--effectors with surprisingly diverse mechanisms of regulation." Biochem J **386**(Pt 2): 201-214.

APPENDIX

Additional Publications

Regulation of the VHL/HIF-1 Pathway by DJ-1

Mohammad Parsanejad, Yi Zhang, Dianbo Qu, Isabella Irrcher, Maxime W.C. Rousseaux, Hossein Aleyasin, Fatemeh Kamkar, Steve Callaghan, Ruth S. Slack, Tak W. Mak, Stephen Lee, Daniel Figeys, and David S. Park

The Journal of Neuroscience, 4 June 2014, 34(23):8043-8050; doi:10.1523/JNEUROSCI.1244-13.2014

From: jn permissions <jnpermissions@sfn.org>
To: Fatemeh Kamkar
Sent: Thursday, July 30, 2015 5:03 PM
Subject: RE: Request for permission to reprint in Dissertation/Thesis

---

Dear Dr. Kamkar,

Thank you for your email. Permission is granted to reproduce the requested material listed below with NO fee in print and electronic format for use in your doctoral thesis/dissertation. Please contact me if you have any questions or if you need another form of permission.

Regards,
Michael
SfN Central Office

Regulation of the VHL/HIF-1 Pathway by DJ-1

Mohammad Parsanejad, Yi Zhang, Dianbo Qu, Isabella Irrcher, Maxime W.C. Rousseaux, Hossein Aleyasin, Fatemeh Kamkar, Steve Callaghan, Ruth S. Slack, Tak W. Mak, Stephen Lee, Daniel Figeys, and David S. Park
The Journal of Neuroscience, 4 June 2014, 34(23):8043-8050; doi:10.1523/JNEUROSCI.1244-13.2014

From: Fatemeh Kamkar
Sent: Tuesday, July 28, 2015 6:49 PM
To: jn permissions
Subject: Request for permission to reprint in Dissertation/Thesis

Dear Sir/Madam,

I am a co-author of the research article published in J Neuroscience. I would like to request permission for reprint of this article to include it in my PhD dissertation, as part of the manuscript collection.

Parsanejad M, Zhang Y, Qu D, Irrcher I, Rousseaux MW, Aleyasin H, Kamkar F,

Callaghan S, Slack RS, Mak TW, Lee S, Figeys D, Park DS. Regulation of the

VHL/HIF-1 pathway by DJ-1. J Neurosci. 2014 Jun 4;34(23):8043-50. doi:

10.1523/JNEUROSCI.1244-13.2014. PubMed PMID: 24899725.

Thank you for your time and consideration.

Regards,

Fatemeh Kamkar

Brief Communications

Regulation of the VHL/HIF-1 Pathway by DJ-1

Mohammad Parsanejad,[1] Yi Zhang,[1] Dianbo Qu,[1] Isabella Irrcher,[1,5] Maxime W.C. Rousseaux,[1] Hossein Aleyasin,[1] Fatemeh Kamkar,[1] Steve Callaghan,[1] Ruth S. Slack,[1] Tak W. Mak,[4] Stephen Lee,[1] Daniel Figeys,[2] and David S. Park[1,5]

[1]Department of Cellular and Molecular Medicine, [2]Institute of Systems Biology, University of Ottawa, Ottawa, Ontario K1H 8M5, Canada, [3]Department of Ophthalmology, Queen's University, Kingston, Ontario K7L 5G2, Canada, [4]The Campbell Family Institute for Breast Cancer Research, Toronto, Ontario M5G 2C1, Canada, and [5]Department of Cogno-Mechatronics Engineering, Pusan National University, Busan 609-735, Korea

DJ-1 (PARK7) is a gene linked to autosomal recessive Parkinson disease (PD). We showed previously that *DJ-1* loss sensitizes neurons in models of PD and stroke. However, the biochemical mechanisms underlying this protective role are not completely clear. Here, we identify Von Hippel Lindau (VHL) protein as a critical DJ-1-interacting protein. We provide evidence that DJ-1 negatively regulates VHL ubiquitination activity of the α-subunit of hypoxia-inducible factor-1 (HIF-1α) by inhibiting HIF–VHL interaction. Consistent with this observation, *DJ-1* deficiency leads to lowered HIF-1α levels in models of both hypoxia and oxidative stress, two stresses known to stabilize HIF-1α. We also demonstrate that HIF-1α accumulation rescues *DJ-1*-deficient neurons against 1-methyl-4-phenylpyridinium-induced toxicity. Interestingly, lymphoblast cells extracted from *DJ-1*-related PD patients show impaired HIF-1α stabilization when compared with normal individuals, indicating that the DJ-1–VHL link may also be relevant to a human context. Together, our findings delineate a model by which DJ-1 mediates neuronal survival by regulation of the VHL–HIF-1α pathway.

Key words: DJ-1; oxidative stress; Parkinson's disease

Introduction

Parkinson's disease (PD) is a neurodegenerative disorder, pathologically characterized by progressive loss of dopaminergic (DA) neurons in the substantia nigra pars compacta (SNc). While most cases are sporadic, 5–10% of the cases are familial and monogenic. Loss of *DJ-1* leads to an early-onset form of PD (Bonifati et al., 2003). We have previously shown that DA neurons in *DJ-1*-deficient mice exhibit hypersensitivity to oxidative stress induced by 1-methyl-4-phenyl-1,2,3,6-tetrahydropyridine (MPTP), H_2O_2, and 1-methyl-4-phenylpyridinium (MPP^+), the active metabolite of MPTP (Kim et al., 2005). We and others have also shown that reactive oxygen species (ROS) is increased in cells/mice lacking *DJ-1* (Taira et al., 2004; Aleyasin et al., 2007). In line with this observation, numerous studies demonstrated that DJ-1 is neuroprotective under oxidative conditions (Aleyasin et al., 2007, 2010; Lee et al., 2009). The mechanisms through which DJ-1 exerts its antioxidant-neuroprotective role are largely unclear.

To identify potential DJ-1-interacting proteins, we performed an unbiased mass spectrometry screen, which indicated Von Hippel Lindau (VHL) protein as a potential interacting partner. VHL is primarily a tumor-suppressor protein (Lonser et al., 2003) and its best-known biochemical role is as an E3 ubiquitin-ligase complex (Lonergan et al., 1998). One of the best-defined substrates of VHL is the α-subunit of hypoxia-inducible factor-1 (HIF-1α), a transcription factor important in the hypoxic response (Kamura et al., 2000; Tanimoto et al., 2000). Under normal levels of oxygen or ROS, HIF-1α is hydroxylated by prolyl-hydroxylase proteins (PHDs; Berra et al., 2003), ubiquitinated by VHL protein, and finally degraded by the proteasome. Hypoxia or increased levels of ROS, however, inhibit PHD, which in turn inhibits VHL-mediated degradation of HIF-1α and induces transcription of genes involved in cellular adaptation to hypoxic and oxidative stress condition, such as vascular endothelial growth factor (*VEGF*) and erythropoietin (*EPO*). Interestingly, HIF-1α expression and its downstream targets are downregulated in the SNc of PD brains (Elstner et al., 2011). Conversely, increase of HIF-1α and/or its targets are protective in several models of PD (Genc et al., 2002; Lee et al., 2009). HIF-1α also upregulates tyrosine hydroxylase and increases dopamine release in PC12 cells and rat ventral mesencephalic cells (Johansen et al., 2010). Given these links of HIF-1α to PD and our observations that VHL could potentially interact with DJ-1, we explored whether DJ-1 could regulate the VHL–HIF pathway. Presently, we provide evidence to support a model by which DJ-1

Received March 20, 2013; revised May 4, 2014; accepted May 5, 2014.

Author contributions: M.P., D.Q., M.W.C.R., H.A., R.S.S., T.W.M., S.L., and D.S.P. designed research; M.P., Y.Z., I.I., S.C., and D.S. performed research; D.Q., F.K., S.C., T.W.M., S.L., and D.F. contributed unpublished reagents/analytic tools; M.P. analyzed data; M.P., Y.Z., and D.S.P. wrote the paper.

This work was supported by grants from the Canadian Institutes of Health Research, Heart and Stroke Foundation of Ontario, Parkinson's Society Canada, Parkinson's Research Consortium, Neuroscience Canada/Kornhill Foundation, and the Centre for Stroke Recovery. This work also was supported by the World Class University program through the National Research Foundation of Korea, funded by the Ministry of Education, Science and Technology, South Korea (Grant: R31-2008-000-20004-0; to D.S.P.). The authors thank Alexander Rovello and Dr. Yasmeide Rodríguez-Gonzalez, University of Ottawa, Ontario, Canada, for their technical assistance. Authors would also like to thank Dr. Patrizia Rizzu, Medical Genomics-VU University Medical Center, The Netherlands, for kindly providing human lymphoblasts.

Daniel Figeys is a Canada Research Chair in Proteomics and Systems Biology.

Correspondence should be addressed to David S. Park, Ottawa Health Research Institute, Neuroscience Group, University of Ottawa, 451 Smyth Road, Ottawa, Ontario K1H 8M5, Canada. E-mail: dpark@ohri.ca.

M.W.C.R.'s present address: Department of Molecular and Human Genetics, Baylor College of Medicine, Houston, Texas 77030.

H.A.'s present address: Feinberg Department of Neuroscience and Friedman Brain Institute, Icahn School of Medicine at Mount Sinai, New York, New York 10029-6574.

DOI:10.1523/JNEUROSCI.1344-13.2014

 0270-6474/14/348043-08$15.00/0